Aus dem Institut für Veterinär-Physiologie
des Fachbereichs Veterinärmedizin
der Freien Universität Berlin

SLC41A1, SLC41A3 and CNNM2: Magnesium responsive genes with potential involvement in human ailments

Inaugural-Dissertation
zur Erlangung des akademischen Doktorgrades
philosophiae doctor (Ph.D.)
in 'Biomedical Science'
an der Freien Universität Berlin

vorgelegt von
Lucia Mastrototaro
Biotechnologin
aus Lecce (Italien)

Berlin 2016

Journal-Nr. : 3915

Gefördert durch ein Elsa-Neumann-Stipendium des Landes Berlin

Gedruckt mit Genehmigung des Fachbereichs Veterinärmedizin
der Freien Universität Berlin

Dekan: Univ.-Prof. Dr. Jürgen Zentek
Erster Gutachter: Univ.-Prof. Dr. Jörg Rudolf Aschenbach
Zweiter Gutachter: Univ.-Prof. Dr. Heidrun Gehlen
Dritter Gutachter: Prof. Dr. Jürgen Vormann

Deskriptoren (nach CAB-Thesaurus):
magnesium, SLC41A1, SLC41A3, CNNM2, neurodegeneration, Parkinson's disease, insulin, intracellular magnesium homeostasis, magnesium mitochondrial efflux system, protein expression, protein localization, transport studies

Tag der Promotion: 05.10.2016

To my family

TABLE OF CONTENTS

LIST OF FIGURES

LIST OF ABBREVIATIONS

aa	Amino acid
ACCA1	Acetyl-/propionyl-coenzyme A carboxylase alpha chain 1
ACD	Ancient conserved domain
ACDP2	Ancient conserved domain protein 2
ADP	Adenosine diphosphate
AD	Alzheimer's disease
ADHD	Attention deficit hyperactivity disorder
ALS	Amyotrophic lateral sclerosis
AMBRA1	Autophagy/beclin-1 regulator
AR	Androgen receptor
AREs	Androgen receptor elements
ATP	Adenosine triphosphate
cAMP	Cyclic adenosine monophosphate
CBS	Cystathionine-beta-synthase
CNNM2	Cyclin M2
COX	Cytochrome C oxidase
DM2	Diabetes mellitus 2
DCT	Distal convoluted tubule
EBP	Emopamil binding protein
ER	Endoplasmic reticulum
FFS	Fast-filter spectrofluorometry
GA	Golgi apparatus
HD	Huntington's disease
HEK293	Human embryonic kidney 293
I1/2	Isophorm 1/2
IMH	Intracellular Mg homeostasis
MagT1	Magnesium transporter 1
MDCT	Mouse distal convoluted tubule cells
Mg	Magnesium
MgtE	Magnesium transporter E
MPC1	Mitochondrial pyruvate carrier 1
MRG	Magnesium responsive gene

NMDG	N-Methyl-D-glucamine
NME	Na^+/Mg^{2+} exchanger
PARK7/DJ1	Parkinson disease 7/ deglycase protein
PCR	Polymerase chain reaction
PD	Parkinson's disease
PKA	Protein kinase A
PKC	Protein kinase C
PINK1	PTEN Induced Putative Kinase 1
RBC	Red blood cells
SLC	Solute carrier
SLC41A1	Solute carrier family 41 member A1
SLC41A3	Solute carrier family 41 member A3
SNP	Single nucleotide polymorphism
SPTBN1	Spectrin β chain 1
SU-YTH	Split-ubiquitin yeast two hybrid
TAL	Thick ascending limb
TM	Transmembrane
TRPM6/7	Transient receptor potential melastatin ion channel 6/7
TUSC3	Tumor suppressor candidate 3

1. GENERAL INTRODUCTION

Magnesium (Mg) plays several crucial roles in eukaryotic cells and in the whole organism. In mitochondria it is a key factor of the adenosine triphosphate (ATP)-synthesizing machinery and its “deficit” or defects in its transport impairs cellular functions, e. g. proliferation rate, which can be reversed by magnesium supplementation.

Therefore it is not surprising that Mg deficiency and/or a change in the intracellular Mg homeostasis (IMH) might lead to a multitude of serious ailments, such as neurodegenerative disorders (Parkinson’s disease (PD) and Alzheimer’s disease (AD)), stroke, diabetes and cardiovascular diseases (1).

The intracellular free Mg^{2+} concentration is in the order of 0.5 mM and it is maintained below the concentration predicted from the transmembrane electrochemical potential. This control is achieved through a balance of Mg^{2+} uptake, intracellular Mg^{2+} storage and Mg^{2+} efflux; clearly, specific magnesium transporters exist for each step and impairment in their function can lead to altered intracellular magnesium levels or magnesium homeostasis. In the last decades, roughly a dozen of candidate genes have been proposed to encode for proteins regulating Mg^{2+} transport in eukaryotic cells, but only few of them have been well characterized as Mg^{2+} transporters. The first mammalian Mg^{2+} transporter to be identified at the molecular level was Mrs2 of the inner mitochondrial membrane (2). Other well characterized channels and transporters are TRPM6/7, MagT1, and SLC41A1 (3). Importantly, SLC41A1 has been identified and characterized as the main Mg^{2+} efflux mechanism in the plasma membrane (4, 5) by members of the supervising team at the Institute of Veterinary Physiology, Berlin, and as Na^{+}/Mg^{2+} exchanger overexpressed in pre-eclamptic women (6).

Several other genes have been described as magnesium responsive genes (MRG) and meanwhile molecularly characterized, but their role in the cellular physiology has long remained uncovered. For example, CNNM2 and SLC41A3 are both listed among the MRG, indeed their mRNA levels rise in mouse distal convoluted tubule cells (MDCT) grown in nominally Mg^{2+}-free medium (7, 8), but data about their cellular localization and their role in magnesium transport are missing.

Thus this thesis has focused on the further investigation of Mg^{2+} efflux mediated by SLC41A1 and its impact on human aliments such as PD and diabetes and on the functional and molecular characterization of SLC41A3 and CNNM2 in order to have a complete frame of the magnesium transport and mobilization in the cells and eventually to better understand the importance of these processes in the cell and in the whole body physiology. This study reveals that a

misbalanced Mg^{2+} influx/efflux, as consequence of an altered magnesium transport function, may represent the trigger for some common human diseases.

2. LITERATURE REVIEW

2.1. Magnesium and its importance in the human body

Magnesium is the fourth most abundant cation in the body and the second most abundant divalent cation in eukaryotic cells (9). Total body magnesium content in the average 70 kg human adult is approximately 25 g (10), of which 50-60% resides in bone (11, 12), 46% in skeletal muscle and soft tissues (11), and less than 1% is found in serum and red blood cells (RBC) (13-15).

In normal adults, the total serum magnesium concentration ranges between 0.65 and 1 mM (16); approximately one third is bound to proteins, primarily albumin and the rest to globulins (17, 18), 61% exists in the free or ionized state and about 5% is complexed with other ions, such as phosphate and citrate (10). The reference range for the concentration of ionized magnesium in human serum (0.54–0.67 mM) is narrower than that for calcium (10, 19). Plasma magnesium concentration in healthy individuals is similar to serum concentration ranging from 0.7 to 1.0 mM (20), while magnesium concentration in RBC is higher (1.65–2.65 mM) (16, 20).

Total intracellular magnesium concentration varies from 14 to 20 mM in different mammalian cells (21). The majority of cellular Mg^{2+} is bound to proteins, phospholipids, nucleic acids and especially ATP (22) or it is sequestered within mitochondria and endoplasmic reticulum, while free ionized Mg^{2+} represents only a small amount, ≈0.2–1 mM (23, 24), approximately 5% of the total cellular Mg. Free intracellular magnesium is maintained within this narrow range by Mg^{2+}-regulatory systems (Mg^{2+}-homeostatic factors and Mg^{2+} transporters), but in extreme situations, such as hypoxia or prolonged magnesium depletion, it may undergo changes. Similar to Ca^{2+}, the free ion is physiologically active in the body (25)..

Serum Mg^{2+} is maintained in a relatively tight range only slightly higher than the intracellular free Mg^{2+}; this makes the reversal potential for Mg^{2+} close to zero. Because the plasma membrane potential is negative, the electrochemical gradient for Mg^{2+} promotes the entrance of Mg^{2+} into the cells. The cellular distribution of magnesium is heterogeneous, with lower concentrations in the peripheral regions of the cytoplasm than in the perinuclear region (26).

The role of Mg^{2+} in the body is manifold, it contributes to the mineralization and growth of bones (27) and it regulates the vascular tone and cardiac rhythm. It is an essential cofactor for more than 300 enzymes (28) and signal-transduction proteins; it is required for transcellular ion transport, neuromuscular transmission, synthesis of carbohydrates, proteins, lipids and nucleic acids, and finally for energy generation and glycolysis, either indirectly as a part of the Mg^{2+}-ATP complex or directly as an enzyme activator (29). It plays also a crucial role in cellular proliferation and division because replicating cells need to synthesize DNA and RNA and the presence of

magnesium is crucial for maintaining an adequate supply of purine and pyrimidine nucleotides (30, 31) and for the correct functioning of DNA polymerases (32). Finally magnesium has an anti-apoptotic effect in the mitochondrial permeability transition (33) and by acting as calcium antagonist it blocks the calcium-induced death cascade (34).

It is evident that adequate magnesium stores are vitally important for life; decreased Mg^{2+} levels have been linked to various adverse health outcomes (35, 36), including cardiovascular diseases (37-40), hemicranias (41), osteoporosis (42), pre-eclampsia/eclampsia (43, 44), diabetes (45) and neurodegeneration (46). Much evidence has demonstrated the benefits of Mg^{2+} supplementation to improve the magnesium balance and for the treatment of the pathologies listed above (37-46).

While hypomagnesaemia is frequently observed in hospitalized individuals and is associated with many pathologic conditions, hypermagnesaemia is less frequent (25) because the kidneys of healthy patients have a large capacity for Mg^{2+} excretion. When the renal threshold for reabsorption is exceeded, most of the excess Mg^{2+} is excreted into the urine. Thus hypermagnesaemia generally occurs in patients consuming an excessive amount of Mg^{2+} or patients with kidney failure. In such instances, reducing the Mg^{2+} intake is enough to restore normal Mg^{2+} levels in the body. Only in severe case of hypermagnesaemia, it is necessary to intervene with hemodialysis or diuretics.

2.2. Magnesium transport into the cell and between intracellular stores

Although the gradient of free Mg^{2+} across the plasma membrane is modest, it may vary and consequently influence many cellular activities.

The main factors influencing the levels of cytosolic free magnesium are the activity of transport systems in the plasma membrane and mitochondria and the concentration of nucleotides, because ATP, for example, binds Mg^{2+} with a high dissociation constant (~30μM) (47). The amount of intracellular free magnesium can therefore undergo some fluctuations as a consequence of changes in the ATP concentration and mitochondrial or plasma membrane transport activity; for example, it would increase in a poor energy state (48) or in anoxia (49).

Magnesium transport into or out of the cell requires the presence of channels and/or carrier-mediated transport systems (50, 51). Taking into account that the membrane potential typically ranges from –40 mV to –80 mV (negative on the cytoplasmic side) and that the extracellular concentration of magnesium is higher than its intracellular concentration (28, 52-55), uptake of Mg^{2+} into the cell can be mediated by channels or channel-like mechanisms. On the contrary, outward transport of Mg^{2+} takes place against the electrochemical gradient, therefore, Mg^{2+}

extrusion must be accomplished by an ATP-dependent transporter or by a secondary active transport mechanism.

Although the role of Mg^{2+} has been extensively established for numerous biochemical processes, details on the transport mechanisms mediating uptake of Mg^{2+} into vertebrate cells, the subsequent storage and its distribution between organelles remain obscure. In the last decade, several proteins have been suggested to be directly involved in Mg^{2+} transport or to act as Mg^{2+} homeostatic factors. In many cases, their biophysical and physiological characterization is still rudimentary but their coordinated functions determine the vertebrate cellular Mg^{2+} homeostasis (Fig. 1).

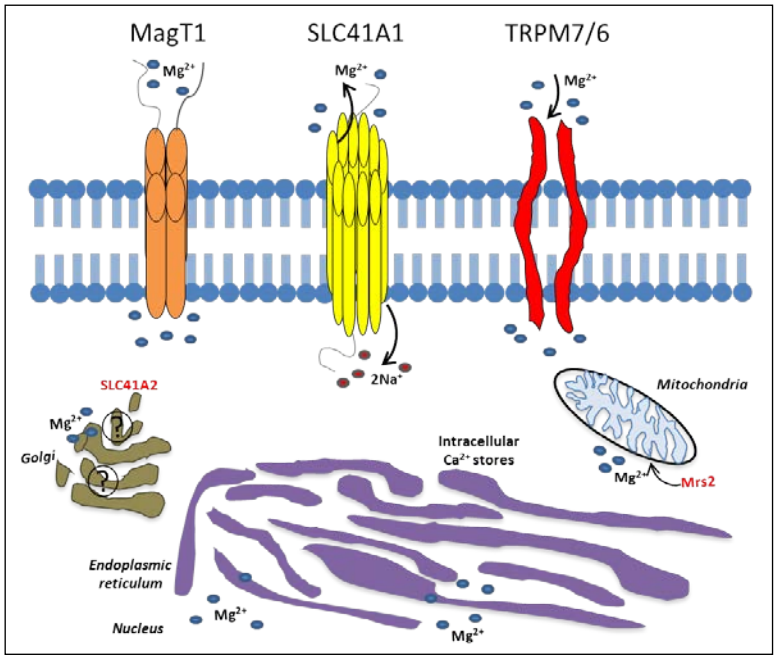

Figure 1. Various proposed Mg^{2+} transporters and their predicted transport mechanisms in vertebrate cells (56): Mrs2, a mitochondrial Mg^{2+} uptake system that transports Mg^{2+} with mitochondrial membrane potential (channel transport mechanism based on similarity with yeast Alr family); **TRPM7/6** channel kinase (channel transport mechanism); **MagT1** thought to be a plasma membrane Mg^{2+} transporter with an ion channel transport mechanism; **SLC41A1** identified as the Na^{+}/Mg^{2+} exchanger (5) represents an exchange mechanism which mediates Mg^{2+} efflux in vertebrate cells; **SLC41A2** has been suggested as the responsible Mg^{2+} transporter in Golgi but its mode of operation is still uncovered. Mg^{2+} transport into both the endoplasmic reticulum and nucleus are very poorly characterized and hence are pictured simply as passive exchange mechanisms. (104 modified after the latest finding of Kolisek et al (5))

It was recently suggested that Mg^{2+} uptake in mammalian cells occurs via the channel kinases TRPM7 (57) and TRPM6 (58, 59). In particular TRPM7 is ubiquitously expressed and it is important to ensure a rapid Mg^{2+} entry during G1 phase of the cell cycle and its activity is

regulated by intracellular Mg^{2+} through a negative feedback mechanism (60). It is considered a master regulator of cellular Mg^{2+} homeostasis.

A recent study shows that in the situation of TRPM7 deficiency, eukaryotic DT40 B cells (chicken B-cell line) increase the expression level of the Mg^{2+} transporter MagT1, indicating that MagT1 might compensate for the lack of TRPM7 (61). A further study (62) characterizes MagT1 and TUSC3 as major mechanisms of Mg^{2+} influx, because a knockdown of either MagT1 or TUSC3 significantly lowers the total and free intracellular Mg^{2+} concentrations in mammalian cell lines.

While TRPM7 is equally distributed in human tissues and organs, the expression of TRPM6 is restricted to kidney and colon where it represents the key protein in the transcellular pathway of intestinal Mg^{2+} absorption and renal reabsorption. When mutated, it causes recessive hypomagnesaemia with secondary hypocalcemia (58, 59). It has been convincingly demonstrated that TRPM6 is responsible for the apical entry pathway of Mg^{2+} in the renal distal convoluted tubule (DCT), but the basolateral extrusion mechanism had not been molecularly characterized. The finding that the renal CNNM2 (cyclin M2) is predominantly localized on the basolateral side of the thick ascending limb of Henle's loop (TAL) and DCT (63) makes this protein a putative candidate for basolateral Mg^{2+} extrusion. Furthermore experimental evidences associate two mutations of CNNM2 to dominant hypomagnesaemia and the same study shows that the protein mediates Mg^{2+}-sensitive Na^{+} currents that are blocked when extracellular Mg^{2+} is increased and diminished when the protein is mutated (63).

The effect of mutations found in CNNM2, its sensitivity to extracellular Mg^{2+} and its basolateral localization suggest a critical role for CNNM2 in epithelial Mg^{2+} transport. It remains still uncertain whether CNNM2 transports Mg^{2+} itself or contributes to a Mg^{2+}-sensing mechanism via the tandem pair of cystathionine-beta-synthase (CBS) domains in the ancient conserved domain (ACD) region. This latter hypothesis is in line with the new data presented in this work, showing that CNNM2 does not mediate any Mg^{2+} efflux or influx but it might represent the first Mg^{2+} homeostatic factor with no transport activity which is instead involved in the coordination of other Mg^{2+} transporters.

With the identification and characterization of TRPM6/7, the claudin family, MagT1 and other transport systems, the picture of mechanisms mediating uptake of Mg^{2+} into vertebrate cells has become more and more comprehensive. However, to regulate the cellular Mg^{2+} homeostasis, mechanisms mediating extrusion of the ion are required as well and the knowledge about these pathways is still rudimentary.

Two mechanisms were postulated to mediate Mg^{2+} extrusion. The first mechanism uses the Na^{+} concentration gradient as the sole energy input for the extrusion of Mg^{2+} and the mechanism was therefore named Na^{+}-dependent exchanger. The second mechanism is Na^{+} independent and different cations (e.g. Ca^{2+} or Mn^{2+}) and anions (e.g. Cl^{-}, HCO_3^{+}) are suspected to act as

counter-transported and cotransported ions in this process, respectively. Both mechanisms were demonstrated experimentally, however, only the Na^+-dependent mechanism has been molecularly identified as being the solute carrier family 41 member A1 (SLC41A1), also called Na^+/ Mg^{2+} exchanger because it extrudes 1 Mg^{2+} in exchange for 2 Na^+ (5).

The intracellular magnesium content depends also on the Mg^{2+} transport between the intracellular stores, in particular mitochondria. Mitochondrial Mg^{2+} is involved in many processes like modulation of anion channels, H^+ gradients and the membrane potential across the mitochondrial membrane (64). Furthermore it has a protective role in the so-called 'mitochondrial permeability transition', a dysfunction characterized by the opening of a multi-protein complex localized in the inner mitochondrial membrane (65), because adequate Mg^{2+} levels reduce the probability of an irreversible pore opening (66).

Therefore, it is really crucial to keep the Mg^{2+} concentration in a tight range since even minimal variations may affect mitochondrial functions and the fate of the whole cell. While the plasma membrane importers control the amount of Mg^{2+} imported into the cells, the maintenance of an appropriate cytosolic Mg^{2+} concentration further depends on storage of Mg^{2+} in organelles, such as the vacuole, which provides a 'buffer' function in addition to chelators (e.g., ATP).

On top of these controls, the importers and exporters in the mitochondria work together cooperatively to well regulate the mitochondrial Mg^{2+} levels; therefore altered expression of the mitochondrial transporters may shift the Mg^{2+} balance. Under Mg^{2+}-deficient states, mitochondria might supply some Mg^{2+} to the cytosol and try to restore the general intracellular Mg^{2+} homeostasis, but this ultimately may compromise their own functions (67).

Mitochondrial Mg^{2+} influx is stimulated by inorganic phosphorus (68). The only known transporter in eukaryotic cells responsible for Mg^{2+} uptake into mitochondria is MRS2 (69, 70). Free magnesium in the mitochondrial matrix varies with the cellular metabolic state: it decreases in the presence of inorganic phosphate and ATP, and increases when ATP is converted into ADP (71).

The pathways involved in Mg^{2+} release from mitochondria are uncovered, but mitochondrial magnesium efflux seems to be stimulated by the increase of free magnesium in the mitochondrial matrix.

Considering that mitochondria act as intracellular Ca^{2+} stores as well and that a Na^+-dependent (Na^+/Ca^{2+} exchanger) and a Na^+-independent efflux mechanism exist for Ca^{2+} (72), it seems reasonable to suspect that similar mechanisms may mediate extrusion of Mg^{2+} from mitochondrial stores.

The molecular identity of a mitochondrial efflux system has remained undiscovered for many years, but the present work has revealed SLC41A3, a member of the SLC superfamily, as a

strong candidate for being the first molecularly identified intracellular Mg^{2+} exchanger, with location on the mitochondrial membrane.

2.3. Hormonal regulation of intracellular magnesium

Clinical and experimental data demonstrate that magnesium transport in mammalian cells is influenced by hormonal and pharmacological factors including β-agonists, growth factors, and insulin (50, 51, 73). It has been suggested that a hormonally regulated magnesium uptake system controls the intracellular magnesium concentration in cellular compartments. Many hormones affect Mg^{2+} transport, including calcitonin (74), parathormone (75), adrenaline and noradrenaline which stimulate magnesium uptake by fat cells while they reduce magnesium uptake by cardiac muscle cells (11). It appears likely, however, the hormonal modulation concerns especially the efflux system because it is energy-dependent. The modulation is usually mediated via intracellular messengers, such as cytosolic free calcium or cAMP, which seem to have a stimulating effect on magnesium efflux in ascites cells (76).

Insulin has also been suggested as a regulatory hormone of magnesium homeostasis. *In vivo* studies conducted on the cortical portion of the thick ascending limb in mouse and rat kidney demonstrated that insulin, acting on the loop of Henle, reduces magnesium extrusion across the basolateral membrane (26). *In vitro* studies on human platelets show that insulin can increase the cellular magnesium uptake in a dose- and time-dependent way (73).

A further study indicates that insulin can modulate the cellular Mg^{2+} content in cardiac cells by limiting the Mg^{2+} extrusion induced by β-adrenoreceptor stimulation and by favoring a Mg^{2+} accumulation in the cell (77). Indeed the administration of β-adrenergic agonists to cardiac cells elicits a remarkable extrusion of cellular Mg^{2+} across the sarcolemma (51, 78) via an increase of cAMP and the activation of a Na^{+}/Mg^{2+} exchanger (53, 79).

Intracellular cAMP can directly inhibit Mg^{2+} uptake and/or transiently increases the concentration of cytosolic Mg^{2+} and therefore its efflux through redistribution of magnesium from internal pools. It has been shown that the addition of nanomolar concentrations of cAMP to permeabilized hepatocytes or to isolated liver mitochondria (80) induces the mobilization of large amounts of Mg^{2+} from the mitochondrial pool. Large Mg^{2+} fluxes may lead to a significant redistribution of Mg^{2+} across the cells and cell compartments, which will affect many cellular functions and metabolic pathways.

The role of insulin on magnesium homeostasis has been broadly examined in this project and the results obtained confirm the beneficial effect of insulin on hypomagnesaemia often observed in diabetes patients. Insulin is known to bind the insulin receptor and activate a downstream cascade which leads to the inhibition of PKA (protein kinase A) and therefore to the inhibition of

SLC41A1, which is activated via cAMP-dependent PKA-mediated phosphorylation. It is shown in the present study that insulin, by inhibiting PKA, reduces the Mg^{2+} extrusion via SLC41A1; on the contrary an increased production of cAMP might result in the activation of SLC41A1 and therefore in an enhanced Mg^{2+} efflux (81).

The above considerations may have particular importance in diabetes, a condition in which insulin signaling as well as Mg^{2+} homeostasis are markedly impaired. Therefore, a further characterization of SLC41A1 appears necessary in order to achieve a better understanding of Mg^{2+} homeostasis in some disease states and to link the mechanisms of Mg^{2+} mobilization across the plasma membrane or between intracellular compartments to mitochondrial dysfunction and hypomagnesaemia-related disorders.

2.4. SLC41 family

The SLC41 family of vertebrate magnesium transporters was first identified and characterized in 2003 (82) and comprises three members – SLC41A1, SLC41A2 and SLC41A3. The three members have been found in all eukaryotes and they display distant homology to the prokaryotic MgtE family of Mg^{2+} transporters (83-85) (Fig. 2). They are characterized by two "MgtE-like domains" denoted D1 (consensus sequence: PX_6GN) and D2 (consensus sequence: $P(D/A)X_4PX_6D$) (82).

The examination of the SLC41 topology suggests the presence of two five-transmembrane (TM) span MgtE domains, connected by a linker helix; therefore the SLC41 family seems to possess the structural features of prokaryotic MgtE transporters, which are characterized by a Mg^{2+}-selective pore created via homodimerization (84).

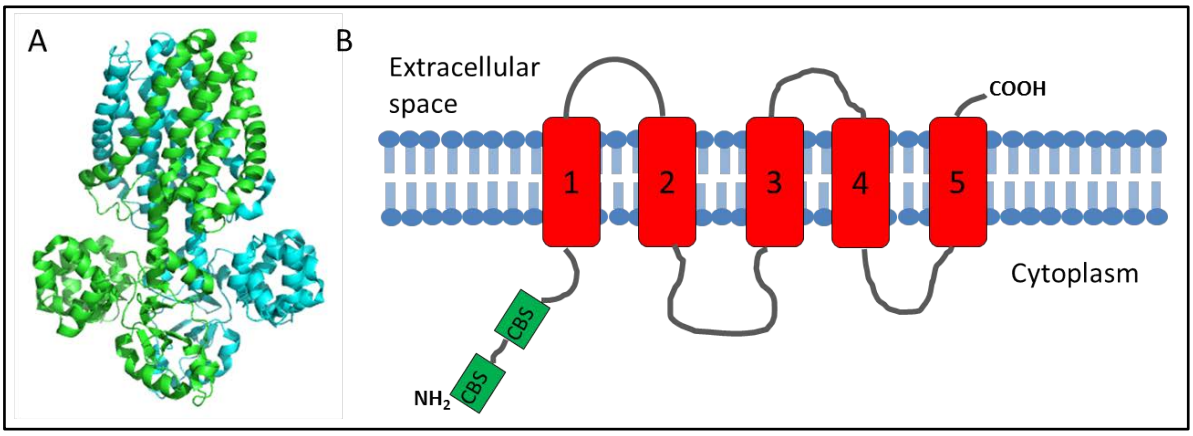

Figure 2. Structural overview of the prokaryotic MgtE transporters: A, Crystal structure of magnesium transporter MgtE (83); **B,** The MgtE dimer is viewed in the plane of the membrane, highlighting the N domain, CBS domains (green), connecting helix (grey), and transmembrane (TM) domain (red) in one subunit. The transmembrane helices of the subunit are numbered.

Using the two-electrode oocyte voltage-clamp model, it has been shown that the three members of the SLC41 family transport Mg^{2+} within its physiological concentration range when heterologously expressed in *Xenopus laevis* oocytes (7, 86, 87). However, electrogenic Mg^{2+} transport by SLC41 family members could not be confirmed in mammalian or avian cellular systems transfected with the human gene (4, 5).

SLC41A1 is the only member which has been well characterized at the molecular and physiological level. From the experimental evidences, A1 is clearly Mg^{2+} transporter and the primary Mg^{2+} efflux system working as a Na^{+}/Mg^{2+} exchanger (5) and not as a cation channel, as it was assumed by Goytain and Quamme (86).

Furthermore, similar to the large N-terminal domains of the prokaryotic MgtE proteins, which are implicated in the regulation of Mg^{2+} transport, the short N-terminal cytoplasmic domain of SLC41A1 has recently been implicated in the regulation of SLC41A1 function (83, 88). Indeed the intracellular N-terminus is involved in Mg^{2+} sensing and it contains several phosphorylation hotspots for PKA and PKC (4).

Finally data are available about SLC41A1 cellular localization, complex-forming ability, spectrum of binding partners (89) and its link to human disorders (90). On the contrary, there is little known on the molecular biology, cellular localization and membrane topology of SLC41A2 and SLC41A3, and there is no information available about their expression across human tissues and organs in peer-reviewed papers. Their exact function in the context of intracellular Mg^{2+} homeostasis is still uncertain as well, but based on the homology with SLC41A1 it can be speculated that both SLC41A2 and SLC41A3 also function as Mg^{2+} carriers.

2.4.1. SLC41A1 as Na^{+}/Mg^{2+} exchanger

SLC41A1 represents the long-searched Na^{+}/Mg^{2+} exchanger of the plasma membrane. It has been first identified by Wabakken et al. (82) and characterized as the first eukaryotic protein with homology to the prokaryotic MgtE family of Mg^{2+} transporters. In particular, the N-terminal region of SLC41A1, named D1, has the highest similarity to the prokaryotic MgtE consensus sequence, whereas the C-terminus, named D2, is less similar. In both, D1 and D2, Wabakken and colleagues identified two conserved motifs which are found in all MgtE-like proteins of eubacteria, archaea and eukaryota.

The human gene has been mapped to chromosome 1q31-32 and computational analysis (TMHMM1.0 program and WHAT program) of the protein predicted SLC41A1 to have 10 putative transmembrane spanning domains with both N- and C-termini, putatively located

intracellularly (82, 86) (Fig. 3) and therefore to be an integral protein of the plasma membrane with a predicted molecular mass of 56 kDa (4, 82).

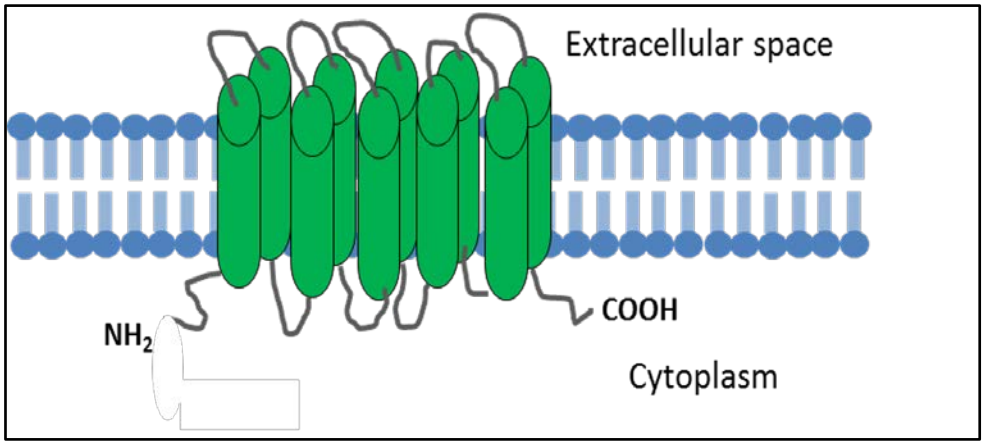

Figure 3. Computer model of hSLC41A1 (56kDa): the most probable computer predicted model of SLC41A1 membrane topology, with 10TM domains (green) and both N- and C-termini located intracellularly (82, 86).

The localization data were confirmed by confocal immunofluorescence, showing that overexpressed *FLAG-hSLC41A1* in HEK293 cells is targeted to the plasma membrane (4).
Although the most probable model, which has been computer-predicted, exhibits 10 TM spans with both termini being oriented intracellularly, a structure-function analysis of heterologous SLC41A1 expression later demonstrated that SLC41A1 has 11 TM domains (Fig. 4). The protein therefore exhibits the same plasma membrane orientation as the homologous bacterial MgtE proteins with an N-terminal flanking region located in the cytosol, which is suspected to be important for the regulation of the Mg^{2+} transport function (88). However, controversy remains about the orientation of the C-terminus, which has lately been proposed to be extracellular in peer-reviewed bibliography (88).
Consequently, a split-ubiquitin functional assay was performed with transgenic SLC41A1 fused N- or C-terminally to a Cub-LexA-VP16 reporter cassette in order to clarify the orientation of the C-terminus. The assay revealed a cytosolic orientation of the C-terminus and therefore confirmed the 10 TM model of SLC41A1 topology, with both termini being oriented intracellularly, as the strongly preferred in silico analyses have proposed (91) (Fig. 4).

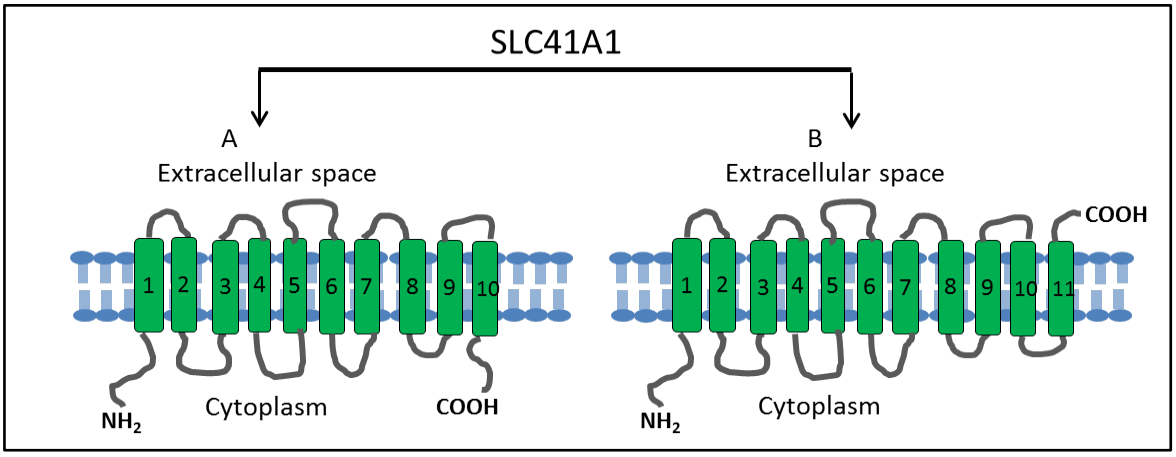

Figure 4. Computer model of hSLC41A1 (56kDa): The two membrane topology models of SLC41A1 constructed according to the available peer-reviewed bibliography; **A**, 10 TM domains model (82, 91); **B**, 11 TM domains model by Mandt et al. (88).

Finally, some recent studies conducted on SLC41A1 showed that its transcript is upregulated in the renal cortex of hypomagnesemic mice and that it mediates electrogenic transport of Mg^{2+} in *Xenopus* oocytes expressing the heterologous protein, thus suggesting that it acts as a channel or channel-like Mg^{2+} uptake system (86). These data could not be confirmed in mammalian HEK293 cells, where SLC41A1 rather mediated Mg^{2+} extrusion.

Final evidence for the nature of SLC41A1 function came from mag-fura 2-assisted measurements of the free intracellular Mg^{2+} concentration ($[Mg^{2+}]_i$): HEK293 cells overexpressing SLC41A1 exhibited a significant decrease of $[Mg^{2+}]_i$ when transferred from a high Mg^{2+}-containing buffer (10 mM) to completely Mg^{2+}-free buffer (4). The efflux capacity of SLC41A1 was strongly dependent on extracellular Na^+. These findings strongly argue for SLC41A1 to act as Na^+/Mg^{2+} exchanger, thereby, representing the main Mg^{2+} extrusion system in mammalian cells.

*h*SLC41A1 is ubiquitously expressed suggesting its important role in cell, tissue, and organ physiology, but the highest levels were found in heart, testis, adrenal and thyroid glands, prostate and ovaries, and lower expression levels were observed in all other tested tissues (82).

Since several lines of evidence point to an involvement of a disturbed Mg^{2+} status in many human disorders and because SLC41A1 is the only known mechanism responsible for Mg^{2+} extrusion from eukaryotic cells, the here-presented studies aimed at a further characterization of SLC41A1 in order to achieve a better understanding of the molecular basis of hypomagnesaemia observed in some disease states.

Currently, several experimental evidences suggest that a disturbed Mg^{2+} status might contribute to the development of preeclampsia. Because a recently published study shows that a lowered

Mg^{2+} intake in mice leads to the overexpression of genes involved in Mg^{2+} transport or homeostasis (7), the expression profile of magnesium responsive genes (MRGs) has been examined in placentas of normoevolutive and preeclamptic women, as preeclampsia is often associated to hypomagnaesemia (6). Among all the tested MRGs, only SLC41A1 was found to be significantly overexpressed in several preeclamptic placentas and therefore it might be the cause of the hypomagnesaemia and the increased local sodium concentration often observed in preeclamptic women (6). This implies that Mg^{2+} might represent an effective treatment of preeclampsia but also that a change in Mg^{2+} homeostasis may contribute to the development of the disease.

The deficiency of magnesium and/or altered IMH have been associated with neurodegenerative, neurological and psychiatric disorders like AD (92), PD (93, 94), stroke (95), aggressive behavior (96) and hyperactivity (97). In particular, there are clinical evidences showing that a low Mg^{2+} intake increases the risk of idiopathic PD (98) and that PD patients have a decreased concentration of free cytosolic Mg^{2+} in the occipital lobes compared with healthy subjects (99).

Although Mg^{2+} intake seems to have beneficial effects in the prevention of PD and/or the deceleration of PD progression, the molecular link between Mg^{2+} and PD pathophysiology has remained obscure until the recent discovery that the Na^{+}/ Mg^{2+} exchanger SLC41A1 is localized in the newly identified PD locus PARK 16 (100-103). Because the amino acid substitution p.A350V of SLC41A1 has been found in one PD patient of Caucasian origin (103), one of the questions of this study has been whether the mutation has an effect on the protein function and therefore a clinical relevance. The results characterized the mutation as a gain-of-function mutation, responsible for an enhanced Mg^{2+} efflux compared with wild type SLC41A1, which might eventually lead to a chronic intracellular Mg^{2+}-deficiency, a condition found in various brain regions of PD patients (90).

Finally magnesium is essential for insulin production, its release and also for insulin signalling (1). Intracellular- and extracellular magnesium deficiency is known as a common complication of chronic stable, mild type 2 *diabetes* (104).

It was already well known that the main mechanism responsible for the Mg^{2+} efflux from the cells is the Na^{+}/Mg^{2+} exchanger (NME) SLC41A1, which is activated via cAMP-dependent PKA-mediated phosphorylation (89), and that insulin activates a downstream cascade (IR-PI3K-PDE3b pathway) which eventually leads to the inhibition of PKA. Therefore, a second question of the project regarding SLC41A1 was whether insulin and various inhibitors, acting on the downstream cascade of the insulin receptor, might have an effect on SLC41A1 activity in vitro.

From the obtained results it has been established that the Na^{+}-dependent Mg^{2+} efflux conducted by SLC41A1 is modulated by insulin which causes a decrease of PKA activity and a subsequent decrease of SLC41A1-mediated Mg^{2+} efflux. However, when the downstream pathway of insulin

signaling is blocked, SLC41A1 efflux ability is not affected. Therefore, it can be speculated that insulin acts as an essential regulator of intracellular magnesium homeostasis. By blocking the Mg^{2+} efflux, it might protect cells from an excessive Mg^{2+} loss and therefore from hypomagnesaemia often observed in diabetes patients.
Taken together, these results support the importance of a balanced Mg^{2+} intake and Mg^{2+} supplementation in several human ailments and the experimental data of this thesis suggest SLC41A1 as a new molecular target to focus on for the prevention of the consequences of disease-associated hypomagnesaemia.

2.4.2. SLC41A3

Member A3 of the SLC41 family has been initially characterized as a rather unspecific Mg^{2+} transporter. Human *SLC41A3* (also called *FLJ20473*, *SLC41A1-L2*, *SLC41A1-like 2*) has been mapped to chromosome 3q21.2-q21.3 and 7 isoforms are predicted to be produced by alternative splicing. The full-length protein (isoform 1) encodes a 507 aa protein with a molecular weight of 54.7 kDa. A significantly high similarity of 71% is found between the most conserved sequence stretch (amino-acid residues138–499) of SLC41A1 and SLC41A3 (82). SLC41A3 has never been investigated in detail, but a structural comparison with the other SLC41 family members has suggested that it consists of eleven TM domains (88), two MgtE-like regions (105–240 and 318–456), one phosphorylation site in position 275, one peroxidase active-site signature (426–437) and one poly-Leu region (378–381).
Two-electrode voltage clamp experiments revealed Mg^{2+}-evoked currents in *Xenopus laevis* oocytes heterologously overexpressing SLC41A3. The SLC41A3-mediated Mg^{2+} currents were saturable and the affinity was calculated to be 1.5 mM (7). Although the protein is also permeable to other divalent cations, indicating low substrate specificity (Quamme, unpublished data), it seems to be primarily a Mg^{2+} transporter, because it mediates Mg^{2+} flux in the concentration range normally found in extracellular and intracellular fluids, as reflected by the K_m value.
Recently SLC41A1 has been extensively characterized as Na^+/ Mg^{2+} exchanger in the plasma membrane; therefore, it is likely that the highly homologous protein SLC41A3 could have a similar function. Since SLC41A1 and SLC41A2 are not differentially regulated in the DCT, de Baaij et al, (105) proposed SLC41A3 as being a DCT-specific Mg^{2+} extrusion mechanism. Indeed by comparing distal convolute tubule expression profiles of mice fed high or low Mg^{2+}-containing diets, they identified SLC41A3 as Mg^{2+}-sensitive DCT gene (105). Furthermore, a study using real-time quantitative PCR showed that the level of *SLC41A3* mRNA expression in mice increases with decreasing $[Mg^{2+}]_i$ (7).

There are no peer-reviewed publications reporting data on the expression pattern of SLC41A3 in different tissues, but according to the Human Protein Atlas (www.proteinatlas.org), the expression pattern of SLC41A3 is quite different from the other two members of the SLC41 family. SLC41A1 and A2 are equally distributed in most tissues and organs; instead, SLC41A3 expression seems to be restricted to certain tissues and cell types. The highest levels are found throughout the central nervous system, in particular neuronal cells of the cerebral cortex, the hippocampus, lateral ventricle, as well as most cell types of the cerebellum; moderate levels are found in most cell types of the digestive tract and the male reproductive system; weak or absent expression was detected in skin, soft tissues and tissues of the immune system (except for hematopoietic cells of the bone marrow which showed high levels of SLC41A3).

The high expression levels in the central nervous system are in line with the observations in a conditional SLC41A3 knockout mouse line (*Slc41a3*$^{tm1a(KOMP)Wtsi}$) created by the International Knockout Mouse Consortium, which exhibits exclusively neurological/behavioral abnormalities, in particular abnormal locomotor coordination including ataxia.

Finally computational analysis predicted SLC41A3 to be primarily targeted to the cytoplasmic membrane (7); however, the present thesis has evaluated the cellular localization of SLC41A3 and shows that it is mainly a mitochondrial protein responsible for the Mg^{2+} extrusion from mitochondria and that the mitochondrial Mg^{2+} efflux is Na^{+}-dependent or, at least, regulated by Na^{+}.

The computer-predicted model (TMpred) proposes 11 TM domains for SLC41A3 with an extracellular N-terminus and a cytoplasmic C-terminus (106) (Fig. 5). However, so far there is no experimental evidence about the number of TM domains and the orientation of N- and C-termini.

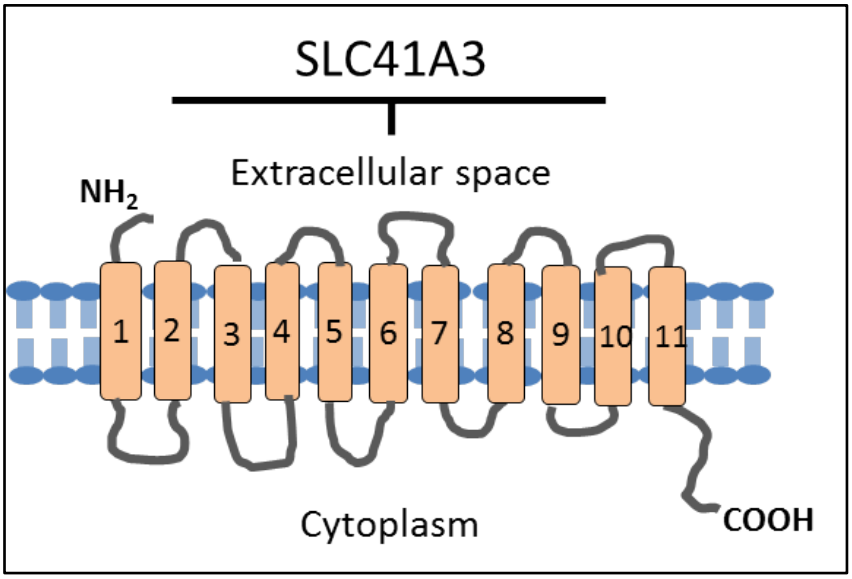

Figure 5. Computer-predicted model (TMpred) of SLC41A3 topology (106): the most probable computer predicted model of SLC41A3 membrane topology, with 11 TM and an extracellular N-terminus and cytoplasmic C-terminus

2.5. CNNM2

CNNM2 has been mapped to chromosome 10q24.32. It is ubiquitously expressed, but the highest levels are found in the brain, placenta and renal TAL and DCT, which are the kidney regions where most of the Mg^{2+} is reabsorbed (8). Originally called ACDP2 (ancient conserved domain protein 2), the protein has later been termed CNNM2 because of its sequence homology and structural similarity with the cyclins, although *in vivo* it doesn't have any cyclin function.

The gene encodes a protein with molecular weight of approximately 97 kDa (*phosphosite.org*). Computer predictions suggested the presence of 4 or 5 transmembrane helices with an extracellular C-terminus (107). Various splicing variants have been identified (3), among them variant 1 and 2 (I1 and I2), which are highly similar and they both contain 2 CBS domains (InterPro 000644), which seem to be essential for intramolecular dimerization (108). However, in complementation tests in *Salmonella enterica sv. Typhimurium* (strain MM281), the two variants demonstrated functional disparity: only the I1 was capable of transporting Mg^{2+}, therefore, complementing the Mg^{2+}-deficient phenotype of strain MM281 (3). Goytain and Quamme (8) demonstrated that only the transient overexpression of I1 in *Xenopus* oocytes was responsible for an electrogenic transport of Mg^{2+}. Interestingly, CNNM2-related Mg^{2+} transport, seen in a heterologous expression system (8), was not confirmed in a homologous expression system (63).

Isoform1 represents the full-length protein (875aa), while I2 lacks the exon 6, which might be crucial for Mg^{2+} binding, for the Mg^{2+} binding site assembly or for the determination of the operation mode.

Recently mutations and sequence variants of CNNM2 have been associated to various pathological conditions. In particular, some sequence variations increase the risk of hypertension and alter the serum Mg^{2+} levels (109). A genome-wide association study established a link between CNNM2 and susceptibility to ischemic stroke and coronary artery disease (110). In addition, the single nucleotide polymorphism (SNP) rs7914558 localized in one CNNM2 intron has been characterized as schizophrenia risk variant (111, 112).

Finally, two mutations in CNNM2 were found in individuals of two unrelated families affected by dominant hypomagnesaemia (63). In detail, a frame-shift mutation which leads to a truncated protein and a missense mutation which causes the substitution p.T568I in a region called ACD (ancient conserved domain), where the CBS domains are located (Fig. 6). This missense mutation impairs the protein function because it alters ATP binding to the CBS domains, but it doesn't induce any change in the protein localization on the kidney basolateral membrane according to Stuiver et al (63) (Fig. 6).

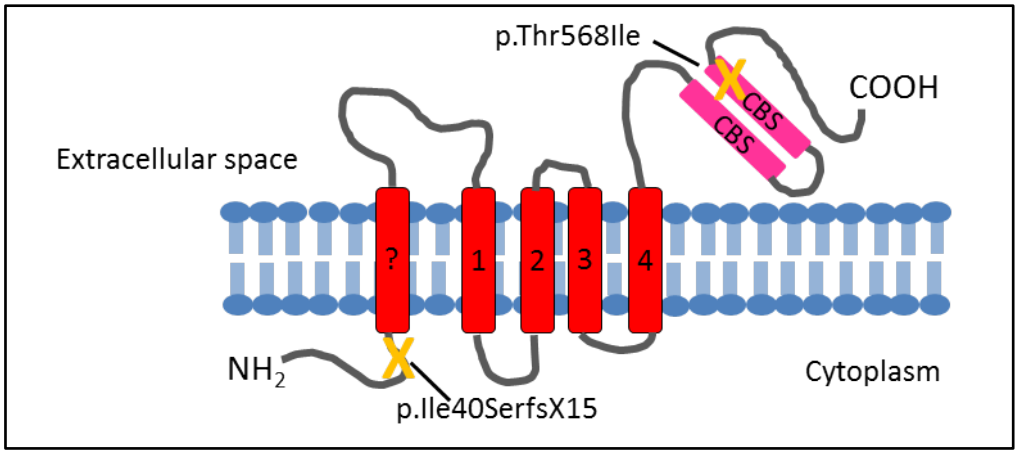

Figure 6. Localization of the mutations in the predicted secondary structure of CNNM2: The predicted transmembrane domains are indicated in red and the CBS domains in pink. The ancient conserved domain is boxed and the mutations associated to hypomagnesaemia are indicated with a yellow cross. (63)

From these data it can be extrapolated that CNNM2 plays a crucial role in the intracellular Mg^{2+} homeostasis, mediating the epithelial transport and the renal reabsorption. Originally CNNM2 was proposed to be a Mg^{2+} transporter (3, 8) and it was found to be overexpressed in mice fed with a low-Mg^{2+} diet (8), but Stuiver and colleagues (63) speculated that CNNM2 senses the

intracellular Mg^{2+} concentration and regulates the activity of other transporters rather than being a Mg^{2+} transporter itself.

Recently De Baaij et al. (113) examined the pathways of CNNM2 maturation and post-translational modification, proposing that a peptidase cleaves a 64 amino acid N-terminal signal peptide in the endoplasmic reticulum. According to this model, the mature protein possesses three TM helices with an extracellular N-terminus and intracellular C-terminus. Further *in silico* analysis of the protein sequence showed that the second TM domain is the shortest and less hydrophobic and it might represent a reentrant loop (Fig. 7).

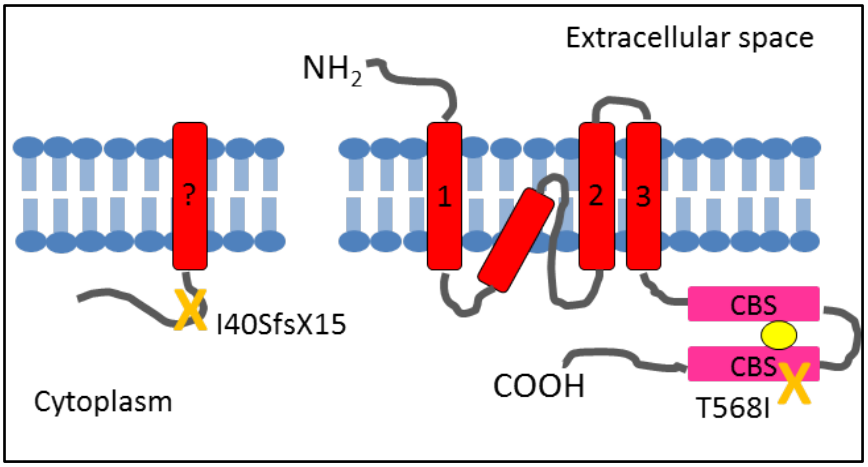

Figure 7. Schematic model of the structure of CNNM2 after endoplasmic processing: The model illustrates the structure of the CNNM2 protein at the plasma membrane and shows the signal peptide cleavage in the endoplasmic reticulum. *Crosses* represent the locations of the two mutations found in individuals with hypomagnesaemia. The TM are represented in red, the CBS domains are represented in the pink box and the binding ATP is illustrated as the yellow circle (113)

The data obtained during the present study support the hypothesis of De Baaij et al., who proposed the cleavage of the N-terminal flanking region and the first transmembrane helix (113). Indeed when Western blot was performed with an antibody directed against the Strep-tagged N-terminus, only a faint signal corresponding to CNNM2 was detected and this can be explained only with the loss of the N-terminal region carrying the Strep-tag.

Based on the above-mentioned evidence that links CNNM2 to impaired IMH, on the broad knowledge that magnesium significantly influences incidence, development, and course of *diabetes mellitus* type 2 and on a previous study (114) showing CNNM2 as being overexpressed in diabetic patients, a further question of the present thesis was whether the expression of CNNM2 is dependent on the extracellular Mg^{2+} concentrations. Its transcript levels have been therefore examined *in vitro* in JVM-13 (lymphoblasts) and Jurkatt (T-lymphocytes) cells after 48 hours of Mg^{2+} starvation and resulted in overexpression in both cells lines tested.

Furthermore, the role of both CNNM2 variants was evaluated in Mg^{2+} transport and the results clearly revealed that I1 and I2 do not transport Mg^{2+} in an electrogenic nor in an electroneutral mode. This is in accordance with the observation that overexpression of both variants in HEK293 cells does not influence total magnesium in correlation with extracellular magnesium concentration.

Based on these results and on the work of Stuiver (63), who associated a mutation in CNNM2 with dominant hypomagnesaemia and suggested an involvement of CNNM2 in IMH, it can be assumed that CNNM2 in human cells is not a Mg^{2+} transporter per se but it might represent the first identified magnesium homeostatic factor.

3. AIMS AND OBJECTIVES OF THE THESIS

Magnesium plays an essential role in all cells: it interacts with polyphosphate compounds such as ATP, DNA and RNA, it is required as cofactor for more than 300 enzymes which regulate central or crucial biochemical reactions in the body, including protein synthesis, muscle and nerve function and blood glucose control (115, 116). Furthermore, magnesium helps to build bones, it is essential for energy production, oxidative phosphorylation, glycolysis and calcium and potassium transport across cell membranes (115).

It is widely known that low intakes of magnesium induce changes in biochemical pathways that can lead to disease conditions over time. A magnesium deficiency is for example associated with hypertension and cardiovascular disease, type 2 diabetes, osteoporosis and migraine.

Over the last decades many studies have been published supporting magnesium's benefits for health, indeed it has been shown to have therapeutic value in treating headaches, chronic pain, asthma, sleep disorders and in reducing the incidence of some conditions such as heart disease, hypertension and diabetes (117-119).

The main goal of this work has been the molecular and physiological characterization of three MRGs, namely SLC41A1, SLC41A3 and CNNM2. By investigating the effects of insulin on SLC41A1-mediated Mg^{2+} efflux and the way of functioning of SLC41A3 and CNNM2, the present thesis provides a comprehensive approach on Mg^{2+} transport across the plasma membrane and between the internal stores in association with some common human ailments.

The main objectives of this work were:

1) To further investigate the role of SLC41A1 and Mg^{2+} efflux in relation to human ailments such as PD and diabetes, because this protein has been previously described by Kolisek et al as the only Mg^{2+} efflux system in eukaryotic cells (5) and has been related, from the same group, to pre-eclampsia, a common disorder of pregnancy (6).
2) To describe the molecular and physiological role of SLC41A3. This protein shows high similarity to SLC41A1 and it is a distant homologue of the prokaryotic Mg^{2+} transporter MgtE. It has therefore been suggested to be involved in magnesium transport but so far no study has described its cellular role or localization.
3) To better characterize CNNM2 because two mutations of this gene had been associated to dominant familial hypomagnesaemia (63) but its function in the cell and its involvement in the Mg^{2+} transport has not yet been elucidated.

4. RESULTS

4.1. Publication I

Nature of SLC41A1 complexes: report on split-ubiquitin yeast two hybrid assay

This chapter has been published in: *Magnesium Research*
2013 Apr-Jun;26(2):56-66. doi: 10.1684/mrh.2013.0339.

Axel Nestler, Gerhard Sponder, Katrin Rutschmann, **Lucia Mastrototaro**, Christoph Weise, Juergen Vormann, Monika Schweigel-Röntgen, Martin Kolisek

You have to read this part online (free of charge).
DOI: http://dx.doi.org/10.1684/mrh.2013.0339

4.2. Publication II

Substitution p.A350V in Na^+/Mg^{2+} exchanger SLC41A1, potentially associated with Parkinson's disease, is a gain-of-function mutation

This chapter has been published in: *PLoS One*
2013 Aug 15;8(8):e71096. doi: 10.1371/journal.pone.0071096. eCollection 2013.

Martin Kolisek, Gerhard Sponder, **Lucia Mastrototaro**, Alina Smorodchenko, Pierre Launay, Juergen Vormann, Monika Schweigel-Röntgen

OPEN ACCESS Freely available online

PLOS ONE

Substitution p.A350V in Na^+/Mg^{2+} Exchanger SLC41A1, Potentially Associated with Parkinson's Disease, Is a Gain-of-Function Mutation

Martin Kolisek[1]*, Gerhard Sponder[1], Lucia Mastrototaro[1], Alina Smorodchenko[2], Pierre Launay[3], Juergen Vormann[4], Monika Schweigel-Röntgen[5]*

1 Institute of Veterinary-Physiology, Free University Berlin, Berlin, Germany, **2** Institute of Physiology, Pathophysiology and Biophysics, University of Veterinary Medicine, Vienna, Austria, **3** INSERM, U699, Paris, France, **4** Institute of Prevention and Nutrition, Ismaning, Germany, **5** Institute for Nutritional Physiology "Oskar Kellner", Leibniz Institute for Farm Animal Biology, Dummerstorf, Germany

Abstract

Parkinson's disease (PD) is a complex multifactorial ailment predetermined by the interplay of various environmental and genetic factors. Systemic and intracellular magnesium (Mg) deficiency has long been suspected to contribute to the development and progress of PD and other neurodegenerative diseases. However, the molecular background is unknown. Interestingly, gene *SLC41A1* located in the novel PD locus *PARK16* has recently been identified as being a Na^+/Mg^{2+} exchanger (NME, Mg^{2+} efflux system), a key component of cellular magnesium homeostasis. Here, we demonstrate that the substitution p.A350V potentially associated with PD is a gain-of-function mutation that enhances a core function of SLC41A1, namely Na^+-dependent Mg^{2+} efflux by 69±10% under our experimental conditions (10-minute incubation in high-Na^+ (145 mM) and completely Mg^{2+}-free medium). The increased efflux capacity is accompanied by an insensitivity of mutant NME to cAMP stimulation suggesting disturbed hormonal regulation and leads to a reduced proliferation rate in p.A350V compared with wt cells. We hypothesize that enhanced Mg^{2+}-efflux conducted by SLC41A1 variant p.A350V might result, in the long-term, in chronic intracellular Mg^{2+}-deficiency, a condition that is found in various brain regions of PD patients and that exacerbates processes triggering neuronal damage.

Citation: Kolisek M, Sponder G, Mastrototaro L, Smorodchenko A, Launay P, et al. (2013) Substitution p.A350V in Na^+/Mg^{2+} Exchanger SLC41A1, Potentially Associated with Parkinson's Disease, Is a Gain-of-Function Mutation. PLoS ONE 8(8): e71096. doi:10.1371/journal.pone.0071096

Editor: Mark R. Cookson, National Institutes of Health, United States of America

Received March 21, 2013; **Accepted** June 24, 2013; **Published** August 15, 2013

Funding: This work was supported by a research grant from the German Research Foundation (DFG), KO-3586/3-1 and KO-3586/3-2 to MK. The funders had no role in study design, data collection and analysis, decision to publish, or preparation of the manuscript.

Competing Interests: MK, JV & MSR are discoverers on the patent application based on the data presented in this manuscript. It is currently submitted for a patent search by IPA-MV AG (no number assigned yet). Responsible Inovations-manager Mr. Tobias Parikh (T.Parikh@pva-mv.de). Dr. Mandana Rezwan (Dualsystems Biotech AG) co-operated with the construction of the cell lines for this study. There are no further patents, products in development or marketed products to declare. This does not alter the authors' adherence to all the PLOS ONE policies on sharing data and materials, as detailed online in the guide for authors.

* E-mail: martink@zedat.fu-berlin.de (MK); roentgen@fbn-dummerstorf.de (MSR)

Introduction

The crucial role of magnesium (Mg) in normal cellular physiology has been described in many reports. Thus, unsurprisingly, Mg^{2+} deficiency and/or changed intracellular Mg homeostasis (IMH) has been associated with a multitude of serious ailments among them neurodegenerative, neurological, and psychiatric disorders such as Alzheimer's disease (AD) [1], stroke [2], aggressive behavior [3], increased stress sensitivity [4], and hyperactivity [5]. In particular, several studies have suggested an association between a disturbed IMH and the incidence of Parkinsons disease (PD) [6,7,8], a chronic, progressive, neurodegenerative disorder of the motor system mainly characterized by the degeneration of neurons in the *substantia nigra pars compacta* and the formation of Lewy bodies [9,10]. PD is estimated to affect ~1% of people over 60 years of age or ~0.3% of the entire population in industrialized countries [11,12]. Oyanagi and colleagues [13,14] have shown that continuous low Mg intake for two generations induces exclusive loss of dopaminergic neurons in rats. In agreement with previous data, the results of a study conducted among the population of Guam [15] and of a more recent case control study in Sweden [6] demonstrate that low Mg intake is linked to an increased risk of idiopathic PD. By means of phosphorus magnetic resonance spectroscopy (^{31}P-MRS), Barbiroli and colleagues [16] have demonstrated a significantly increased content of inorganic phosphate accompanied by a decreased concentration of free cytosolic Mg^{2+} ($[Mg^{2+}]_i$) in the occipital lobes of PD patients compared with healthy subjects. On the other hand, Mg has been shown to decrease negative interactions between environmental (herbicides) and molecular factors (α-synuclein) that are known to be involved in PD pathophysiology [17]. Moreover, Hashimoto and colleagues [18] have reported the significant preventive effects of Mg against 1-methyl-4-phenylpyridinium (MPP+) toxicity [19] to dopaminergic neurons.

Although these studies have demonstrated a beneficial effect of sufficient Mg intake for PD prevention and/or the deceleration of PD progression in patients, and despite an obvious link between IMH and PD pathophysiology, the underlying mechanism(s) has (have) remained elusive until now. However, the recent discovery of SLC41A1 as a Na^+/Mg^{2+} exchanger (NME; Mg^{2+}-efflux

system) [20] and its localization within the newly identified PD locus *PARK16* [21,22,23,24] makes this protein an interesting candidate to explain the involvement of disturbed intracellular Mg^{2+} homeostasis in PD pathophysiology.

Human *SLC41A1* has been mapped to chromosome 1q31-32 and encodes a protein consisting of 513 amino acids having a molecular mass of 56 kDa [25]. Its 5-kb transcript has been detected in most of the tested tissues in humans and mice (notably in heart, muscle, testis, thyroid gland, and kidney) [25,26]. SLC41A1 has been characterized as an integral protein that is located in the cytoplasmic membrane [27] and that possesses 10 (strongly preferred computer-predicted model) or 11 transmembrane domains [28] with the N-terminus being oriented intracellularly [27,28]. SLC41A1 has also been demonstrated to form hetero-oligomeric complexes. However, the identities of its binding partners and their relevance for the normal NME function of SLC41A1 *in vivo* remain uncertain [27].

The evidence for NME being involved in PD etiology has further been strengthened by the identification of PD-specific SLC41A1 variants (c.436A>G resulting in p.K146E; c.1440A>G resulting in p.P480P; and c.552+50G>A) in the Chinese population [24] and of the variant of SLC41A1 carrying the amino acid substitution p.A350V (c.1049C>T) in one PD patient of Caucasian origin [23]. Noteworthy is also the fact that *SLC41A3*, also a member of the SLC41 family, when knocked-out in mice displayed abnormal locomotor coordination (www.knockoutmouse.org; [29]).

Furthermore, the null mutation c.698G>T resulting in skipping of exon 6 of SLC41A1 (an in-frame deletion of a transmembrane helix) has been associated with a nephronophthisis-like phenotype (NPHP), therefore, suggesting that the disturbed renal Mg^{2+} homeostasis may lead to tubular defects that result in a phenotype similar to NPHP [30]. Also, SLC41A1 has been found to be over-expressed in preeclamptic placental samples with an approximately five times higher frequency than in normoevolutive placental samples [31].

In this study, we have mainly examined the effect of the substitution p.A350V potentially related to PD on the performance of the Na^+/Mg^{2+} exchanger SLC41A1. Our findings show that the substitution p.A350V in SLC41A1 is a gain-of-function mutation leading to increased Mg^{2+} extrusion from the cell.

Materials and Methods

HEK293-derived cell lines/growth media and culture conditions

Tetracycline-inducible HEK293-(HA-strep-SLC41A1) and HEK293-(HA-strep-SLC41A1-p.A350V) were constructed in co-operation with Dualsystems Biotech AG. Briefly, full-length human wild-type (wt) and point-mutation-carrying *SLC41A1* cDNA was cloned into p*NTGSH* vector (Dualsystems Biotech AG) with an N-terminal HA-strep tag. Point mutation c.1049C>T (p.A350V) was introduced by PCR-site-directed mutagenesis [32]. Introduction of the mutation was confirmed by bidirectional sequencing. The obtained p*NTGSH-HA-strep-SLC41A1* and p*NTGSH-HA-strep-SLC41A1-c.1049C>T* were separately electroporated into the Flp-In™ T-REx™ HEK293 cell line (Invitrogen). Cells were placed under hygromycin selection; hygromycin-resistant clones were screened for tet-inducible expression of the wt or mutated (p.A350V) HA-strep-tagged SLC41A1. Protein expression was induced by the addition of tetracycline (1 $\mu g.ml^{-1}$) for 24 hours.

HEK293-(HA-strep-SLC41A1) and HEK293-(HA-strep-SLC41A1-p.A350V) cells were cultured in Dulbecco's modified Eagle's medium (PAN Biotech) containing 10% fetal bovine serum (PAN Biotech), 4.5 $g.l^{-1}$ glucose (Sigma-Aldrich), 2 mM glutamine (PAN Biotech), PenStrep (PAN Biotech), Normocin™ (0.1 $mg.ml^{-1}$, Cayla), blasticidin (15 $\mu g.ml^{-1}$, Cayla), and hygromycin (0.1 $mg.ml^{-1}$, Cayla).

The preparation (cloning protocol) and culture conditions of tetracycline-inducible HEK293-(flag-SLC41A1) were as previously described [20,27].

Cell survival assay

HEK293 cells inducibly over-expressing wt or the p.A350V variant were grown to approximately 80% confluency, rinsed twice with PBS (PAN Biotech) and provided with fresh culture medium. Cell viability was determined, with a TC10 automated cell counter (BioRad), at 0 h and 24 h from the beginning of the induction.

Quantitative real time PCR

To determine the transcription activity of both transgenic variants of *SLC41A1*, namely *wt* and *c.1049C>T*, by the quantitative real time PCR (q-RT-PCR) method in induced (+tet) and non-induced (-tet) cells, we used the following primers: *hSLC41A1fw*, 5′-TTGGACGCTCGCCTTGCCTG-3′ and *hSLC41A1rev*, 5′-TGGTGTGGAACACCTGCGCC-3′. Expression activities of *SLC41A2* and *SLC41A3* were determined with following primer pairs: *hSLC41A2fw*, 5′-TGGTTATAAGTAG-CATTGGGGGCCT-3′ and *hSLC41A2rev*, 5′-TCCTGCTAGCCTGAATGGCCA -3′; *hSLC41A3fw*, 5′-CA-CAAAGATAGTCGGTATCTGACG-3′and *hSLC41A3rev*, 5′-GACCATGGCCAGGATGATT-3′. Total RNA isolation, the determination of its integrity, purity, and quantity, cDNA synthesis, and q-RT-PCR were performed as described by Kolisek and colleagues [20]. Data were evaluated with software application FK-Wolf-01, developed by Katharina Wolf (FU Berlin). Statistical evaluation was performed with data sets acquired from three biological preparations for each condition loaded in triplicate.

Protein detection in tet-inducible HEK293 cell lines

HEK293 cells, over-expressing flag- or HA-strep-tagged wt or p.A350V, and the respective uninduced controls were lysed with RIPA buffer for 30 min. Centrifugation was performed to pellet unsolubilized material (14000 rpm, 30 min, 4°C). The total protein concentration was determined with the Bradford protein assay (Biorad). For the flag-tagged wt variant, samples containing 10 µg total protein and, for the HA-strep-tagged wild-type variant and the p.A350V mutant, 30 µg total protein were run on a 10% SDS-polyacrylamide gel and transferred to a polyvinylidene difluoride (PVDF) membrane. Immunoblotting was performed in TBS-TWEEN plus 2.5% dry milk with antibodies against the flag-tag (HRP-conjugated anti-flag M2, Sigma-Aldrich) and the strep-tag (Qiagen). Anti-mouse IgG linked to horseradish peroxidase (HRP; Cell Signaling Technology) was used as the secondary antibody for the anti-strep antibody. The antibody against RPL19 (Abnova), together with the anti-mouse secondary antibody stated above, was used to detect the loading control. Proteins were visualized by use of the SuperSignal™ West Dura system (Pierce). Image J software (http://rsb.info.nih.gov/ij/) was used for the densitometric analyses.

Membrane protein enrichment

The ProteoExtract™ native membrane protein extraction kit (Calbiochem) was used to extract and enrich membrane proteins

from HEK293 cell lines over-expressing wt or p.A350V according to the manufacturer's protocol. Proteins (25 μg) were separated on a 10% SDS-polyacrylamide gel. Immunoblotting was performed as previously described. The soluble protein RPL19 was used to control the specificity of the separation between soluble and membrane proteins.

Subcellular fractionation of proteins

For fractionation of proteins according to their subcellular localization, we used the Qproteome cell compartment kit (Qiagen). Wt or p.A350V cells were induced or left untreated. Cells (4×10^6) were processed according to the manufacturer's protocol. The obtained fractions (cytosolic, membrane, nuclear, and cytoskeletal) were electroseparated on an 8.5% SDS-polyacrylamide gel, and SLC41A1 variants were immuno-detected as described previously. As a control for the specificity of the fractionation, parallel blots were run and probed with antibodies against RPL19 (cytosolic fraction), PMCA4 (membrane fraction; Sigma-Aldrich), or Lamin A (nuclear fraction; Sigma-Aldrich). Mouse secondary antibody conjugated to HRP (Cell Signaling Technology) was used for RPL19 and PMCA4, and an HRP-coupled rabbit antibody was used for Lamin A (Cell Signaling Technology).

Determination of the phosphorylation status of wt and p.A350V variant

The PhosphoProtein Purification Kit (Qiagen) was used according to the manufacturer's instructions. 1.5×10^7 cells of the stably transfected HEK293 cell lines expressing strep- or flag-tagged wt or strep-tagged variant p.A350V (HA-Strep-tagged) were used as starting material. 2.5 mg of total protein was used for the affinity purification of phosphorylated proteins. Flow through (unphosphorylated proteins) and elution fractions (phosphorylated proteins) were precipitated with 8% (weight/volume) trichloroacetic acid and washed once with acetone. The pellets were dissolved in 0.1 M Tris.HCl buffer containing 2 M urea. Proteins were separated on a 10% SDS-polyacrylamide gel, transferred to a PVDF membrane and immunostained with a primary anti-strep antibody and a secondary HRP-coupled mouse antibody. For the flag-tagged cell line M2 antibody was used. To detect the phosphorylated form of Akt, the phospho-akt (Ser473) primary antibody (Cell Signaling Technology) and the secondary mouse antibody were used. Images were acquired with the BioRad ChemiDoc™ MP System (BioRad).

Blue native electrophoresis and Western blot analysis of SLC41A1- and SLC41A1 p.A350V-protein complexes

Samples containing 10 and 20 μg of strep-affinity purified proteins (IBA & Qiagen) were loaded onto a native 5–18% polyacrylamide gradient gel, and blue native electrophoresis was performed according to Schägger and Jagow [33]. Electroseparated proteins were transferred to a PVDF membrane. Wt and p.A350V protein complexes were immuno-detected as described previously. NativeMark™ unstained protein standard (Invitrogen) was used as size marker.

Confocal Microscopy

Specimens were prepared according to Kolisek and coworkers [27] except that, for fixation and permeabilization, we used methanol-acetone, and blocking was performed with 10% goat serum. For detection of strep-tagged wt and p.A350V, we used a primary anti-strep antibody (diluted 1:500; Qiagen). The Alexa Fluor-647-conjugated WGA (Invitrogen) was used as a cell membrane marker. Processed samples were mounted with Fluoroshield-DAPI (abcam). Confocal images were taken with a Confocal Laser Scanning Microscope LSM 510 META (Carl Zeiss) equipped with a 63x oil-immersion objective. For the excitation of Alexa-488, Alexa-647, and DAPI, an argon-ion laser (488 nm), helium-neon laser (647 nm), and blue diode laser (405 nm) were used respectively. Image J software (http://rsb.info.nih.gov/ij/) was used for the image merging and correction, as well as to quantify the percentage of co-localization.

Determination of free intracellular Mg^{2+} by mag-fura 2 FF-Spectrofluorometry

The -tet and +tet wt and *p.A350V* cells were rinsed twice with ice-cold, completely divalent-free, Dulbecco's phosphate-buffered saline (DPBS), detached by HyQtase, centrifuged, washed twice in completely Ca^{2+}- and Mg^{2+}-free Hank's balanced solution (CMF-HBS) supplemented with 10 mM HEPES and 1.36 mM L-glutamine (CMF-HBS+), and finally resuspended in the same solution. Then, the cells were loaded with 7.5 μM mag-fura 2-AM (30 min, 37°C) in the presence of the loading-facilitator Pluronic F-127 (both from Life Technologies/Molecular Probes). After being washed in CMF-HBS+, cells were incubated for a further 30 min at 37°C to allow for the complete de-esterification of the fluorescence probe, washed twice in CMF-HBS+ to remove extracellular mag-fura 2 and stored in CMF-HBS supplemented with 10 mM HEPES, 5 mM glucose, and 0.4 mM Mg^{2+} until the start of the experiments. Directly before measurements, all cells were Mg^{2+}-loaded by a 20-min pre-incubation in CMF-HBS+ supplemented with 10 mM Mg^{2+} (influx conditions; $[Mg^{2+}]_e >> [Mg^{2+}]_i$). Then, after the remaining extracellular Mg^{2+} had been washed out by rinses in CMF-HBS+, the $[Mg^{2+}]_i$ of cells was continuously determined for 10 min in CMF-HBS+ (efflux conditions in which $[Mg^{2+}]_i >> [Mg^{2+}]_e = 0$ mM; $[Na^+]_i << [Na^+]_e = 145$ mM); CMF-HBS+ supplemented with 5 mM Mg^{2+}; or CMF-HBS+ supplemented with 10 mM Mg^{2+}. Differentiation of NME from other transport components was performed by means of the NME inhibitor imipramine (250 μM) [20] or the NME stimulator dB-cAMP (100 μM) [20,34].

Measurements were performed at 37°C in 3 ml cuvettes containing 2 ml cell suspension (cytocrit: 10%) while being stirred in a spectrofluorometer LS50-B (PerkinElmer) [20,27]. $[Mg^{2+}]_i$ values were calculated from the 340 to 380 nm ratio according to the formula of Grynkiewicz *et al.* [35] and as described in Kolisek *et al.* [20,27]. SLC41A1-dependent Mg^{2+} extrusion from induced SLC41A1 (wt) and p.A350V cells was determined from the $[Mg^{2+}]_i$ changes observed in Mg^{2+}-loaded cells during recovery in CMF-HBS+ solution and calculated by subtracting the respective values of uninduced cells.

If not otherwise stated, data are presented as means ± SE. All statistical calculations were performed with Sigma-Stat (Jandel Scientific). Significance was determined by Student's *t*-test or Mann-Whitney rank sum test as appropriate; $P\leq0.05$ was considered to be significant.

Impedance-based measurement of cell adhesion and proliferation

The xCELLigence system (RTCA-SP, ACEA Biosciences Inc.) was used according to the manufacturer's instructions for the continuous real-time monitoring of cell adhesion and proliferation by cell-electrode impedance [36] displayed as the dimensionless Cell Index (CI). By using the RTCA Analyser, electrical impedance changes were measured across interdigitated micro-electrodes integrated on the bottom of a specialised 96-well plate

(E-Plate 96) and sent to the RTCA Control Subunit. The latter used the RTCA Software (version 2.0) for CI calculation from the frequency-dependent electrode resistances and real-time display of data.

Background impedance of E-Plate 96 wells was determined with 50 µl culture medium only or culture medium containing respective concentrations of tetracycline, imipramine, or dB-cAMP. Subsequently, per well, 5×10^5 wt or p.A350V cells were plated in a final volume of 100 µl culture medium and half of the samples were induced with tetracycline. Then, localized on the RTCA SP Station the E-Plate 96 was placed into the CO_2-incubator, and the CI was monitored every 15 minutes over a period of 48 hours. After about 24 h in culture, cells were either treated with medium or with compounds known to inhibit (imipramine, 250 µM) or activate (dB-cAMP, 100 µM) SLC41A1-dependent Mg^{2+} efflux.

Results

Characterization of tet-induced over-expression of SLC41A1 wt and p.A350V variants in HEK293 cells

Functional examination of both variants was performed in the newly generated HEK293 cell lines with tet-regulated expression of stably transfected HA-strep-SLC41A1 (HEK293-(HA-strep-SLC41A1); referred to further only as wt cells) and HA-strep-SLC41A1-p.A350V (HEK293-(HA-strep-SLC41A1-p.A350V); referred to further only as p.A350V cells). Thus, the basic characteristics of each cell line were acquired before the physiological characterization of the potentially PD-associated variant of SLC41A1, p.A350V, was performed.

Previously, we had observed that longer tet-induction (20–24 hours) of flag-SLC41A1 in HEK293 cells (clone 17) led to increased death rates of the cells [20]. Therefore, we examined whether a 24-h over-expression of SLC41A1 wt (further only wt) and SLC41A1 p.A350V (further only p.A350V) variants would be tolerated, or whether it would also result in increased death rates. After tet-induction (+tet), we determined 93% to 100% viability of the cells over-expressing either wt or p.A350V. Viability of uninduced (-tet) wt or -tet p.A350V cells ranged after 24 h between 95% and 100%, and therefore, we concluded that a 24-h tet-induced over-expression of the wt or p.A350V variant had no significant effect on cell viability. Weaker expression of wt and p.A350V was also demonstrated by the finding that we had to load a 3-fold greater amount of the protein onto the gel to be able to obtain a SLC41A1 signal equally strong as that in clone 17 (Fig. 1C) [20].

Next, we quantified the transcriptional activity of both transgenic *SLC41A1* variants after 24 h of tet-induction and in -tet cells. A significantly higher amount of ~11.25-fold (+tet wt ddCt mean 123.72±7.42/-tet wt ddCt mean 11.0±0.48; P = .89e-09) of the wt *SLC41A1* transcript and a significantly higher amount of ~14.25 fold (+tet c.1049C>T ddCt mean 144.9±34.62/-tet c.1049C>T ddCt mean 10.17±0.79; P = 1.84e-08) of the *SLC41A1*-c.1049C>T transcript was detected, when compared with -tet cells (Fig. 1A and 1B). Therefore, we concluded that both wt and p.A350V cells produced similar amounts of transcript after 24 h of tet-induction. We also wished to know whether the over-expression of wt *SLC41A1* or *c.1049C>T* mutant could influence the expression of *SLC41A2* and/or *SLC41A3* in +tet and -tet wt and p.A350V cells, respectively. Indeed, we did not detect any significant influence of wt or p.A350V over-expression on the expression of SLC41A2 and SLC41A3 (data not shown). This also confirmed the specificity of the *hSLC41A1fw* and *hSLC41A1rev* primers.

Leaky expression of the gene of interest can often complicate functional studies [27,37]. Therefore, we tested whether wt and p.A350V over-expressing cell lines exhibited considerable levels of leaky expression of the wt and p.A350V variants. As a control, we used clone 17 of HEK293-(flag-SLC41A1) cells as previously characterized by Kolisek et al. [20,27]. Western blot analysis revealed bands specific for the wt and p.A350V variants (both ~56 kDa) almost exclusively in +tet cells (Fig. 1C). These data confirmed that both tested cell lines exhibited a negligible leaky expression of the transgenic SLC41A1 variants and, therefore, were suitable for downstream experimentation. Next, we determined whether wt and p.A350V cells expressed comparable amounts of SLC41A1 protein. With densitometric analyses performed on three blots with equal amounts of protein isolates from wt and p.A350V cells, we calculated that the density of p.A350V-specific bands was ~1% lower compared with that of wt-specific bands. Therefore, we concluded that both wt and p.A350V cells produced nearly identical amounts of the respective SLC41A1 variants after 24 h of tet-induction. These data further underlined the suitability of both cell lines for further functional experimentation.

SLC41A1 p.A350V localizes within the cytoplasmic membrane

Next, by performing Western blot analysis of the soluble protein- and membrane-protein-enriched cellular fractions (SF, MF) and of subcellular protein fractions (cytosolic, membrane, nuclear, and cytoskeletal), we examined whether the potentially PD-associated variant p.A350V of SLC41A1 was properly targeted into the cytoplasmic membrane, as demonstrated for wt SLC41A1 [20,27]. Figure 1D shows a Western blot analysis of MF and SF isolated from -tet and +tet wt and p.A350V cells. The ~56 kDa bands corresponding to wt and p.A350V were predominantly detected in the MF, with markedly lower abundance in SF of +tet cells. Flag-hSLC41A1 was used as a positive control [27]. Cytosolic protein RPL19 was used to control the specificity of the membrane fraction enrichment and, as expected, was detected only in the soluble protein fraction. We also performed subcellular protein fractionation with HEK293 cells over-expressing wt or p.A350V (Fig. 1E). Probing of the electroseparated fractions with an antibody against the strep-epitope resulted in the almost exclusive detection of both the wt and the p.A350V variants in the fraction enriched in plasma membrane proteins. The specificity of the fractionation was controlled by running and probing parallel blots with antibodies against PMCA4 (membrane fraction; positive control; Fig. 1E), against RPL19 (cytosolic fraction, data not shown), or against Lamin A (nuclear fraction; data not shown). These results were in accordance with our confocal microscopy data, which revealed that both wt and p.A350V SLC41A1 variants were predominantly localized in the plasma membrane. This was shown by co-localization of the green fluorescent signal of immunolabeled SLC41A1 variants (anti-strep:GAM-Alexa-488), with the red fluorescent signal of wheat germ agglutinin conjugated to Alexa-647 (Fig. 2). Colocalization correlation analysis between Alexa-488- and Alexa-647-specific signals in wt and p.A350V variants revealed a 94.5±1.8% (N = 6) and 92±2.3% (N = 7) overlap of the green and red pixels, respectively. In contrast, no wt- or p.A350V-specific fluorescence was seen in -tet cells (Figure S1). Taken together, these data demonstrated the plasma membrane localization of the potentially PD-related p.A350V variant of SLC41A1. Thus, we conclude that the mutation p.A350V does not affect the intracellular localization of SLC41A1.

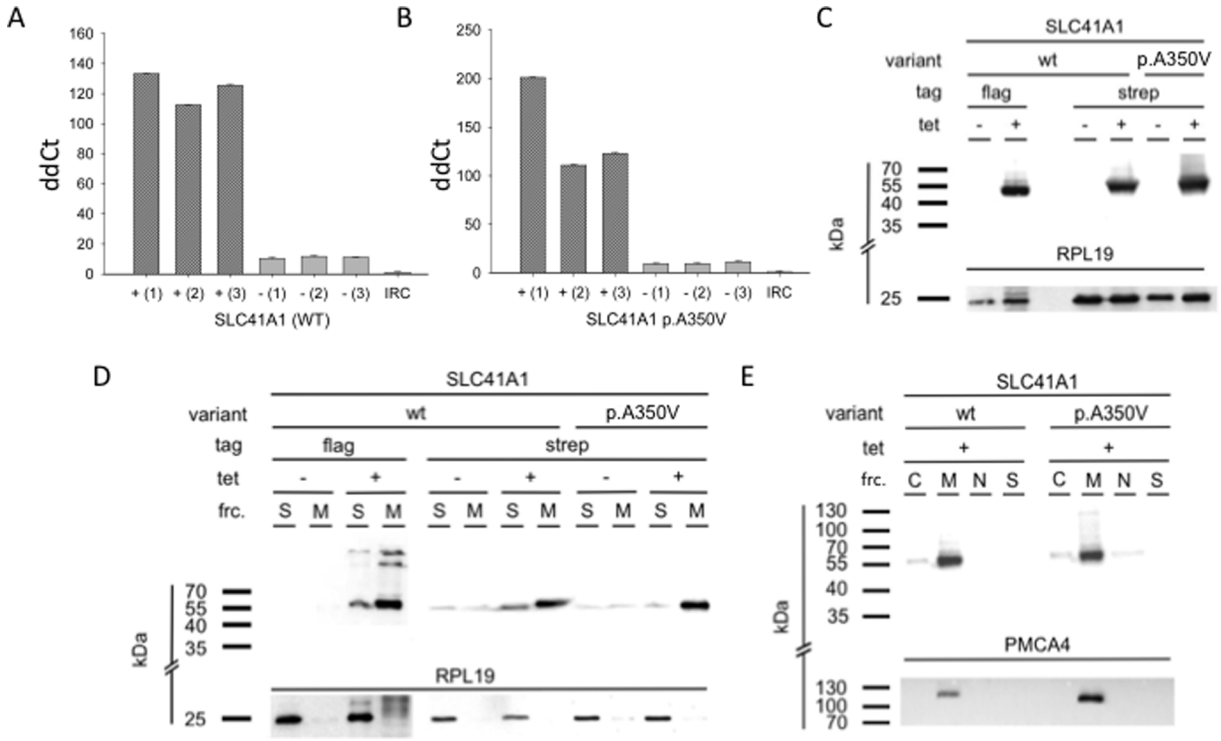

Figure 1. (A) Quantitative real time PCR analysis of *SLC41A1* (*wt*) expression in -tet and +tet cells. The ddCt values of three independent +tet samples and three independent -tet samples are shown. Each biological sample was loaded in triplicate. IRC indicates inter-run control. (B) Quantitative real time PCR analysis of *SLC41A1-(c.1049C>T)* expression in -tet and +tet cells. The ddCt values of three independent +tet samples and three independent -tet samples are given. Each biological sample was loaded in triplicate. IRC indicates inter-run control. (C) Immunodetection of recombinant HA-strep-SLC41A1(wt) and HA-strep-SLC41A1-p.A350V in total protein isolate from -tet and +tet (24 h) cells. Strep-tagged wt and p.A350V were detected only in tet-induced cells. Positive control: flag-tagged SLC41A1 isolated from HEK293 cells, clone 17, which was extensively characterized in [20,27]. Loading was controlled by immunodetection of RPL19 protein. (D) Immunodetection of recombinant HA-strep-SLC41A1(wt) and HA-strep-SLC41A1-p.A350V in soluble and membrane-protein-enriched fractions isolated from -tet and +tet (24 h) cells. Strep-tagged wt and p.A350V were detected almost exclusively in tet-induced cells and predominantly in membrane (M) protein fractions and in much lower quantities in soluble (S) protein fractions. Positive control: flag-tagged SLC41A1 isolated from HEK293 cells (clone 17). Soluble RPL19 was used to control the specificity of the separation between soluble and membrane proteins. (E) Immunodetection of recombinant HA-strep-SLC41A1(wt) and HA-strep-SLC41A1-p.A350V in subcellular protein fractions isolated from +tet (24 h) cells. Wt and p.A350V were predominantly detected in membrane (M) protein fractions with much lower quantities in cytosolic (C) protein fractions and also for p.A350V in traces in the nuclear (N) protein fraction. Transgenic variants were not detected in cytoskeletal (S) fractions. Specificity of the fractionation was controlled on a parallel blot by immunodetection of PMCA4 (M).
doi:10.1371/journal.pone.0071096.g001

p.A350V exhibits identical complex-forming abilities as SLC41A1 wt in HEK293 cells

SLC41A1 forms transient multimeric complexes *in vivo* [27]. Therefore, we wondered whether the mutation p.A350V could affect the complex-forming characteristics of SLC41A1. Figure 3 shows Western blot analysis performed on strep-affinity purified native protein isolations separated with blue native electrophoresis [27,33]. Wt and p.A350V variants showed identical separation patterns (Fig. 3), both forming two identical complexes with molecular masses between 242 and 480 kDa. This leads us to the assumption that the mutation p.A350V has no obvious effect on the complex-forming abilities of the SLC41A1 protein.

Amino acid substitution p.A350V in human SLC41A1 induces increased Mg^{2+} efflux

As in our previous study [20], -tet and +tet wt and p.A350V cells were Mg^{2+}-loaded by a 20-min pre-incubation in solutions containing 10 mM Mg^{2+}, and subsequently, the $[Mg^{2+}]_i$ was measured over a 10–min period in completely Mg^{2+}-free solutions containing 145 mM Na^+ (efflux conditions). $[Mg^{2+}]_i$ values determined at the end of each period are shown in Table 1. Uninduced wt cells and p.A350V cells regulate their $[Mg^{2+}]_i$ at stable levels of 0.36 ± 0.01 mM. Compared with -tet controls, the $[Mg^{2+}]_i$ of +tet cells was increased by 25% (wt) and 33% (p.A350V) when incubated in 10 mM Mg^{2+} solution. After resuspension in absolutely Mg^{2+}-free solutions, loaded +tet cells normalized their $[Mg^{2+}]_i$ to values no longer different from those of -tet cells (Table 1).

The $[Mg^{2+}]_i$ decrease observed in +tet cells was previously shown to reflect the SLC41A1-dependent Mg^{2+} efflux [20]. The results for +tet wt and +tet p.A350V cells are summarized in figure 4 showing a significantly stronger Mg^{2+} extrusion of 81.2 ± 4.7 μM/10 min ($Np._{A350V} = 113$) in p.A350V cells compared with 48.2 ± 7.0 μM/10 min ($N_{wt} = 82$) in the wt cells used as control. These data clearly demonstrate an increased efflux capacity of p.A350V cells.

However, if the measurements were performed in solutions containing 5 or 10 mM Mg^{2+}, thereby lowering the inside-out Mg^{2+} gradient, no Mg^{2+} extrusion occurred from Mg^{2+}-loaded +tet wt and +tet p.A350V cells. Instead, as can be seen in figure 4, the $[Mg^{2+}]_i$ increased by 41.1 ± 15.0 μM/10 min and 83.5 ± 22.3 μM/10 min in wt cells (Nwt; $_{[Mg^{2+}]e\ (5\ mM)} = 14$ &

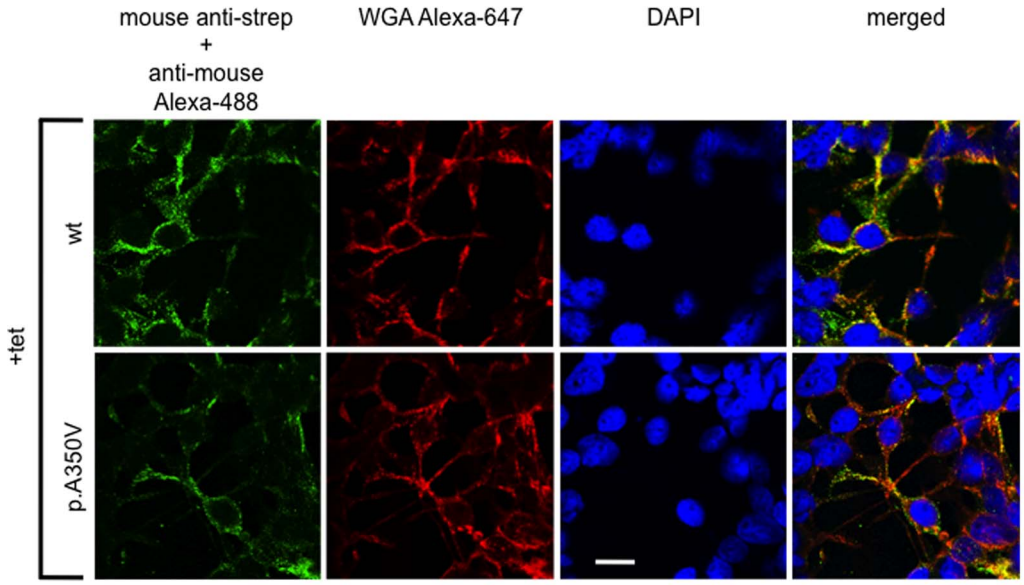

Figure 2. Confocal immunolocalization of HA-strep-SLC41A1 (wt) and HA-strep-SLC41A1-p.A350V in +tet (24 h) cells. Strep-tagged wt and p.A350V were immunolabeled with primary mouse anti-strep and secondary GAM Alexa-488 antibodies (green signal). Plasma membranes were fluorescently contrasted with wheat germ agglutinin (WGA) conjugated to Alexa-647 (red signal). Nuclei were stained with DAPI (blue signal). The merged images show that both Alexa-488 and Alexa-647 signals co-localize in +tet cells. Scale bar indicates 10 μm.
doi:10.1371/journal.pone.0071096.g002

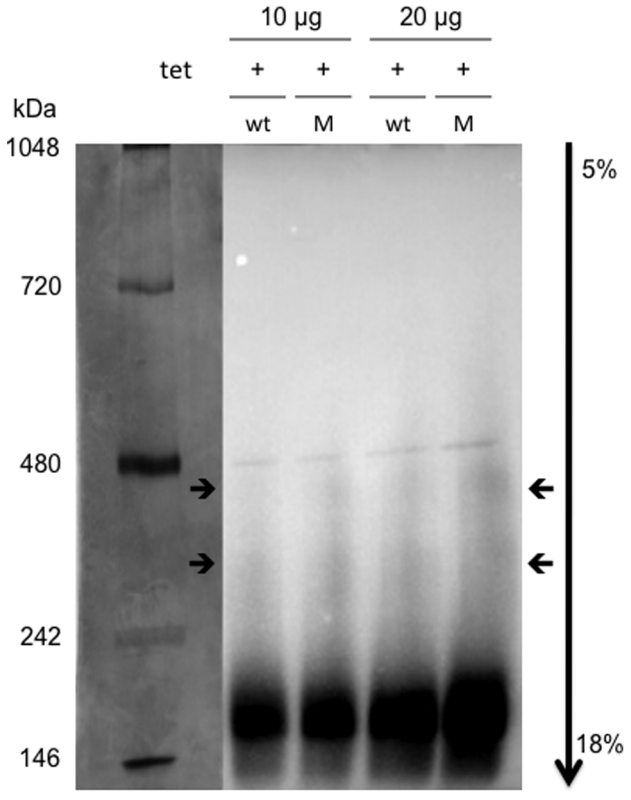

Figure 3. Gradient blue native PAG electroseparation (5–18%) and Western blot analysis of SLC41A1(wt) and p.A350V (M) complexes. Both wt and p.A350V variants form identical complexes (two; labeled with arrows) with molecular masses between 242 and 480 kDa.
doi:10.1371/journal.pone.0071096.g003

Nwt; $_{[Mg^{2+}]e\ (10\ mM)}$ = 14) and by 73.6±16.4 μM/10 min and 103.2±21.5 μM/10 min in p.A350V cells ($N_{p.A350V;\ [Mg^{2+}]e\ (5\ mM)}$ = 13 & $N_{p.A350V;\ [Mg^{2+}]e\ (10\ mM)}$ = 13) incubated in 5 or 10 mM Mg^{2+}, respectively, during the measurements.

Effects of imipramine and of dB-cAMP on SLC41A1-related Mg^{2+} efflux from +tet wt and p.A350V cells

In both wt- and p.A350V-over-expressing cells, the observed $[Mg^{2+}]_i$ decrease (−60.5±9.2 μM/10 min, N_{wt} = 21; and 101.7±9.2 μM/10 min, $N_{p.A350V}$ = 26) was nearly completely abolished (−0.7±13.5 μM/10 min, N_{wt} = 21; and 8.7±9.1 μM/10 min, $N_{p.A350V}$ = 26) by the tricyclic antidepressant imipramine (Fig. 5A) known to inhibit the NME function of SLC41A1 [20].

In our previous study [20], we have demonstrated that phosphorylation, postulated to be a mechanism for the activation of Mg^{2+} extrusion [20,34], regulates NME activity of SLC41A1 and that wt is being detectable in the phosphoprotein-specific fraction (P). To this end we performed Western blot analysis on fractionated protein lysates of induced +tet flag-wt, strep-wt, and strep-p.A350V. Figure 6 demonstrates that the ~56 kDa bands corresponding to wt and p.A350V were detected in the P fractions. The specificity of the fractionation was controlled with an antibody exclusively recognizing phosphorylated Akt.

We also tested whether the SLC41A1-dependent Mg^{2+} efflux from +tet wt and p.A350V cells could be further stimulated by the application of dibutyryl-cAMP (dB-cAMP), a membrane-permeant cAMP analog that activates the holoenzyme complex of protein kinase A (PKA) [20]. No additional effects on Mg^{2+} extrusion from p.A350V cells were observed after the application of 100 μM dB-cAMP ($N_{p.A350V}$ = 15; Fig. 5B). However, as shown in figure 5B, dB-cAMP increased Mg^{2+} release by 77±20% (N_{wt} = 15) in wt controls.

Table 1. $[Mg^{2+}]_i$ (mM) of uninduced (-tet) and induced (+tet) HEK293-(HA-strep-SLC41A1), and HEK293-(HA-strep-SLC41A1-p.A350V) cells.

$[Mg^{2+}]_e$ mM	HEK293-(HA-strep-SLC41A1) (control)		HEK293-(HA-strep-SLC41A1p.A350V)	
	-tet (N = 82)	+tet (N = 82)	-tet (N = 113)	+tet (N = 113)
10	0.36±0.01	0.45±0.01**	0.36±0.01	0.48±0.01**
0	0.36±0.01	0.40±0.01[a]	0.37±0.01	0.40±0.01[a]

$[Mg^{2+}]_i$ values for cells successively incubated for 20 min in solutions containing 10 mM Mg^{2+} (loading conditions) and for 10 min in completely Mg-free media (efflux conditions) are given. Data are presented as means ± SE. N is being indicated. **P<0.001 vs. control (-tet cells); [a]P<0.001 vs. loaded +tet HEK293-(HA-strep-SLC41A1) or HEK293-(HA-strep-SLC41A1-p.A350V) cells.
doi:10.1371/journal.pone.0071096.t001

Amino acid substitution p.A350V in human SLC41A1 effects cell growth

The 48-h growth curves of +tet p.A350V cells and wt cells obtained under control conditions and with imipramine or dB-cAMP in the culture medium are displayed in figure 5C. Compared with +tet wt cells, the normalized CI (nCI) of +tet p.A350V cells was reduced (2.03±0.03 vs. 2.26±0.08; P<0.001) after 48 h in culture (Fig. 5C). Application (24 h after seeding) of imipramine and of dB-cAMP in parallel to its effects on NME activity decreases and increases the 48-h nCI of +tet wt and p.A350V cells compared with control values (Fig. 5C). After imipramine application, the 48-h nCI amounted to 0.18±0.17 in wt and to 0.26±0.40 in p.A350V cells, thus showing a strong reduction in both groups. However, the dB-cAMP-induced increase of the 48-h nCI was much stronger in +tet wt cells compared with +tet p.A350V cells (2.81±0.08 vs. 2.55±0.08; P<0.001).

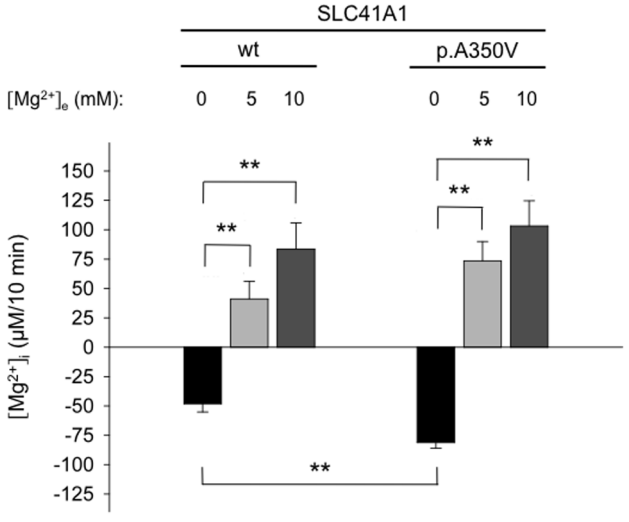

Figure 4. SLC41A1-related Mg^{2+} efflux in p.A350V cells compared with wt cells. Before measurements, cells were pre-loaded with Mg^{2+} as described in Material and Methods ($[Mg^{2+}]_e$ = 10 mM). The $[Mg^{2+}]_i$ change obtained after 10 min in media containing 145 mM Na^+ is given for the following conditions: (1) completely Mg^{2+}-free media ($N_{p.A350V}$ = 113 & N_{wt} = 82); (2) media supplemented with 5 mM Mg^{2+} ($N_{p.A350V}$ = 13 & N_{wt} = 14); and (3) media supplemented with 10 mM Mg^{2+} ($N_{p.A350V}$ = 13 & N_{wt} = 14). Values have been corrected for $[Mg^{2+}]_i$ changes in -tet cells and are given as means ± SE; **P<0.001.
doi:10.1371/journal.pone.0071096.g004

Discussion

Most PD cases are sporadic with unclear multifactorial etiologies (idiopathic PD). Only approximately 3% to 5% among all sporadic PD cases are attributable to defects in seven PD-associated genes: *SNCA* (autosomal dominant pattern of inheritance; (ADPI)), *LRRK2* (ADPI), *EIF4G1* (ADPI), *VPS35* (ADPI), *parkin/PARK2* (autosomal recessive pattern of inheritance; (ARPI)), *DJ-1/PARK7* (ARPI), and *PINK1* (ARPI) [38,39]. However, changes in several other genes have been suggested as causes for recessive neurological/neurodegenerative disorders that may include PD: hereditary ataxias (*ATXN2/3*, *FMR1*), frontotemporal dementia (e.g. *MAPT*) and others (e.g. *ATP13A2*, *PLA2G6*, *FBXO7*) [39].

RAB7L1, and *SLC41A1* have been identified within the newly revealed PD-susceptibility locus *PARK16* at chromosome 1q32 [21,22,23,24]. SLC41A1 has been shown by our group to be a cell-membrane-localized Mg^{2+} carrier, conducting the exchange of intracellular Mg^{2+} for extracellular Na^+ (NME) [20,27]. NME has been shown to be functionally active in nearly all investigated cells and tissues including neurons [34,40,41,42,43]. It has also been shown to be responsible for the maintenance of an optimal $[Mg^{2+}]_i$ for a variety of processes critical for the cell such as bioenergetics [44], the regulation of cellular pH, volume, and the total ion balance, [45,46], and cell proliferation and differentiation [47,48].

Recently, in one PD patient, Tucci and colleagues [23] have found a coding variant of SLC41A1, carrying substitution p.A350V. Here, we have investigated if this potentially PD-associated mutation affects the molecular and/or functional properties of SLC41A1. Our experiments have revealed no changes regarding the cellular localization, phosphorylation status, or complex-forming ability of the p.A350V variant when compared with the wt protein. However, we have demonstrated that +tet p.A350V cells are able to perform Mg^{2+}-efflux more efficiently than +tet wt cells. Under our experimental conditions, short-term, 10-min Mg^{2+} release is increased by 69±10% (P<0.001) after the induction of p.A350V over-expression compared with cells over-expressing wt. Moreover, as a consequence of an enhanced NME activity, we found a reduced proliferation rate in p.A350V compared to wt cells. As the growth experiments were performed for long periods (48 h) and with cells incubated in complete culture media containing 1.2 mM Mg^{2+}, the effects of the p.A350V mutation seem to be of relevance also under physiological conditions.

In both cell lines, Mg^{2+} extrusion is blocked by >90% after imipramine application, clearly showing that it results from SLC41A1-mediated NME activity [42]. Imipramine, which besides quinidine, is the current pharmacological choice for NME inhibition [20,49], is known to act on the extracellular Na^+-binding site of the NME, and competition between these two compounds slows Mg^{2+} efflux. In agreement with this, the

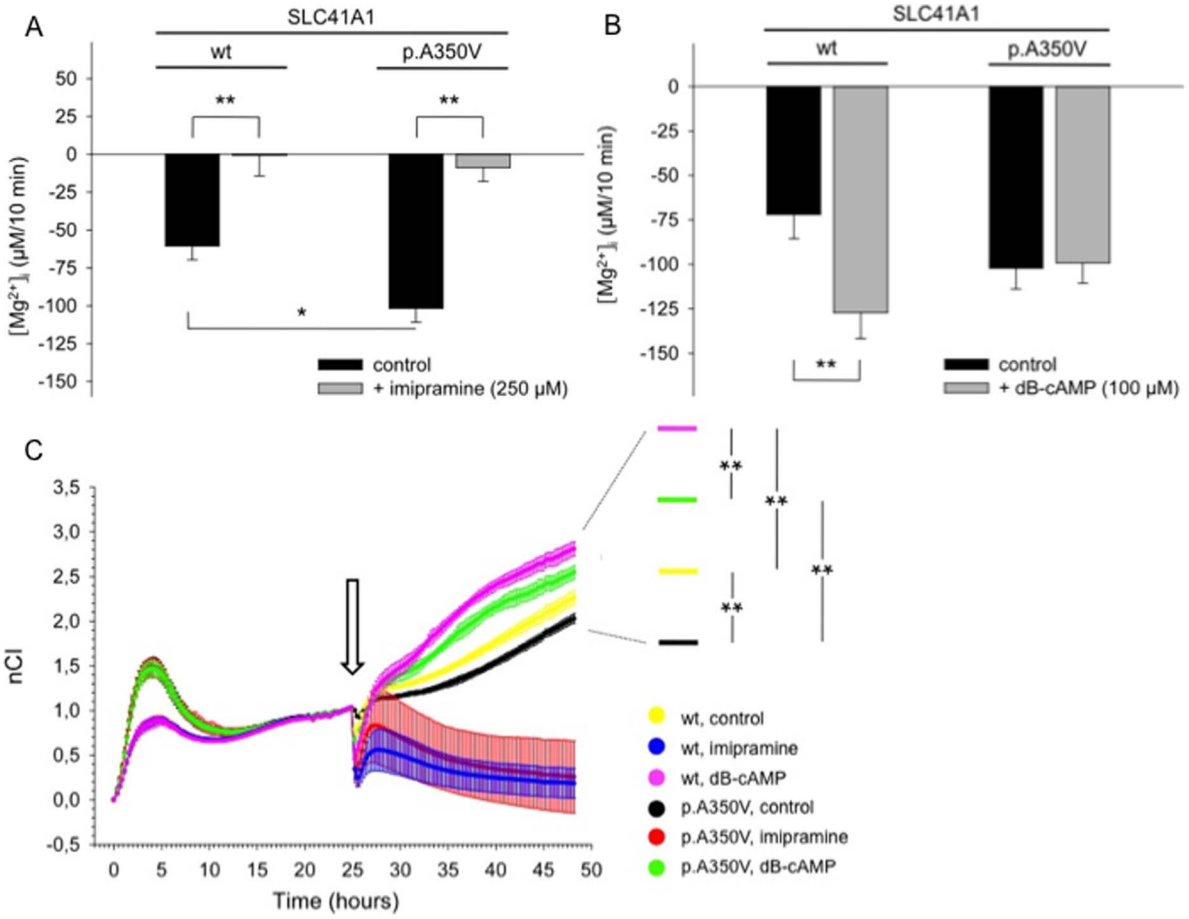

Figure 5. Effect of imipramine and of cAMP-dependent PKA phosphorylation on SLC41A1-related $[Mg^{2+}]_i$ changes, cell adhesion, and cell proliferation in +tet p.A350V cells and wt cells. A: Summary of $[Mg^{2+}]_i$ changes after resuspension of Mg^{2+}-loaded +tet p.A350V cells and wt cells in completely Mg^{2+}-free Na^+-containing solutions with or without (control) the Na^+/Mg^{2+} exchanger inhibitor imipramine (250 µM). Values have been corrected for $[Mg^{2+}]_i$ changes in -tet cells and given as means ± SE; $N_{p.A350V} = 26$ & $N_{wt} = 21$ single experiments per condition; *P = 0.03; **P<0.005. B: Summary of $[Mg^{2+}]_i$ changes after resuspension of Mg^{2+}-loaded +tet p.A350V cells and wt cells in completely Mg^{2+}-free Na^+-containing media with or without (control) the Na^+/Mg^{2+} exchanger activator dB-cAMP (100 µM). Values have been corrected for $[Mg^{2+}]_i$ changes in -tet cells and are means ± SE; Np.A350V = 15 & Nwt = 15 single experiments per condition; **P = 0.01. C: Original growth curves of +tet p.A350V cells and wt cells under control conditions and after application of 250 µM imipramine and of 100 µM dB-cAMP. Cells were seeded at a density of 10×10^5 per well, induced with tetracycline, and allowed to attach and proliferate for 24 h prior to treatment with the compounds (indicated by the arrow). The Cell Index, a dimensionless parameter reflecting cell adherence and number, was normalized (nCI) to the time just before modulator application. Values are means ± SD; N = 6 single experiments per condition; **P<0.001.
doi:10.1371/journal.pone.0071096.g005

inhibitory effect of imipramine is in the order of that of sodium withdrawal, which amounts to 91% in our previous study with SLC41A1-over-expressing HEK293 cells [20].

Another characteristic feature of NME is its activation by PKA-dependent phosphorylation [20,34]. Elevation of the intracellular cAMP concentration specifically stimulates Na^+-dependent efflux either directly via an increased affinity of the transporter for intracellular Mg^{2+} [34,50] or by Mg^{2+} mobilization from intracellular organelles, e.g. from mitochondria [51]. Interestingly, the application of dB-cAMP (a cell-membrane-permeant cAMP-analog) increased (77±20%) Mg^{2+} efflux only in +tet wt cells, whereas no effect has been seen in p.A350V cells. This insensitivity of mutant NME to cAMP stimulation might be of pathophysiological importance as under normal conditions various hormones or mediators, e.g., adrenergic substances, prostaglandin E2, and angiotensin II, use this pathway to induce a transient $[Mg^{2+}]_i$ decrease that directly or indirectly influences cellular transport mechanisms and physiological functions [49,51,52]. For example, in this study, the growth-promoting effect of dB-cAMP is reduced in p.A350V-over-expressing cells compared with wt cells. The inability further to increase p.A350V-related NME function via cAMP also suggests maximum or near-maximum activation of the transporter and is in accordance with the observation of enhanced Mg^{2+} efflux in mutants compared with wt cells. The $[Mg^{2+}]_i$, a main determinant of NME activity [53], is similar (0.44±0.01 mM) between wt and p.A350V cells. Therefore, one can speculate that the p.A350V mutation augments the affinity of the transport protein for intracellular Mg^{2+}, changes the Mg^{2+}-carrier-complex formation, or dysregulates transporter gating to facilitate the Mg^{2+} transport rate.

In the long-term, the increased activity of the NME might contribute to the development of intracellular Mg^{2+} deficiency [43], if not compensated for by Mg^{2+} influx. Mg deprivation, whether by gene defects such as p.A350, toxins (rotenone, MPTP), or restricted Mg intake, induces and/or exacerbates processes such as oxidative stress accompanied by an increase in NO and free

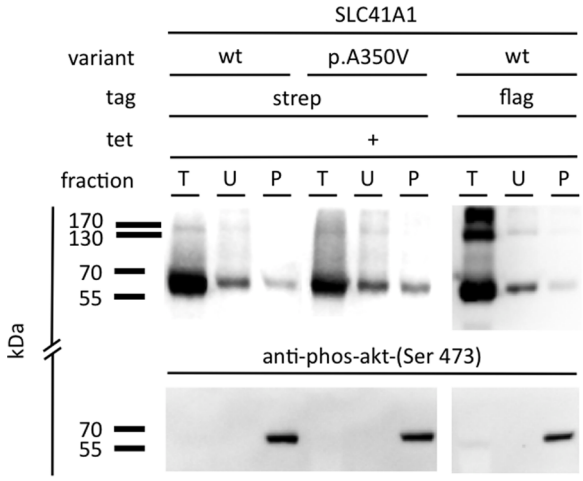

Figure 6. Immunodetection of phosphorylated recombinant flag-SLC41A1 (wt), HA-strep-SLC41A1 (wt), and HA-strep-SLC41A1-p.A350V with the PhosphoProtein purification kit (Qiagen). Total (T), flow-through (U; containing unphosphorylated proteins) and elution (P; containing phosphorylated proteins) fractions were probed with antibodies against strep- or flag-tag. A signal specific for phosphorylated wt or p.A350V was detected in all three cell lines. The specificity of the fractionation was controlled with an antibody against phosphorylated Akt.
doi:10.1371/journal.pone.0071096.g006

radicals [54,55], dysfunction of mitochondria and the endoplasmic reticulum [56,57], impairment of Ca^{2+} homeostasis [58], iron accumulation [59], alterations in the autophagy-lysosome pathways, protein mishandling, and inflammatory responses [58], all of which are known to trigger neuronal damage in neurodegenerative diseases including PD [56,60,61]. In accordance, Oyanagi and colleagues [14] have been able to induce the severe loss of dopaminergic neurons in rats fed for one year with an Mg-restricted diet containing only one-fifth of the normal Mg content. Furthermore, a lower concentration of Mg in various brain regions and in the cerebrospinal fluid of PD patients has been found [16,62,63]. On the other hand, a high extracellular [Mg] of $\geq$1.2 mM has been demonstrated to protect dopaminergic neurons of the *substantia nigra* from MPP+ toxicity [18] and, because of its Ca^{2+}-antagonizing effects, to reduce neuroinflammation [64]. Moreover, spontaneous and Fe^{2+}-induced accelerated aggregation of α-synuclein can be inhibited by 0.8 mM Mg^{2+} [65]. In this study, by using an extracellular [Mg] of 5 and 10 mM, we have been able to block SLC41A1-related Mg^{2+} efflux in both wt and p.A350V cells. Increasing the extracellular Mg^{2+} concentration will reduce the driving force for an electroneutral Mg^{2+} efflux and suggests that the exchanger switches to the reverse mode, thereby performing Mg^{2+} uptake [27,42]. Thus, Mg supplementation might be useful for preventing a loss of intracellular Mg^{2+}, a loss that is detrimental to neurons.

Under physiological conditions, an adequate Mg intake should be seen as an important positive environmental factor protecting neurons against accelerated ageing caused by slowly acting deleterious environmental factors (e.g. toxins) and/or genetic risk factors. With regard to the latter, Mg^{2+} is an essential co-factor in almost all enzymatic systems involved in DNA processing and in nucleotide excision repair, base excision repair, and mismatch repair [66]. Furthermore, PD-relevant genes with a recessive pattern of inheritance (*parkin/PARK2*, *PINK1*, and *DJ-1/PARK7*) are all related to mitochondria dysfunction and oxidative stress making it possible that defects in these genes and disturbances of IMH intervene in these pathways to induce nigral mitochondrial cytopathy [67].

Conclusions

Magnesium deficiency (both systemic and intracellular) has long been suspected to be involved in various human disease complexes such as metabolic syndrome and neurodegeneration in general including PD. An obvious molecular link between disturbed IMH and PD is however missing. In this study, we have examined the functional properties of a recently identified potentially PD-associated coding variant of the NME SLC41A1, p.A350V. We have demonstrated that p.A350V is able to perform Mg^{2+}-extrusion more efficiently than wt NME and shows insensitivity to cAMP stimulation and have found a reduced proliferation rate in p.A350V compared with wt cells. Our data therefore indicate that the rare conservative substitution p.A350V is a gain-of-function mutation leading to an increased Mg^{2+} efflux capacity with likely a long-term consequence in systemic deterioration, particularly under conditions of low extracellular Mg^{2+} concentration. By extrapolation, our data are in agreement with the findings of epidemiological and case-control studies and suggest that the chronic loss of Mg^{2+} from brain tissue and, thus, latent intracellular hypomagnesemia, contributes to neurodegeneration. Na^+/Mg^{2+} exchange in neurons and SLC41A1 *per se* might therefore represent a PD-relevant therapeutic target, with Mg^{2+} supplementation of PD patients possibly being beneficial.

Supporting Information

Figure S1 Confocal immunolocalization of HA-strep-SLC41A1 (wt) and HA-strep-SLC41A1-p.A350V in -tet (24 h) cells. Strep-tagged wt and p.A350V were immunolabeled with primary mouse anti-strep and secondary GAM Alexa-488 antibodies (green signal). Plasma membranes were fluorescently contrasted with wheat germ agglutinin (WGA) conjugated to Alexa-647 (red signal). Nuclei were stained with DAPI (blue signal). Scale bar indicates 10 μm.
(DOC)

Acknowledgments

Our gratitude is due to Heike Pröhl (FBN Dummerstorf), Martin Marak, and Katarina Wolf (both FU Berlin) for competent technical support of the project, to Dr. Mandana Rezwan (Dualsystems Biotech AG) for cooperation with the construction of the cell lines and to Dr. Theresa Jones for linguistic corrections.

Author Contributions

Conceived and designed the experiments: MK MSR . Performed the experiments: MK GS LM AS PL JV MSR . Analyzed the data: MK GS LM AS PL JV MSR. Contributed reagents/materials/analysis tools: MK MSR. Wrote the paper: MK MSR.

References

1. Barbagallo M, Belvedere M, Di Bella G, Dominguez LJ (2011) Altered ionized magnesium levels in mild-to-moderate Alzheimer's disease. Magnes Res 24: S115–121.
2. Nie ZL, Wang ZM, Zhou B, Tang ZP, Wang SK (2012) Magnesium intake and incidence of stroke: Meta-analysis of cohort studies. Nutr Metab Cardiovasc Dis [Epub ahead of print].

3. Johnson S (2001) The multifaceted and widespread pathology of magnesium deficiency. Med Hypotheses 56: 163–170.
4. Sartori SB, Whittle N, Hetzenauer A, Singewald N (2012) Magnesium deficiency induces anxiety and HPA axis dysregulation: modulation by therapeutic drug treatment. Neuropharmacology 62: 304–312.
5. Mousain-Bosc M, Roche M, Rapin J, Bali JP (2004) Magnesium VitB6 intake reduces central nervous system hyperexcitability in children. J Am Coll Nutr 23: 545S–548S.
6. Ådén E, Carlsson M, Poortvliet E, Stenlund H, Linder J, et al. (2011) Dietary intake and olfactory function in patients with newly diagnosed Parkinson's disease: a case-control study. Nutr Neurosci 14: 25–31.
7. Miyake Y, Tanaka K, Fukushima W, Sasaki S, Kiyohara C, et al. (2011) Dietary intake of metals and risk of Parkinson's disease: a case-control study in Japan. J Neurol Sci 306: 98–102.
8. Lovitt B, Vanderporten EC, Sheng Z, Zhu H, Drummond J, et al. (2010) Differential effects of divalent manganese and magnesium on the kinase activity of leucine-rich repeat kinase 2 (LRRK2). Biochemistry 49: 3092–3100.
9. Hutchinson M, Raff U (2000) Structural changes of the substantia nigra in Parkinson's disease as revealed by MR imaging. AJNR Am J Neuroradiol 21: 697–701.
10. Wakabayashi K, Tanji K, Mori F, Takahashi H (2007) The Lewy body in Parkinson's disease: molecules implicated in the formation and degradation of alpha-synuclein aggregates. Neuropathology 27: 494–506.
11. Nussbaum RL, Ellis CE (2003) Alzheimer's disease and Parkinson's disease. N Engl J Med 348: 1356–1364.
12. de Lau LM, Breteler MM (2006) Epidemiology of Parkinson's disease. Lancet Neurol 5: 525–535.
13. Oyanagi K (2005) The nature of parkinsonism-dementia complex and amyotropic latheral sclerosis of Guam and magnesium deficiency. Parkinsonism Relat Disord 11: S17–23.
14. Oyanagi K, Kawakami E, Kikuchi-Horie K, Ohara K, Ogata K, et al. (2006) Magnesium-deficiency over generations in rats with special references to the patogenesis of the Parkinsonism-dementia complex and amyotropic lateral sclerosis of Guam. Neuropathology 26: 115–128.
15. Garruto RM, Yanagihara R, Gajdusek DC (1985) Disappearance of high-incidence amyotrophic lateral sclerosis and parkinsonism-dementia on Guam. Neurology 35: 193–198.
16. Barbiroli B, Martinelli P, Patuelli A, Lodi R, Iotti S, et al. (1999) Phosphorus magnetic resonance spectroscopy in multiple system atrophy and Parkinson's disease. Mov Disord 14: 430–435.
17. André C, Truong TT, Robert JF, Guillaume YC (2005) Effect of metals on herbicides-alpha-synuclein association: a possible factor in neurodegenerative disease studied by capillari electrophoresis. Electrophoresis 26: 3256–3264.
18. Hashimoto T, Nishi K, Nagasao J, Tsuji S, Oyanagi K (2008) Magnesium exerts both preventive and ameliorating effects in an in vitro rat Parkinson disease model involving 1-methyl-4-phenylpyridinium (MPP+) toxicity in dopaminergic neurons. Brain Res 1197: 143–151.
19. Gessner W, Brossi A, Shen RS, Abell CW (1985) Further insight into the mode of action of the neurotoxin 1-methyl-4-phenyl-1,2,3,6-tetrahydropyridine (MPTP). FEBS Lett 183: 345–348.
20. Kolisek M, Nestler A, Vormann J, Schweigel-Röntgen M (2012) Human gene SLC41A1 encodes for the Na^+/Mg^{2+} exchanger. Am J Physiol Cell Physiol 302: C318–326.
21. Satake W, Nakabayashi Y, Mizuta I, Hirota Y, Ito C, et al. (2009) Genome-wide association study identifies common variants at four loci as genetic risk factors for Parkinsoǹs disease. Nat Genet 41: 1303–1307.
22. Simón-Sánchez J, Schulte C, Bras JM, Sharma M, Gibbs JR, et al. (2009), Genome-wide association study reveals genetic risk underlying Parkinson's disease. Nat Genet 41: 1308–1312.
23. Tucci A, Nalls MA, Houlden H, Revesz T, Singleton AB, et al. (2010) Genetic variability at the PARK16 locus. Eur J Hum Genet 18: 1356–1359.
24. Yan Y, Tian J, Mo X, Zhao G, Yin X, et al. (2011) Genetic variants in the RAB7L1 and SLC41A1 genes of the *PARK16* locus in Chinese Parkinson's disease patients. Int J Neurosci 121: 632–636.
25. Wabakken T, Rian E, Kveine M, Aasheim HC (2003) The human solute carrier SLC41A1 belongs to a novel eukaryotic subfamily with homology to prokaryotic MgtE Mg^{2+} transporters. Biochem Biophys Res Commun 306: 718–724.
26. Goytain A, Quamme GA (2005) Functional characterization of humanSLC41A1, a Mg^{2+} transporter with similarity to prokaryotic MgtE Mg^{2+} transporters. Physiol Genomics 21: 337–342.
27. Kolisek M, Launay P, Beck A, Sponder G, Serafini N, et al. (2008) SLC41A1 is a novel mammalian Mg^{2+} carrier. J Biol Chem 283: 16235–16247.
28. Mandt T, Song Y, Scharenberg AM, Sahni J (2011) SLC41A1 Mg^{2+} transport is regulated via Mg^{2+}-dependent endosomal recycling trough its N-terminal cytoplasmic domain. Biochem J 439: 129–139.
29. Gerdin A (2010) The Sanger Mouse Genetics Programme: high throughput characterisation of knockout mice. Acta Opthalmologica 88:0. Doi:10.1111/j.1755-3768.2010.4142.x.
30. Hurd TW, Otto EA, Mishima E, Gee HY, Inoue H, et al. (2013) Mutation of the Mg^{2+} Transporter SLC41A1 Results in a Nephronophthisis-Like Phenotype. J Amer Soc of Nephrol, ahead of print.
31. Kolisek M, Galaviz-Hernández C, Vázquez-Alaniz F, Sponder G, Javaid S, et al. (2013) *SLC41A1* is the only magnesium responsive gene significantly overexpressed in placentas of preeclamptic women. Hypertens Pregnancy, accepted for publication.
32. Reikofski J, Tao BY (1992) Polymerase chain reaction (PCR) techniques for site-directed mutagenesis. Biotechnol Adv 10: 535–547.
33. Schägger H, von Jagow G (1991) Blue native electrophoresis for isolation of membrane protein complexes in enzymatically active form. Anal Biochem 199: 223–231.
34. Günther T, Vormann J (1992) Activation of Na+/Mg^{2+} antiport in thymocytes by cAMP. FEBS Lett 297: 132–134.
35. Grynkiewicz G, Poenie M, Tsien RY (1985) A new generation of Ca^{2+} indicators with greatly improved fluorescence properties. J Biol Chem 260: 3440–3450.
36. Xi B, Yu N, Wang X, Xu X, Abassi YA (2008) The application of cell-based, label-free technology in drug discovery. Biotech J 3: 484–495.
37. Pham DH, Moretti PAB, Goodall GJ, Pitson SM (2008) Attenuation of leakiness in doxycycline-inducible expression via incorporation of 3′ AU-rich mRNA destabilizing elements. BioTechniques 45: 155–162.
38. Bekris LM, Mata IF, Zabetian CP (2010) The genetics of Parkinson disease. J Geriatr Psychiatry Neurol 23: 228–242.
39. Puschmann A (2013) Monogenic Parkinson's disease and parkinsonism: clinical phenotypes and frequencies of known mutations. Parkinsonism Relat Disord 19: 407–415.
40. Günther T, Vormann J, Förster R (1984) Regulation of intracellular Mg^{2+} by Mg^{2+} efflux. Biochem Biophys Res Commun 119: 124–131.
41. Günther T, Vormann J (1985) Mg^{2+} efflux is accomplished by an amiloride-sensitive Na^+/Mg^{2+} antiport. Biochem Biophys Res Comm 130: 540–545.
42. Schweigel M, Vormann J, Martens H (2000) Mechanisms of Mg^{2+} transport in cultured ruminal epithelial cells. Am J Physiol Gastrointest Liver Physiol 278: G400–408.
43. Stout AK, Li-Smerin Y, Johnson JW, Reynolds IJ (1996) Mechanisms of glutamate-stimulated Mg^{2+} influx and subsequent Mg^{2+} efflux in rat forebrain neurones in culture. J Physiol 492: 641–657.
44. Dolder M, Walzel B, Speer O, Schlattner U, Wallimann T (2003) Inhibition of the mitochondrial permeability transition by creatine kinase substrates. J Biol Chem 278: 17760–17766.
45. Agus ZS, Morad M (1991) Modulation of cardiac ion channels by magnesium. Anu Rev Physiol 53: 299–307.
46. Yamaguchi S, Ishikawa T (2008) The electrogenic Na^+-HCO_3^- cotransporter NBCe1-B is regulated by cellular Mg^{2+}. Biochem Biophys Res Commun 376: 100–104.
47. Wolf FI, Trapani V, Simonacci M, Boninsegna A, Mazur A, et al. (2009) Magnesium deficiency affects mammary epithelial cell proliferation: involvement of oxidative stress. Nutr Cancer 61: 131–136.
48. Covacci V, Bruzzese N, Sgambato A, Di Francesco A, Russo MA, et al. (1998) Magnesium restriction induces granulocyte differentiation and expression of p27Kip1 in human leukemic HL-60 cells. J Cell Biochem 70: 313–322.
49. Schweigel M, Park HS, Etschmann B, Martens H (2006) Characterization of the Na^+-dependent Mg^{2+} transport in sheep ruminal epithelial cells. Am J Physiol Gastrointest Liver Physiol 290: G56–65.
50. Wolf FI, Di Francesco A, Covacci V, Cittadini A (1994) cAMP activates magnesium efflux via the Na/Mg antiporter in ascites cells. Biochem Biophys Res Comm 202: 1209–1214.
51. Fatholati M, LaNoue K, Romani A, Scarpa A (2000) Relationship between total and free cellular Mg^{2+} during metabolic stimulation of rat cardiac myocytes and perfused hearts. Arch Biochem Biophys 374: 395–401.
52. He Y, Yao G, Savoia C, Touyz RM (2005) Transient receptor potential melastatin 7 ion channels regulate magnesium homeostasis in vascular smooth muscle cells (Role of angiotensin II). Circ Res 96: 207–215.
53. Büttner S, Günther T, Schäfer A, Vormann J (1998) Magnesium metabolism in erythrocytes of various species. Magnesium-Bulletin 20 : 101–109.
54. Bussiere FI, Gueux E, Rock E, Girardeau JP, Tridon A, et al. (2002) Increased phagocytosis and production of reactive oxygen species by neutrophils during magnesium deficiency in rats and inhibition by high magnesium concentration. Br J Nutr 87: 107–113.
55. Regan RF, Jasper E, Guo Y, Panter SS (1998) The effect of magnesium on oxidative neuronal injury in vitro. J Neurochem 70: 77–85.
56. Hattingen E, Magerkurth J, Pilatus U, Mozer A, Seifried C, et al. (2009) Phosphorus and proton magnetic resonance spectroscopy demonstrates mitochondrial dysfunction in early and advanced Parkinsoǹs disease. Brain 132: 3285–3297.
57. Lodi R, Iotti S, Cortelli P, Pierangeli G, Cevoli S, et al. (2001) Deficient energy metabolism is associated with low free magnesium in the brains of patients with migraine and cluster headache. Brain Res Bulletin 54: 437–441.
58. Malpuech-Brugère C, Nowacki W, Daveau M, Gueux E, Linard C, et al. (2000) Inflammatory response following acute magnesium deficiency in the rat. Biochem Biophys Acta 1501: 91–98.
59. Vormann J, Günther T, Höllriegel V, Schümann K (1995) Effect of various degrees and duration of magnesium deficiency on lipid peroxidation and mineral metabolism in rats. Nutr Biochem 6: 681–688.
60. Cannon JR, Greenamyre JT (2011) The role of environmental exposures in neurodegeneration and neurodegenerative diseases. Toxicological Sciences 124: 225–250.
61. Abou-Sleimann PM, Muqit MM, Wood NW (2006) Expanding insights of mitochondrial dysfunction in Parkinsoǹs disease. Nat Rev Neurosci 7: 207–219.

62. Uitti RJ, Rajput AH, Rozdilsky B, Bickis M, Wollin T, et al. (1989) Regional metal concentrations in Parkinsonˆs disease, other chronic neurological diseases, and control brains. Can J Neurol Sci 16: 310–314.
63. Bocca B, Alimonti A, Senofonte O, Pino A, Violante N, et al. (2006) Metal changes in CSF and peripheral compartments of parkinsonian patients. J Neurol Sci 248: 23–30.
64. Jantaratnotai N, McGeer PL, McLarnon JG (2012) Mechanisms of Mg^{2+} inhibition of BzATP-dependent Ca^{2+} responses in THP-1 monocytes. Brain Res 1442: 1–8.
65. Golts N, Snyder H, Frasier M, Theisler C, Choi P, et al. (2002) Magnesium inhibits spontaneous and iron-induced aggregation of alpha-synuclein. J Biol Chem 277: 16116–16123.
66. Hartwig A (2001) Role of magnesium in genomic stability. Mutation Res 475: 113–121.
67. McCoy MK, Cookson MR (2012) Mitochondrial quality control and dynamics in Parkinson's disease. Antioxidants & Redox Signaling 16: 869–882.

4.3. Publication III

Insulin Modulates the Na^+/Mg^{2+} Exchanger SLC41A1 and Influences Mg^{2+} Efflux from Intracellular Stores in Transgenic HEK293 Cells.

This chapter has been published in: *Journal of Nutrition*
2015 Nov;145(11):2440-7. doi: 10.3945/jn.115.213918. Epub 2015 Sep 9.

Lucia Mastrototaro, Uwe Tietjen, Gerhard Sponder, Jürgen Vormann, Jörg R Aschenbach, Martin Kolisek

You have to read this part online (free of charge).

DOI: http://dx.doi.org/10.3945/jn.115.213918

4.4. Publication IV

Human CNNM2 is not a Mg^{2+} transporter per se

This chapter has been published in: *Pflügers Archiv - European Journal of Physiology*
Epub 2016 Apr, doi 10.1007/s00424-016-1816-7

Gerhard Sponder, **Lucia Mastrototaro**, Katharina Kurth, Lucia Merolle, Zheng Zhang, Nasrin Abdulhanan, Alina Smorodchenko, Katharina Wolf, Andrea Fleig, Reinhold Penner, Stefano Iotti, Jörg R. Aschenbach, Jürgen Vormann, Martin Kolisek

Data in figures 2-4-5-8-10 of the paper “Human CNNM2 is not a Mg^{2+} transporter per se” have been already presented in the thesis of Lucia Mastrototaro “Current re-evaluation of magnesium in human pathophysiology. Role of clinical biochemistry.”- Universitá Cattolica del Sacro Cuore (Roma, Italy).

You have to pruchase this part online.

DOI: http://dx.doi.org/10.1007/s00424-016-1816-7
Pflügers Archiv - European Journal of Physiology, Juli 2016, Vol. 468, Issue 7, pp 1223-1240

4.5. Publication V

Solute carrier 41A3 encodes for a mitochondrial Mg^{2+} efflux system

This chapter has been published in: *Scientific Reports.*
2016 Jun 15, 6:27999. doi: 10.1038/srep27999.

Lucia Mastrototaro, Alina Smorodchenko, Jörg R. Aschenbach, Martin Kolisek, Gerhard Sponder

SCIENTIFIC REPORTS

OPEN

Solute carrier 41A3 encodes for a mitochondrial Mg^{2+} efflux system

Lucia Mastrototaro[1], Alina Smorodchenko[2], Jörg R. Aschenbach[1], Martin Kolisek[1] & Gerhard Sponder[1]

Received: 30 January 2016
Accepted: 24 May 2016
Published: 15 June 2016

The important role of magnesium (Mg^{2+}) in normal cellular physiology requires flexible, yet tightly regulated, intracellular Mg^{2+} homeostasis (IMH). However, only little is known about Mg^{2+} transporters of subcellular compartments such as mitochondria, despite their obvious importance for the deposition and reposition of intracellular Mg^{2+} pools. In particular, knowledge about mechanisms responsible for extrusion of Mg^{2+} from mitochondria is lacking. Based on circumstantial evidence, two possible mechanisms of Mg^{2+} release from mitochondria were predicted: (1) Mg^{2+} efflux coupled to ATP translocation via the ATP-Mg/Pi carrier, and (2) Mg^{2+} efflux via a H^+/Mg^{2+} exchanger. Regardless, the identity of the H^+-coupled Mg^{2+} efflux system is unknown. We demonstrate here that member A3 of solute carrier (SLC) family 41 is a mitochondrial Mg^{2+} efflux system. Mitochondria of HEK293 cells overexpressing SLC41A3 exhibit a 60% increase in the extrusion of Mg^{2+} compared with control cells. This efflux mechanism is Na^+-dependent and temperature sensitive. Our data identify SLC41A3 as the first mammalian mitochondrial Mg^{2+} efflux system, which greatly enhances our understanding of intracellular Mg^{2+} homeostasis.

The key role of magnesium (Mg^{2+}) in a plethora of biochemical processes requires the tight regulation of intracellular Mg^{2+} homeostasis (IMH). The intracellular Mg^{2+} concentration $[Mg^{2+}]_i$ is regulated by the modulation of cellular uptake and efflux and by intracellular storage[1]. Several channels or transporters have been characterized as mediating the uptake of Mg^{2+} (e.g., TRPM6/7, MagT1, or NIPA1) or its extrusion (SLC41A1) across the cytoplasmic membrane[2–5].

Member A1 of the solute carrier family 41 (SLC41A1; further referred to as A1) has been characterized as being a ubiquitous Na^+-dependent Mg^{2+} efflux system integral to the plasma membrane[6,5]. Whereas the characterization of plasma membrane-localised Mg^{2+} transporters is improving, the transporters for intracellular Mg^{2+} are largely unexplored. To date, the mitochondrial channel Mrs2[7,8] and Golgi-localised MMgt1/2[9] are the only known Mg^{2+} transport systems integral to membranes of subcellular compartments. Their discovery supports an earlier assumption that mitochondria, the endoplasmic reticulum (ER), and the Golgi apparatus serve as intracellular Mg^{2+} stores[10,11].

Kubota and colleagues have documented the release of Mg^{2+} from mitochondria upon their depolarization in PC12 cells[10]. Furthermore, long-chain fatty acids induce the rapid release of Mg^{2+} from rat liver mitochondria in alkaline media, presumably via an Mg^{2+}/Me^+ or an Mg^{2+}/H^+ exchanger[12]. Despite the increasing evidence in favour of such a mitochondrial exchanger (Mg^{2+} efflux system), its molecular identity in mammalian cells is as yet unknown. Recently, Cui *et al.* have characterized the protein Ymr166c/Mme1 (mitochondrial magnesium exporter 1) as the first known Mg^{2+} exporter in yeast mitochondria. Reconstitution experiments in proteoliposomes have shown that this transport activity is dependent on the presence of ATP, although ATP hydrolysis is not required. The authors therefore speculate that Mme1 acts as ATP/ATP-Mg exchanger[13]. In a subsequent study, the same group has identified the gene *CG3476* as a *Drosophila melanogaster* orthologue of Mme1. The heterologous expression of *CG3476* in yeast significantly reduces their mitochondrial Mg^{2+} levels. Knock-down or overexpression of the gene both reduces the viability of *Drosophila*. However, the precise mode of function of Ymr166c/Mme1 remains to be elucidated[14].

The present study was based on the hypothesis that SLC41A3 can carry out Mg^{2+} export in eukaryotic cells, similarly to that of SLC41A1. Like the two other members of solute carrier family 41 (SLC41A1 and A2) SLC41A3 contains two "MgtE-like domains" displaying homology to the prokaryotic Mg^{2+} transporter MgtE[15,16]. Human *SLC41A3* has been mapped to chromosome 3q21.2–q21.3, and seven alternative splice variants are predicted to

[1]Institute of Veterinary-Physiology, Free University of Berlin, Oertzenweg 19b, Berlin, D-14163, Germany. [2]Institute of Vegetative Anatomy, Charité, Universitätsmedizin Berlin, Campus Charité-Mitte, Berlin, D-10117, Germany. Correspondence and requests for materials should be addressed to G.S. (email: gerhard.sponder@fu-berlin.de)

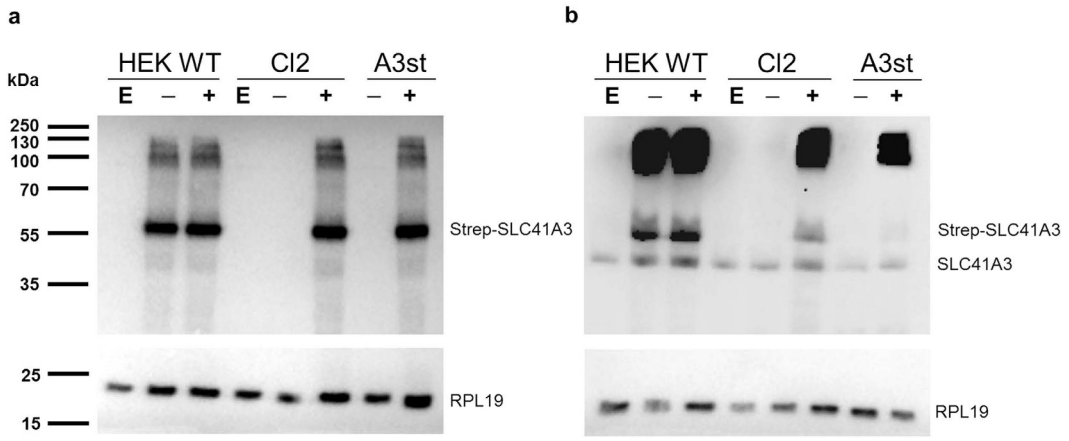

Figure 1. Comparison of SLC41A3 protein levels in various HEK293 cell lines. HEK293 WT cells (HEK WT) or the HEK293 cell line with stably integrated Tet-repressor (Cl2) were transiently transfected with pcDNA5TO-SLC41A3 (− and +) or the empty vector control (E). Protein expression in the transiently transfected cell lines (HEK WT and Cl2) and in the stably transfected cell line (A3st) was induced by addition of tetracycline to a final concentration of 1 μg/ml (+). Uninduced control cells remained untreated (−). Cells were harvested after 24 hours of induction and lysed in RIPA buffer. Total protein extracts were analyzed on an 8.5% PAA-SDS gel and immunodetection of SLC41A3 (55 kDa) was either performed with an antibody directed against the Strep-tag (**a**) or against the native protein (**b**). The signals for the monomeric forms of native and Strep-tagged SLC41A3 are indicated. The ribosomal protein RPL19 (23 kDa) served as loading control and was detected by reprobing the membranes with the respective antibody.

be produced. The full-length protein consists of 507 amino acids with a molecular weight of 54.7 kDa. *SLC41A3* transcripts have been detected in various murine tissues, with the highest levels occurring in the central nervous system (in particular, in the neuronal cells of the cerebral cortex, the hippocampus, and lateral ventricle and in most cell types of the cerebellum)[17]. The anticipated importance of SLC41A3 (further referred to as A3) in CNS is further supported by the detection of neurological and behavioural abnormalities and, in particular, the abnormal locomotor coordination with ataxia, in the conditional knock-out mouse line *Slc41a3*$^{tm1a(KOMP)Wtsi}$ (http://www.mousephenotype.org/). Furthermore, the expression of *A3* is significantly increased in mice fed a Mg^{2+}-deficient diet suggesting the importance of A3 for IMH[18,19]. The heterologous overexpression of A3 in *Xenopus* oocytes is associated with electrogenic Mg^{2+} conductance. These currents are saturable with a K_m of 1.5 mM. Moreover, other ions have been identified as being transported via A3, a finding suggesting that A3 is an unspecific cation channel with a broad permeation profile[20]. The A3-specific electrogenic Mg^{2+} conductance seen in *Xenopus* oocytes has not been detected in mammalian cells. Sahni and colleagues have reported that A3 overexpressed in TRPM7-deficient B lymphocytes fails to restore normal Mg^{2+} homeostasis in these cells[15].

We have therefore examined the cellular localisation of A3 and its ability to transport Mg^{2+}. The presented data provide convincing evidence that SLC41A3 encodes a mitochondrial Mg^{2+} transporter responsible for the Na^+-dependent efflux of the ion.

Results

Creation of tet-inducible HEK293 cell lines overexpressing SLC41A3. To study the function and cellular localisation of A3, a tet-inducible stably transfected cell line was newly generated expressing the protein with an N-terminal HA-Strep tag (A3st). At 24 hours after the addition of tetracycline, efficient inducible expression was detected by Western blot analysis with an antibody against the Strep tag (Fig. 1a, A3st). Furthermore, a HEK293 cell line stably expressing the tetracycline repressor (tetR) was constructed that served as a host for the regulated transient expression of A3. Wild-type HEK293 cells were transfected with the linearized plasmid pcDNA6/TR and cultured under blasticidin selection. Clones that stably expressed the tet repressor were subsequently transfected with the pcDNA5/TO-SLC41A3 construct and tested for their ability to down-regulate the expression of A3 in the absence of tetracycline. Amongst all transiently A3-expressing cell lines, "Clone2" (Cl2) exhibited the lowest level of A3 expression in the absence of tetracycline and abundant expression after induction and was therefore used for further experimentation (Fig. 1a). In contrast to Cl2, protein expression in HEK293 wild-type cells transiently transfected with pcDNA5/TO-SLC41A3 (HEK WT) was independent of the presence of tetracycline due to the absence of the tet repressor (Fig. 1a). We furthermore sought to compare the expression levels of native and overexpressed A3. In parallel to the detection of overexpressed A3, the same samples were analysed on a parallel blot with an antibody directed against native A3 (Fig. 1b). Specificity of this antibody was confirmed in a blocking peptide competition assay (Supplemental Fig. S1). Immunodetection with the A3 antibody yielded two different signals, one for the monomeric form of untagged and one for the monomeric form of Strep-tagged A3. The apparent size difference is due to the HA-Strep tag which increases the molecular weight of SLC41A3 by approx. 4,3 kDa (Fig. 1b). Both antibodies furthermore detected high molecular weight signals between 100 and 250 kDa (Fig. 1a,b). These signals might arise from A3-containing, protein complexes that are

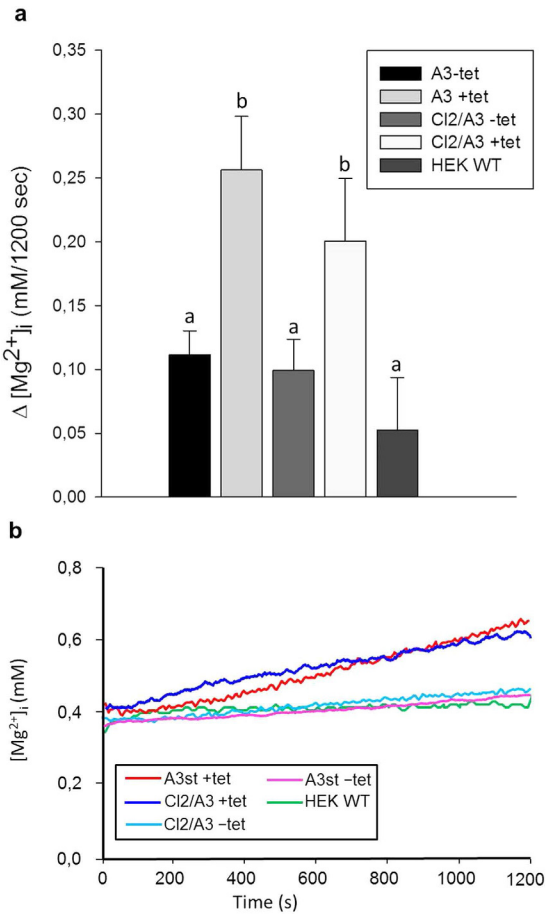

Figure 2. Effect of the expression of SLC41A3 on the change of the intracellular free magnesium concentration ($\Delta[Mg^{2+}]_i$) in HEK293 cells. (a) Tetracycline-induced (+tet) and uninduced (−tet) cells of the SLC41A3 overexpressing cell lines A3st (stable A3 expression) and Clone2 (transient A3 expression) were loaded with Mg^{2+}, and changes of $[Mg^{2+}]_i$ after 1,200 s in completely Mg^{2+}-free solution were determined. Wild-type HEK293 cells (HEK WT) served as a control. Values are given as means ± SEM. Number of measurements: $N_{A3\ -tet} = 17$; $N_{A3\ +tet} = 12$; $N_{Cl2/A3\ -tet} = 10$; $N_{Cl2/A3\ +tet} = 10$; $N_{HEK\ WT} = 6$. ^{a,b}Columns with different letters differ significantly in pairwise comparisons. ($P < 0.05$). **(b)** Representative original recordings of $[Mg^{2+}]_i$ changes of Mg^{2+} -preloaded cells measured in completely Mg^{2+}-free external buffer solution.

not readily dissolved in sample loading buffer. Alternatively, these signals might be A3 aggregates resulting from the strong overexpression of the protein.

SLC41A3 does not mediate Mg^{2+} transport across the plasma membrane but leads to an increase in the free cytoplasmic $[Mg^{2+}]$ when overexpressed. Member A1 of solute carrier family 41 has been extensively characterized as the major Mg^{2+}-extrusion system in the plasma membrane[6,5,21]. The amino acid sequences of A1 and A3 display 56.3% sequence identity and 72.7% sequence similarity (calculated with EMBOSS 6.3.1:matcher, http://mobyle.pasteur.fr/cgi-bin/portal.py?#forms::matcher), respectively. According to the prediction program PSORTII (http://psort.hgc.jp/), the probability for the plasma membrane localisation of A3 is 78.3%, and only 21.7% for its localisation in the endoplasmic reticulum. Based on these data, a functional similarity to the well-characterized plasma membrane Na^+/Mg^{2+} exchanger A1 was assumed. To examine the anticipated function of A3, we investigated the effect of A3 overexpression on Mg^{2+} fluxes in intact cells. By using the Mg^{2+}-sensitive fluorescent dye mag-fura 2, we first examined the ability of SLC41A3 to mediate Mg^{2+} extrusion (efflux condition). Cells were loaded with mag-fura 2 and subsequently incubated in a buffer solution containing 10 mM $MgCl_2$ for 20 min. Thereafter, the Mg^{2+}-fluxes were measured over a time period of 1,200 s in nominally Mg^{2+}-free buffer solution containing 145 mM NaCl. Surprisingly, induced cells of the stable cell line (A3st +tet) and of the transiently transfected cells (Cl2/A3 +tet) did not exhibit Mg^{2+} extrusion but rather an increase in $[Mg^{2+}]_i$ of 0.26 ± 0.04 and 0.20 ± 0.05 mM/1,200 s (Fig. 2a,b), respectively. In contrast, uninduced A3st (A3st −tet; 0.11 ± 0.02 mM/1,000 s), transiently transfected uninduced Cl2/A3 cells (Cl2/A3 −tet; 0.10 ± 0.02 mM/1,000 s), and wild-type HEK293 cells (HEK WT; 0.05 ± 0.04 mM/1,000 s) exhibited significantly lower changes of $[Mg^{2+}]_i$ ($P < 0.05$). These data indicate that the increase in $[Mg^{2+}]_i$ in induced cells was A3 related. Given that the experiments were carried out in completely Mg^{2+}-free buffer solution, the increase in the cytoplasmic free Mg^{2+} concentration in SLC41A3-overexpressing cells could not have been caused by Mg^{2+} influx across the plasma membrane.

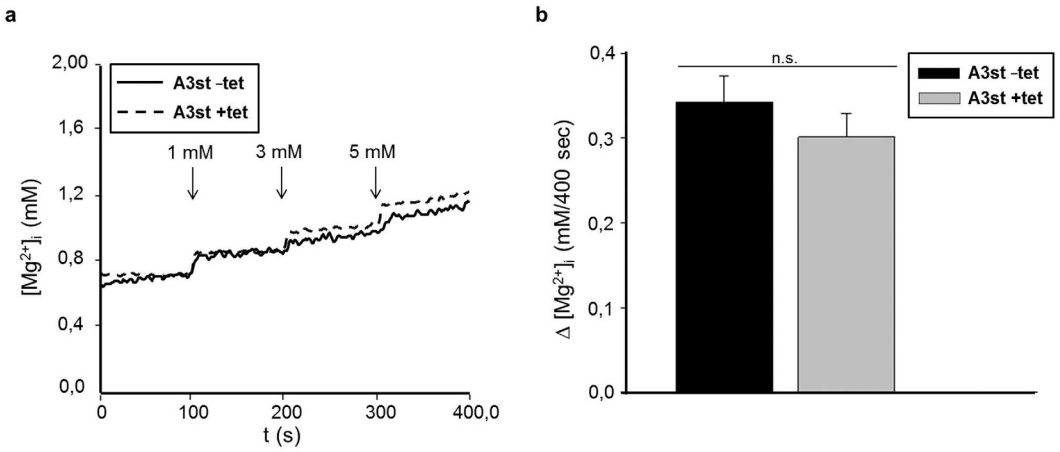

Figure 3. Overexpression of SLC41A3 does not alter the Mg^{2+} uptake capacity across the plasma membrane in HEK293 cells. (a) Tetracycline-induced (+tet) or uninduced (−tet) A3st cells were loaded with mag-fura 2, and measurements were carried out in completely Mg^{2+}-free buffer solution to which Mg^{2+} was added after 100 s (1 mM), 200 s (3 mM), and 300 s (5 mM final concentration). **(b)** Changes in the intracellular Mg^{2+} concentration (Δ $[Mg^{2+}]_I$), calculated from averaged concentrations of the first and the last 50 s of the measurement, were 0.34 mM ± 0.03 for uninduced control cells and 0.30 ± 0.03 mM for induced cells. (n.s., not significant).

To substantiate the inability of SLC41A3 to mediate flux of Mg^{2+} across the plasma membrane, Mg^{2+} influx experiments were performed. A3st cells were induced with tetracycline for 24 hours or left untreated and loaded with mag-fura 2. Subsequently, $[Mg^{2+}]_i$ was measured over a period of 400 s in which Mg^{2+} was added stepwise to final extracellular concentrations of 1, 3 and 5 mM. The shorter duration of 400 s was chosen to minimize the release of Mg^{2+} from intracellular stores. Representative curves for HEK293 cells overexpressing SLC41A3 and for uninduced control cells are shown in Fig. 3a. As expected, in the presence of an inwardly directed Mg^{2+} gradient, −tet and +tet A3st cells exhibited the uptake of the ion into the cell. However, the overexpression of the protein did not result in a significantly different uptake capacity (Fig. 3b), implying that SLC41A3 did not mediate the influx of Mg^{2+} across the plasma membrane under our experimental conditions. Thus, the only logical explanation is that, in response to the overexpression of SLC41A3, Mg^{2+} stored in organelles is released, thereby increasing the cytoplasmic Mg^{2+} concentration.

SLC41A3 is a mitochondrial protein. Next, we performed subcellular fractionation using the Qproteome cell compartment kit (Qiagen) to assess the localisation of SLC41A3 within the cell. In uninduced A3st cells (−tet) a band of ~55 kDa corresponding to A3 was almost exclusively detected in the membrane fraction when using an antibody recognizing native A3 (M; Fig. 4). In induced A3st cells (+tet) detection with the native antibody yielded two signals, one for native A3 and one for the overexpressed Strep-tagged protein. In addition, a weak signal was detected in the fraction containing soluble proteins (C); this signal might have been caused by minor contamination during the sequential isolation of the various fractions. No signal for SLC41A3 was detected in the fractions enriched for nuclear (N) or cytoskeletal proteins (fraction S; Fig. 4). The specificity of the fractionation process was controlled by probing parallel blots with antibodies against the cytosolic ribosomal protein (RP)L19 (fraction S) and the plasma membrane protein PMCA4 (membrane fraction, M). The cytosolic protein RPL19 was detected only in the soluble protein fraction, and the plasma membrane Ca^{2+} ATPase PMCA4 was found, as expected, in the membrane fraction. These data clearly characterize SLC41A3 as being a membrane protein.

As mentioned above, SLC41A3 is predicted to be most likely targeted to the plasma membrane and less probably to the ER. To clarify further the subcellular localisation of SLC41A3 and to exclude potential targeting to the ER, we used an ER isolation kit (Fig. 5a). Various organelle marker proteins were used to control the specificity of the isolation process: Golgin-97 as a Golgi marker, ERp72 for the ER, and COX IV for mitochondria. Most importantly, the experiment was performed with wild-type HEK293 cells, and only endogenous levels of SLC41A3 were detected with an antibody directed against the native protein. As shown in Fig. 5a, various fractions were collected during the differential centrifugation process. SLC41A3 was predominantly detected in fraction M, which mainly contained mitochondrial membranes as verified by the strong signal for COX IV in this fraction. A signal for SLC41A3 was also observed in fraction P1, which contained unbroken cells and plasma membrane. The highly pure ER fraction did not contain SLC41A3. Golgi vesicles were mainly found in fraction SN, which also did not overlap with the signal for native SLC41A3. Taken together, these data clearly argue for the localisation of SLC41A3 in mitochondria and exclude that the protein is targeted to the ER under physiological expression levels.

Next, we sought to confirm the cellular distribution of A3 by fluorescence microscopy. To this end, we performed double-stain immunofluorescence with an antibody directed against the native protein together with an antibody against the mitochondrial marker protein COX IV. Induced and uninduced A3st cells were used to

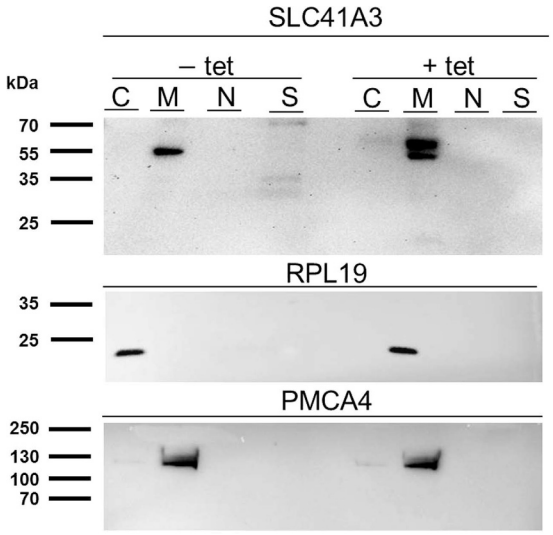

Figure 4. Immunodetection of SLC41A3 after subcellular fractionation. Cytosolic (C), membrane (M), nuclear (N), and cytoskeletal (S) protein-enriched fractions were isolated from −tet and +tet A3st cells and analysed by Western blot. Immunodetection was performed with an antibody directed against native SLC41A3. Immunosignals were detected exclusively in the membrane protein fraction (M) in −tet cells as a single band corresponding to the native protein and, in +tet cells, as two bands corresponding to native and Strep-tagged SLC41A3, respectively. To confirm the specificity of the fractionation, PMCA4 was used as a control for the membrane fraction (M) and RPL19 for the cytoplasmic protein fraction (C).

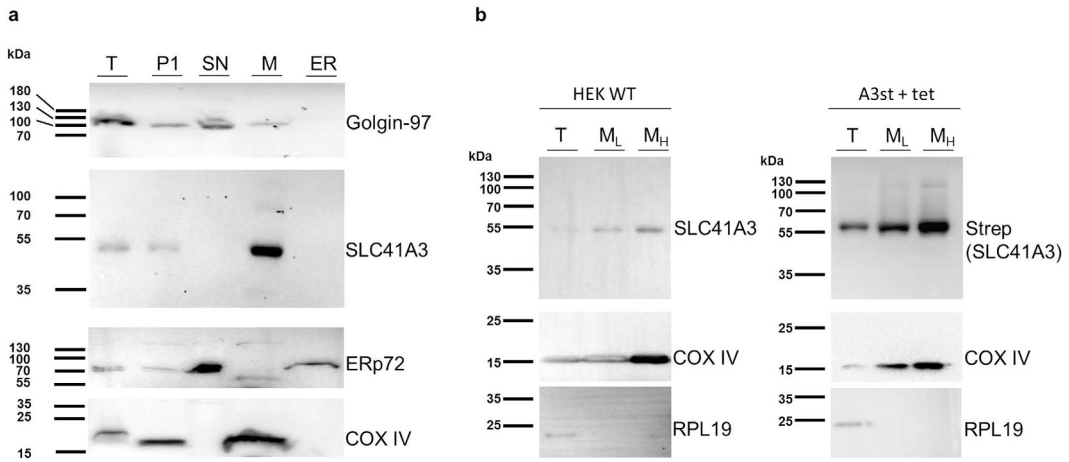

Figure 5. SLC41A3 is primarily localised in mitochondria. (a) Western blot analysis of the total protein fraction (T) and the various fractions (pellet 1, P1; supernatant, SN; mitochondrial pellet, M; endoplasmic reticulum, ER) obtained by using an ER isolation kit and differential centrifugation. SLC41A3 was detected with an antibody recognizing the native protein. Golgin-97 served as a Golgi marker, ERp72 as a marker for the ER, and COX IV for mitochondria. **(b)** A mitochondria isolation kit (Sigma-Aldrich) was used to isolate mitochondria-enriched fractions of wild-type HEK293 cells (HEK WT) and of tetracycline-induced A3st (A3st +tet) cells. The total protein fraction (T) was obtained by solubilizing intact cells. The second fraction and third fractions (M_L and M_H) were enriched in mitochondria. The more purified "heavy" fraction M_H was obtained by low-speed centrifugation (3,500 *g*), whereas the light M_L fraction was isolated by high-speed centrifugation (11,000 *g*). The antibody recognizing native SLC41A3 was used to detect the protein in fractions obtained from HEK WT cells. An anti-Strep antibody was used for the detection of overexpressed SLC41A3 in fractions of A3st +tet cells. Respiratory chain complex IV (COX IV) served as a mitochondrial loading control and the soluble protein RPL19 for the total protein fraction.

detect potential mistargeting and any aberrant localisation within the cell attributable to the overexpression of the protein (Fig. 6). Strong colocalisation of the two signals was observed in A3st +tet and notably also in A3st −tet cells. These data confirm our previous observations and again suggest that A3 is targeted to mitochondria, both when overexpressed and when under the control of its endogenous promoter. Furthermore, we performed

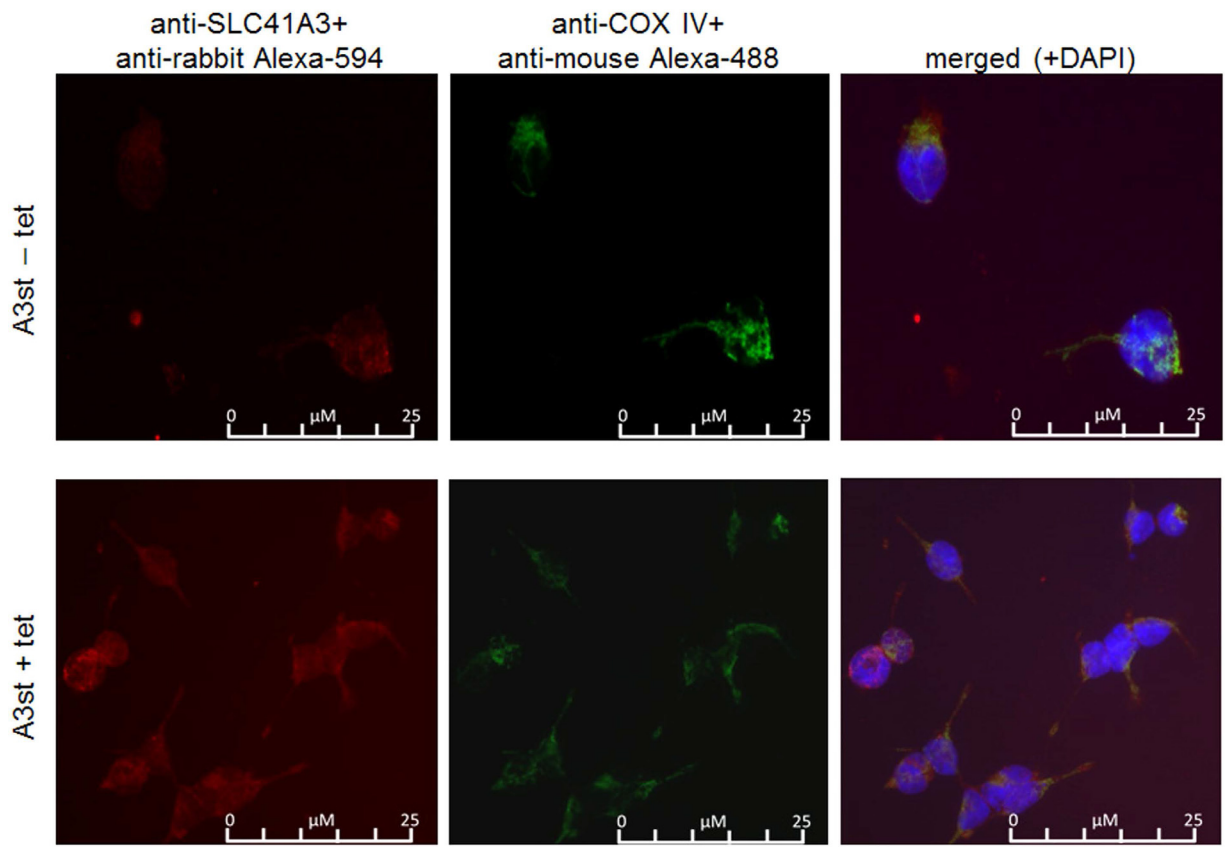

Figure 6. Fluorescence visualization of mitochondrial SLC41A3 localisation. Triple-staining with anti-SLC41A3 antibody (red), anti-COX IV antibody (green) and DAPI (Blue, ony shown in merged) was performed. The merged picture shows that immunosignals for SLC41A3 and COX IV colocalised in uninduced (A3st −tet) and induced (A3st +tet) cells with a stronger intensity upon tetracycline induction.

double-stain immunofluorescence in uninduced and induced A3st cells with the anti-Strep antibody in combination with either the mitochondrial marker COX IV, ERp72 for the endoplasmic reticulum or Glogin-97 as Golgi marker. These results are summarized in Supplemental Figs S2–S4. Similar to the results obtained with the native antibody, significant colocalisation was only observed with the mitochondrial protein COX IV (Supplemental Fig. S2).

Finally, we directly isolated mitochondria from HEK WT and A3st +tet cells. After the homogenization step, the obtained suspension was first centrifuged at low speed (3,500 rpm) to obtain a more purified fraction of "heavy" mitochondria. The remaining supernatant was then centrifuged at high speed (10,000 rpm) to yield a fraction enriched in "light" mitochondria. Both fractions were analysed by Western blot, together with the total protein extract. The inner mitochondrial membrane protein COX IV was used as a marker protein to control the specificity of the fractionation process. In the fractions obtained from HEK WT cells, A3 was detected in the two mitochondrial fractions with the antibody recognizing the native protein and was clearly enriched, in particular, in the purer "heavy" mitochondrial fraction compared with the total protein extract (Fig. 5b). In A3st +tet cells, overexpressed A3 was detected with the anti-Strep antibody. The fact that Strep-tagged A3 is enriched particularly in the "heavy" mitochondrial fraction confirmed that also the overexpressed protein is efficiently target to mitochondria.

Overexpression of SLC41A3 increases the efflux of Mg^{2+} from mitochondria. The above presented data clearly argue for the mitochondrial localisation of SLC41A3 and open up the possibility that the protein functions as a Mg^{2+} extrusion system in the inner mitochondrial membrane. To test this hypothesis, we established a "Mg^{2+}-loading" protocol for isolated, respiring mitochondria similar to that used successfully to study the function of SLC41A1 in whole cells[6,5]. Mitochondrial Mg^{2+} loading takes advantage of the strong inside-negative membrane potential of −150 to −180 mV that is the major driving force for the high capacity Mg^{2+} uptake system, the Mg^{2+}-selective channel Mrs2. Incubation of isolated respiring mitochondria in Mg^{2+}-containing buffer solutions results in the rapid regulated uptake of the ion. Accordingly, we made use of the observation that isolated mitochondria can be efficiently "loaded" with Mg^{2+} [7] and investigated the effect of overexpression of SLC41A3 on the Mg^{2+} efflux capacity out of the organelle (Fig. 7a,b). Isolated mitochondria were first loaded with the membrane-permeable acetoxymethyl ester (AM) of mag-fura 2 in the presence of 10 mM $MgCl_2$, followed by an activation/loading step. During the latter step, the dye was activated by intra-organellar esterases in the presence of $MgCl_2$. The intramitochondrial free Mg^{2+}-concentration $[Mg^{2+}]_m$ was then determined over a time

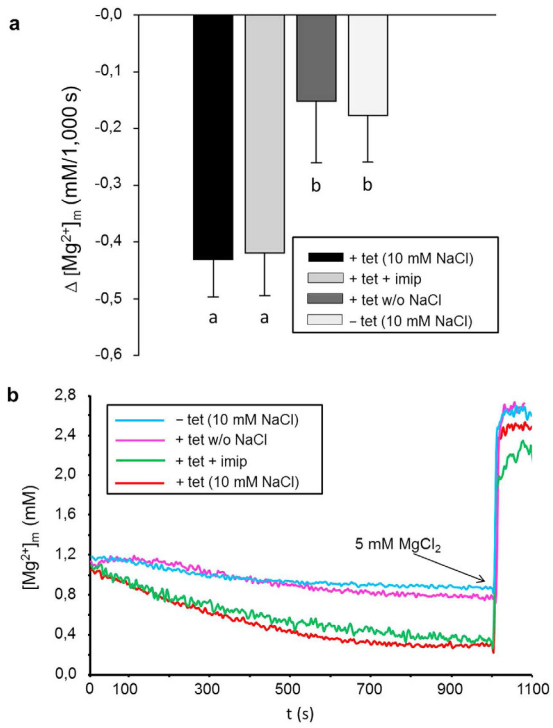

Figure 7. Effect of the overexpression of SLC41A3 on the mitochondrial free magnesium concentration ($[Mg^{2+}]_m$) in HEK293 cells. (a) Mitochondria of tetracycline-induced (+tet) and uninduced (−tet) cells of the SLC41A3 stable cell line A3st were loaded with Mg^{2+}, and changes of $[Mg^{2+}]_m$ during 1,000 s in completely Mg^{2+}-free solution were determined. All solutions contained 10 mM NaCl, except solution +tet without NaCl. The imipramine concentration was 250 μM. Values are given as means ± SEM. Number of measurements: $N_{A3\ -tet\ (10\,mM\ NaCl)} = 12$; $N_{A3\ +tet+imip} = 6$; $N_{A3\ +tet\ (without\ NaCl)} = 5$; $N_{A3\ -tet} = 13$; [a,b]Columns with different letters differ significantly in pairwise comparisons ($P < 0.01$). **(b)** Representative original recordings of $[Mg^{2+}]_m$ changes of isolated mitochondria in completely Mg^{2+}-free medium with or without Na^+ in the external buffer solution. Before the measurements, mitochondria were loaded with Mg^{2+} by incubating them in Mg^{2+}-containing buffer solution (10 mM) for 20 min. Imipramine (imip) was added to the buffer solution directly before measurements were recorded. After 1,000 s, $MgCl_2$ was added to give a final concentration of 5 mM, resulting in a steep increase of the mitochondrial $[Mg^{2+}]$.

period of 1,000 s in nominally Mg^{2+}-free buffer solution. After the 1,000 s efflux period, Mg^{2+} was added to give a final concentration of 5 mM in order to demonstrate that the mitochondria maintained their vitality and were able to rapidly increase their free $[Mg^{2+}]_m$ upon external Mg^{2+} exposure. Figure 7b shows representative curves for mitochondria isolated from overexpressing cells and control cells, whereas Fig. 7a shows summarized data for $\Delta[Mg^{2+}]_m$ over the efflux period. Overexpression of SLC41A3 significantly ($P < 0.01$) increased the efflux capacity by ~55% compared with control cells (−0.43 ± 0.07 mM/1,000 s vs. −0.18 ± 0.08 mM/1,000 s). Moreover, the higher rate of Mg^{2+} efflux was also reflected by the lower free $[Mg^{2+}]_m$ at the start of each efflux measurement. The starting $[Mg^{2+}]_m$ (value calculated as the average of the first 50 s of each measurement) of mitochondria isolated from SLC41A3 overexpressing cells was significantly ($P < 0.05$) reduced by 21.2% compared with that of uninduced control cells. This indicates that the mitochondria of SLC41A3 overexpressing cells are loaded less effectively with Mg^{2+} because of a stronger activity of the extrusion system.

Mg^{2+} efflux from mitochondria overexpressing SLC41A3 is dependent on the presence of Na^+. Interestingly, the SLC41A3-dependent increase in the efflux capacity was only observed when 10 mM NaCl was present in the external buffer solution. In NaCl-free buffer solution, the efflux capacity of mitochondria isolated from induced cells (−0.15 ± 0.11 mM/1,000 s) was reduced to levels comparable with that of uninduced control mitochondria (Fig. 7). To investigate further the role of Na^+ in Mg^{2+} extrusion, we performed efflux measurements in the presence of various NaCl concentrations (Fig. 8). Increasing the Na^+ concentration in the measurement buffer solution to 20 and 40 mM resulted in higher Mg^{2+} extrusion rates compared with measurements performed in the presence of 10 mM NaCl (Fig. 8b). As shown in Fig. 8a, when Mg^{2+} efflux in the presence of 10 mM NaCl was set at 100%, the presence of 20 mM or 40 mM NaCl in the buffer solution increased the efflux capacity to 177 ± 21% and 246 ± 45%, respectively ($P < 0.01$). Next, we investigated the effect of replacing Na^+ in the measurement solution with N-methyl-D-glucamine (NMDG). The presence of 10 mM NMDG-Cl instead of 10 mM NaCl almost abolished the Mg^{2+} efflux capacity of mitochondria (34.5 ± 7.9%).

SLC41A3-mediated Mg^{2+} efflux is temperature-sensitive but not affected by imipramine. We furthermore investigated whether imipramine, a known inhibitor of Na^+/Mg^{2+} exchange mediated via SLC41A1[5],

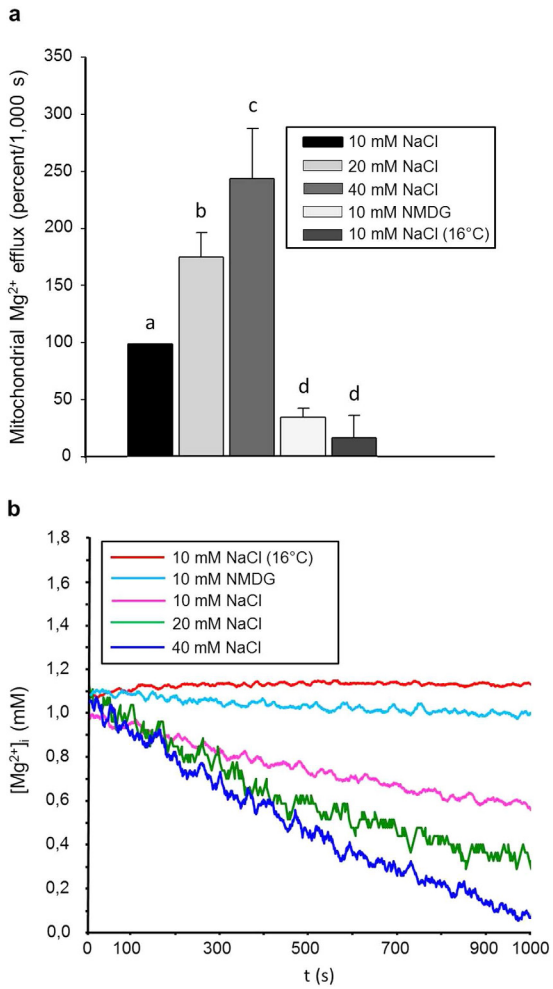

Figure 8. SLC41A3-mediated efflux of Mg^{2+} is dependent on the Na^+ concentration in the external buffer solution and is temperature-sensitive. (a) Mitochondria of tetracycline-induced (+tet) cells of the SLC41A3 stable cell line were loaded with mag-fura2 and Mg^{2+}, and the changes of $[Mg^{2+}]_m$ during 1,000 s in completely Mg^{2+}-free solution were determined. The external buffer solution contained various concentrations of NaCl. Values obtained with 10 mM NaCl were set as 100% efflux activity. The efflux capacity increased with increasing NaCl concentrations in the measurement solution. Mitochondria measured at 16 °C exhibited a strongly reduced efflux of Mg^{2+}. Similarly, replacement of NaCl with NMDG significantly reduced Mg^{2+} extrusion to approx. 34% of the standard efflux activity. Values are given as means ± SEM. Number of measurements: $N_{10\,mM\,NaCl} = 9$; $N_{20\,mM\,NaCl} = 7$; $N_{40\,mM\,NaCl} = 7$; $N_{10\,mM\,NMDG} = 5$; $N_{10\,mM\,NaCl\,(RT)}$ 5. ^{a,b,c,d}Columns with different letters differ significantly in pairwise comparisons ($P < 0.01$). **(b)** Representative original recordings of $[Mg^{2+}]_m$ changes of isolated mitochondria in completely Mg^{2+}-free medium with various concentrations of NaCl in the external measurement medium. N-Methyl-D-glucamine (NMDG) was used to replace sodium in the measurement buffer.

affected Mg^{2+} extrusion from mitochondria isolated from cells overexpressing SLC41A3. Under our experimental conditions, the application of 250 μM imipramine did not reduce the efflux capacity (Fig. 7). Finally, we tested whether the observed Mg^{2+} efflux was sensitive to changes in incubation temperature. At the lower temperature of 16 °C, Mg^{2+} efflux from mitochondria was almost completely abolished and was similar to that of mitochondria incubated in the absence of Na^+ (Fig. 8).

The effect of SLC41A3 overexpression on cellular ATP levels under Mg^{2+} starvation conditions. To get a first insight into the physiological role of SLC41A3 we investigated the effect of A3 overexpression in complete medium and under conditions of reduced Mg^{2+} availability on the total levels of cellular ATP. As cells under culture conditions usually exhibit a high glycolytic activity, thereby masking a potential mitochondrial dysfunction, cells were forced to switch to mitochondrial respiration by replacing glucose/glutamine by galactose/glutamine. A3st cells were seeded and grown for 24 h in DMEM/Gal medium. Thereafter, expression of A3 was induced by addition of tetracycline for another 24 h. The DMEM/Gal medium was then exchanged either for HBSS medium with 0.8 mM $MgSO_4$ or for HBSS medium without $MgSO_4$. Control cells remained in DMEM/Gal medium. After an incubation period of 8 h a luminescence based assay was performed to determine cellular ATP

levels. As shown in Supplemental Fig. S5, relative ATP levels of A3st cells continuously grown in DMEM/Gal or incubated for 8 h in Mg^{2+}-containing HBSS medium were unaffected by the expression level of A3. In contrast, cells overexpressing A3 exhibited lower cellular ATP levels than uninduced cells if cultured under Mg limiting conditions. However, due to the high inter-assay variability in luminescence counts the observed reduction in cellular ATP was statistically not significant. Nevertheless, these data imply that overexpression of A3 has a strong tendency to impair mitochondrial ATP production by reducing the Mg^{2+} availability in mitochondria.

Discussion

Magnesium is vital for normal cellular bioenergetics. In mitochondria, Mg^{2+} not only chelates and stabilizes ATP, but also serves as a cofactor of enzymes involved in cellular respiration and energy production[22]. Moreover, isolated, energized mitochondria are able to accumulate Mg^{2+} up to concentrations that are 3 to 5 times higher than those in cytoplasm[7]. Mg^{2+} has been demonstrated to permeate into the mitochondrial matrix via the high-conductance channel Mrs2, which is powered by a steep negative membrane potential on the inner mitochondrial membrane[7].

The demonstration that Mrs2 constitutes a major mitochondrial Mg^{2+} influx system adds the desired molecular ratio to the formerly proposed hypothesis that mitochondria represent the major intracellular Mg^{2+} storage compartment[7,8,10,23]. Mitochondria must therefore be a dynamic, tightly regulated, open system able not only to accumulate, but also to release Mg^{2+}. Salvi *et al.* demonstrated that besides inducing mitochondrial permeability transition, gliotoxin activates a specific Mg^{2+} efflux system in brain mitochondria[24]. To date, two possible mechanisms of Mg^{2+} release from mitochondria have been suggested: (1) a Mg^{2+} transport (efflux) coupled to ATP translocation via an ATP-MgP_i carrier (APC)[25–27], and (2) a Mg^{2+} efflux system powered by H^+ motive force[23,28,29].

The H^+ gradient perpetually building-up on the inner mitochondrial membrane represents the major motive force powering the transport of various solutes across the inner mitochondrial membrane. The Na^+ contribution to the generation of the membrane potential on the inner mitochondrial membrane is thought to be only secondary. However, the role of Na^+ in the transport physiology of mitochondria is indisputable. Na^+ homeostasis in mitochondria is governed by transport mechanisms such as the Na^+/H^+ exchanger (mNHE, Na^+ efflux mechanism[30]), Na^+-HCO_3^- symporter (mNHCO_3 (SLC4A7), Na^+ influx mechanism[31]), and the Na^+/Ca^{2+} exchanger (mNCE, Na^+ influx mechanism[32]). The paucity of data on the matrix Na^+ homeostasis in respiring mitochondria leaves the field largely unexplored. Jung *et al.* have reported that, in isolated respiring mitochondria, the $[Na^+]_m$ is approximately 1/8 of that in the cytosol[30]. However, the gradient might be less pronounced for mitochondria *in situ*[33]. Nevertheless, studies of permeabilized cardiac myocytes have confirmed that the matrix $[Na^+]_m$ is lower than cytosolic $[Na^+]_i$ in energized mitochondria[30,34].

In metabolically inhibited, non-permeabilized MDCK cells, $[Na^+]_m$ reaches striking 113 +/−7 mM, which is approximately double the concentration of Na^+ in the cytoplasm of the same cells[35]. The accumulated Na^+ is then used to "fuel" the influx of Ca^{2+} via mNCE into the mitochondria[35]. This study has shown that mitochondria possess a large potential to accumulate Na^+ that can be used to support the transport of other solutes via Na^+-dependent transport mechanisms under various physiological and pathophysiological situations.

Our data unequivocally demonstrate that SLC41A3 is a protein integral to the inner mitochondrial membrane and that it functions as an Mg^{2+} efflux system coupled with the influx of Na^+. Based on its similarity with member A1 of the same protein family, namely a Na^+/Mg^{2+} exchanger integral to the cytoplasmic membrane, we can assume that the coupling between the Mg^{2+} efflux conducted via SLC41A3 and the Na^+ influx is direct; however, further thorough experiments must be carried out to support this notion. Moreover, we observed a strong temperature dependence of the Mg^{2+} extrusion process mediated by SLC41A3. Reducing the incubation temperature to 16 °C lowered the efflux capacity by ~85% compared with measurements performed at 37 °C. A similar reduction was also observed for the plasma membrane Na^+/Mg^{2+} exchanger SLC41A1[6]. In contrast, Mg^{2+} influx mediated by the high-conductance channel Mrs2 is entirely insensitive to a reduction of the temperature[7]. This is a further indication that the transport conducted by SLC41A3 is a carrier/exchange mechanism. Interestingly, application of the Na^+/Mg^{2+} transport inhibitor imipramine had no effect on the SLC41A3-based Mg^{2+} efflux from mitochondria. This is surprising, since imipramine is a potent inhibitor of the plasma membrane localised Na^+/Mg^{2+} exchanger SLC41A1[5]. However, it can be explained either by stereochemical differences between the Na^+-binding sites in SLC4A1 and in SLC41A3, or by indirect coupling of SLC41A3-mediated Mg^{2+} efflux to Na^+ counter-transport. This issue will need further examination.

Many degenerative diseases are hallmarked by a deranged Mg homeostasis at both the cellular and organism levels[36]. In particular, diseases that belong to hereditary or age-related mitopathies have been demonstrated to be characterized by aberrant mitochondrial homeostasis and the consequent loss of control over cellular energy turnover (e.g., Alzheimer's and Parkinson´s diseases, *diabetes mellitus* type 2, schizophrenia). Furthermore, these diseases are often associated with Mg deficiency[36–42]. To date, the mitochondrial Mg^{2+} channel Mrs2 is the only transport mechanism that might link Mg deficiency with disturbed mitochondrial homeostasis[43]. Indeed, Kuramoto *et al.* have found that the abrogation of Mrs2 function in the CNS of rats causes massive demyelination and have concluded that normal mitochondrial Mg^{2+} homeostasis is essential for the maintenance of myelin and, thus, CNS functions[44]. Mastrototaro *et al.* have recently suggested a role of the insulin signalling cascade in the regulation of cellular magnesium homeostasis via the Na^+/Mg^{2+} exchanger SLC41A1 and also via an early onset of Mg^{2+} efflux from intracellular stores, such as mitochondria, the Golgi apparatus, and the endoplasmic reticulum[45]. However, no molecular mechanism could be proposed to explain the efflux of Mg^{2+} from mitochondria. The discovery of SLC41A3 as a mitochondrial Na^+-dependent Mg^{2+}-efflux system now offers the possibility to examine further the effect of insulin on the deposition and reposition of Mg^{2+} under normal and also pathological (diabetic) conditions. Further research on SLC41A3 will lead to the better understanding of the orchestration between extramitochondrial and intramitochondrial Mg homeostasis and their interrelationship with the energy metabolism of the cell. The observation that under Mg^{2+} starvation conditions ATP levels

are reduced in SLC41A3 overexpressing cells, suggests an important role of SLC41A3 in mitochondrial energy metabolism. We hypothesise that the joint activity of the Mg^{2+} influx system Mrs2 and the Mg^{2+} efflux system SLC41A3 plays a central role for Mg^{2+} homeostasis in mitochondria. This might be of particular importance for improving the therapeutic strategies and management of age-related mitopathies with simple measures such as Mg supplementation.

Materials and Methods

Cell line generation, growth media, and cell culture. To study the localisation and function of SLC41A3, a tetracyclin-(tet)-inducible stably transfected cell line (A3st) was constructed in cooperation with DualSystems Biotech (Schlieren, Switzerland). Briefly, full-length human *SLC41A3* cDNA was cloned into the p*NTGSH* expression vector with an N-terminal HA-Strep tag. The p*NTGSH-HA-Strep-SLC41A3* was electroporated into the Flp-In™ T-REx™ HEK293 cell line (Life Technologies, Darmstadt, Germany) and recombined into a defined genomic integration locus that was inserted into the host cell line. Cells were placed under hygromycin B (Hyg) and blasticidin S (Bla) selection in order to select for cells containing the integrated expression construct. Stable resistant clones were harvested and seeded in fresh medium containing Hyg and Bla and finally screened for tet-inducible expression of the HA-Strep-tagged SLC41A3.

The tet-inducible HEK293 cells with stably integrated SLC41A3 were grown at 37 °C under a 5% CO_2 atmosphere in Dulbecco's modified Eagle's medium (DMEM) supplemented with 10% FBS, 1% penicillin/streptomycin (Pen/Strep), 15 μg/mL Bla, and 100 μg/mL Hyg.

To confirm the results obtained in the genetically modified SLC41A3-HEK293 cells, a cell line transiently expressing SLC41A3 was constructed by using the pcDNA5/TO vector system (Life Technologies, Darmstadt, Germany), which allowed tet-inducible expression.

First, HEK293 cells were stably transfected with the plasmid pcDNA6/TR in order to generate a host cell line constitutively expressing the tet-repressor protein. This plasmid also included the Bla resistance gene under the control of the SV40 promoter; expression of this gene allowed the selection of cells stably transfected with the plasmids. We first determined the minimum Bla concentration necessary to kill wild-type HEK 293 cells within 20 days. The selective medium was replenished every 3 days for a time period of 20 days. The appropriate Bla concentration for our HEK 293 cell line was determined to be 15 μg/mL. In the next step, HEK 293 cells were transfected with pcDNA6/TR by using the transfection reagent polyethylenimine (PEI). At 48 hours after the transfection, the cells were serially diluted to obtain single clones able to grow in medium containing Bla (15 μg/mL). Colonies formed under Bla selection integrated the vector stably into their genome and expressed the tet-repressor gene. Several cell foci were picked, further expanded, and tested for tet-inducible gene expression by transiently transfecting them with pcDNA5/TO-SLC41A3. The clone, termed "Clone 2 (Cl2/A3)", showed the well-regulated expression of SLC41A3 (low background expression in the absence of tet and significant induction of expression upon tet addition).

Cl2/A3 cells were grown at 37 °C and under a 5% CO_2 atmosphere in DMEM supplemented with 10% FBS, 1% Pen/Strep, and 15 μg/mL Bla.

Cloning of SLC41A3 into pcDNA™5/TO. The human gene SLC41A3 was synthetized with an N-terminal HA-Strep tag and cloned via 5′ KpnI and 3′ NotI into the expression vector pcDNA™5/TO under the control of a tet-inducible promoter.

Protein expression and Western blot. SLC41A3 protein expression was induced by the addition of 1 μg/mL tet for 24 hours. After induction, cells were harvested, washed twice in ice-cold phosphate-buffered saline (PBS) and resuspended in lysis buffer (50 mM Tris HCl pH 8.0, 150 mM sodium chloride, 1.2% Triton X-100, 0.1% SDS, 1 mM EDTA, and protease inhibitor cocktail (cOmplete mini, EDTA-free, Roche Diagnostics)). Lysis was performed for 20 min at 4 °C with gentle agitation followed by a clarifying spin (20 min, 14,000 rpm, 4 °C). The supernatant was then resolved on a 10% polyacrylamide-gel (SDS-PAGE). Following electrophoresis, semi-dry blotting to a polyvinylidene difluoride (PVDF) membrane was performed. A primary mouse antibody directed against the Strep-tag (1:2,500, Qiagen, Hilden, Germany) or a rabbit antibody against the N-terminus of native SLC41A3 (Santa Cruz Biotechnology, Heidelberg, Germany) in combination with the respective horseradish peroxidase (HRP)-conjugated secondary antibodies (anti-mouse, 1:1,000; anti-rabbit, 1:2,000; both from Cell Signaling Technology, Frankfurt, Germany) were used to detect SLC41A3. Proteins were visualized by use of the SuperSignal™ West Dura system (Pierce, Dreieich, Germany).

Blocking peptide competition assay with the antibody recognizing native SLC41A3. The SLC41A3-specific rabbit antibody was purchased from Santa Cruz Biotechnology (Heidelberg, Germany) together with the blocking peptide. To test the specificity of the antibody a competition assay was performed. Total protein samples (5 and 15 μg) of HEK293 wild type cells and of induced A3st cells were separated in triplicate on two 8.5% SDS-PAA gels and blotted to a PVDF membrane. Each membrane was cut into three strips. The first strip was incubated with the SLC41A3-specific antibody at a concentration of 0.125 μg/μl in 2.5% milk/TBS-T. The second strip was incubated in a mixture of anti-SLC41A3 antibody (0.125 μg/ml) and blocking peptide (0.25 μg/μl). The third membrane strip was incubated with a mixture of anti-SLC41A3 antibody and blocking peptide with the concentrations mentioned above together with anti-Strep antibody (0.8 μg/μl). After over-night incubation of the membranes with the primary antibody, one membrane was incubated with the anti-rabbit secondary antibody (dilution: 1:2,000, suitable for the anti-SLC41A3 antibody); the second membrane was incubated with the secondary anti-mouse antibody (dilution 1:1,000, suitable for the primary anti-Strep antibody). Proteins were visualized by use of the Clarity™ Western ECL Blotting Substrate (Bio-Rad, Munich, Germany).

Gross cell-compartment specific localisation of SLC41A3. The Qproteome Cell Compartment Kit (Qiagen) was used according to the manufacturer's instructions to isolate sequentially the proteins associated with the cytosol, nucleus, cellular membranes, or cytoskeleton. The various fractions were analysed by Western blotting. For detection of SLC41A3, the above-described antibody recognizing the native protein was used. Specificity of the isolation was controlled with a mouse antibody against the cytosolic marker protein RPL19 (cytosolic ribosomal protein (RP)L19, Abnova, Heidelberg, Germany) and a mouse antibody directed against the plasma membrane Ca^{2+}-ATPase (PMCA4, Sigma-Aldrich, Munich, Germany). Secondary antibodies were the same as those mentioned above.

Isolation of various cellular membranes/organelles from HEK293 cells. The Endoplasmic Reticulum Isolation Kit (Sigma-Aldrich, Munich, Germany) was used for the isolation of intracellular organelles by differential centrifugation. The experiments were performed according to the manufacturer's protocol. In brief, 3×10^8 wild-type HEK293 cells were collected and washed with PBS. Cells were first resuspended in hypotonic extraction buffer, incubated for 20 min at 4 °C, and centrifuged again. The pellet was resuspended in isotonic extraction buffer, and cells were homogenized by using a Dounce homogenizer. An aliquot of the homogenate was saved for Western blot analysis (total protein fraction in Fig. 5a). The homogenate was centrifuged at 1,000 *g* and 4 °C for 10 min. The post-nuclear supernatant was transferred to a new tube. An aliquot was stored for later analysis (fraction SN in Fig. 5a). The remaining supernatant was centrifuged at 12,000 *g* and 4 °C for 15 min. The supernatant represented the post-mitochondrial fraction, whereas the pellet contained the mitochondrial membranes. The pellet was therefore stored for protein extraction and further analysis (fraction M in Fig. 5a). From the post-mitochondrial supernatant, ER-enriched microsomes were prepared by $CaCl_2$ precipitation according to the protocol (fraction ER in Fig. 5a). For Western blot analysis, supernatant fractions were mixed with 4× SDS-sample buffer, and proteins from the pellet fractions were extracted with standard RIPA buffer. Proteins were resolved on 10% polyacrylamide-gels (SDS-PAGE) and blotted to polyvinylidene difluoride (PVDF) membranes. The above-described rabbit antibody was used for detecting native SLC41A3. Antibodies for controlling the specificity of the fractionation were: Golgin-97 as a Golgi network marker, protein disulphide isomerase family A member 4 (ERp72) as an ER marker, and cytochrome c oxidase (COX IV) for mitochondria (all from Cell Signaling Technology, Frankfurt, Germany). Secondary antibodies were used as mentioned above.

Isolation of mitochondria for protein analysis. For the small-scale isolation of an enriched mitochondrial fraction, the Mitoiso2 kit for cultured cells (Sigma-Aldrich, Taufkirchen, Germany) was used according to the manufacturer's protocol. All experiments were performed according to the "homogenization" method. The first "heavy" mitochondrial fraction was obtained by centrifugation at 3,500 *g*, and the remaining supernatant was then centrifuged at 11,000 *g,* yielding the "light" mitochondrial fraction. The obtained fractions were analysed by Western blotting either with the antibody recognizing native SLC41A3 or with the antibody directed against the Strep tag as described previously. RPL19 (mouse anti-RPL19, Abnova, Heidelberg, Germany) was used as a cytosolic marker protein and cytochrome c oxidase (rabbit anti-CoxIV, Cell Signaling Technology, Frankfurt, Germany) as a mitochondrial marker. Secondary antibodies were the same as those mentioned above.

Fluorescence microscopy. Cells were grown on glass coverslips in 12-well plates. At 80% confluence, protein expression was induced by the addition of tetracycline. At 24 hours after induction, cells were treated 15 minutes with 4% paraformaldehyde and then washed 3 times in PBS. Blocking was performed with 10% normal goat serum (NGS) in PBS for 1 hour. The cells were then incubated for 1 hour with the primary antibody against native SLC41A3 diluted 1:500 in 1% NGS, washed three times in PBS and finally incubated 1 hour with a goat anti-rabbit secondary antibody labelled with Alexa red-fluorescent dye (excitation at 561 or 594 nm) at a dilution of 1:500 in 1% NGS. Subsequently, the cells were incubated with a primary antibody against the mitochondrial protein COX IV diluted 1:200, washed three times in PBS and then incubated with a goat anti-mouse secondary antibody labelled with Alexa green-fluorescent dye (excitation at 488 nm) at a dilution of 1:500 in 1% NGS.

Double-stain immunofluorescence was performed also with the two primary antibodies anti-Strep (1:500) and anti-COX IV (1:1000) with the respective secondary antibodies conjugated to Alexa green-fluorescent and Alexa red-fluorescent dyes.

Another aliquot of cells were immunostained with a primary antibody against Strep-tagged SLC41A3 (1:500) and a secondary goat anti-mouse antibody (1:500), followed by an incubation with the primary antibody specific for the Golgi marker protein Golgin-97 (1:100) or the ER marker protein ERp72 (1:100) followed by a secondary goat anti-rabbit antibody (1:500).

Finally the cells were washed in PBS. The coverslips were mounted with the mounting medium Fluoroshield with DAPI (Sigma-Aldrich, Munich, Germany) to visualize cell nuclei and inverted onto glass slides suitable for microscopy. Digital images were acquired with an automated inverted microscope (Leica DMI 6000 B) and analysed with the microscope imaging software Las AF (Leica).

Quantification of intracellular Mg^{2+}. In order to characterize the Mg^{2+} transport activity of SLC41A3, the Mg^{2+}-sensitive fluorescent dye mag-fura 2 was used under influx or efflux conditions. $[Mg^{2+}]_i$ was determined by measuring the fluorescence of the mag-fura-2-loaded cells in an LS55 spectrofluorometer (PerkinElmer) by using the fast filter application with alternating excitation at 340 nm and 380 nm and emission at 515 nm. SLC41A3-HEK cells (stably transfected) were grown to 80% confluence; protein expression was induced by the addition of tetracycline (tet, 1 μg/mL) for 24 hours. Subsequently, cells were gently scraped, washed in Ca^{2+}- and Mg^{2+}-free HBSS (137 mM NaCl; 5.36 mM KCl; 0.34 mM Na_2HPO_4; 0.44 mM KH_2HPO_4; 5.55 mM glucose; 4.17 mM $NaHCO_3$, 20 mM Hepes) and then loaded for 20 min with mag-fura 2 AM (7.5 μM) on a shaking plate at 37 °C. Following mag-fura 2 loading, the cells were incubated for another 20 min at 37 °C in HBSS to allow the

complete de-esterification of the fluorescent probe, washed twice with HBSS to remove extracellular mag-fura 2, and resuspended in completely Mg^{2+}- and Ca^{2+}-free HBSS. Measurements of Mg^{2+} influx were performed at 37 °C in 3-ml cuvettes containing 2 ml cell suspension that was constantly stirred. Extracellular Mg^{2+} was added stepwise at increasing concentrations, ranging from 1 to 5 mM, during the measurement. For the Mg^{2+} efflux experiments, the cells were incubated with 10 mM $MgCl_2$ at 37 °C for 20 min after mag-fura 2 loading, washed twice in Mg^{2+}- and Ca^{2+}-free HBSS, and finally measured in Mg^{2+}- and Ca^{2+}-free HBSS at 37 °C in 3-ml cuvettes.

Large-scale isolation of mitochondria for mag-fura 2 measurements. Cells were harvested in ice-cold PBS, centrifuged, and washed in ice-cold isolation buffer (IB; 210 mM Mannitol, 70 mM sucrose, 5 mM Hepes-KOH pH 7.2, and 0.5% BSA). The cell pellet was resuspended (4 mL IB/g cells), and digitonin (10 mg/mL in DMSO) was added stepwise to permeabilise the cells. The permeabilisation efficiency was controlled by trypan blue staining. After sufficient permeabilisation was reached, 5 ml IB was added, and the suspension was centrifuged (3,000 *g*, 5 min, 4 °C). The pellet was resuspended in IB, and the suspension was homogenized by using a Dounce homogenizer. IB without BSA (3 times the volume of the homogenate) was added, and unbroken cells and cell debris were pelleted by centrifugation (1,200 *g*, 3 min, 4 °C). This clarifying step was repeated once before the suspension was finally centrifuged (10,000 *g*, 20 min, 4 °C) to pellet the mitochondria. The mitochondrial pellet was resuspended in 1 mL IB without BSA supplemented with 0.5 mM ATP, 0.2% succinate, and 0.01% pyruvate.

Quantification of free magnesium in mitochondria. Mitochondria were loaded with mag-fura 2 AM (7.5 μM) for 20 min on a shaking plate at 37 °C in IB without BSA+S (S: supplemented with 0.5 mM ATP, 0.2% succinate, and 0.01% pyruvate). Following mag-fura 2 loading, mitochondria were incubated in IB without BSA+S with 10 mM $MgCl_2$ at 37 °C for 20 min (mag-fura 2 AM activation) and then washed twice in Mg^{2+} and Ca^{2+}-free IB without BSA+S. Finally, $[Mg^{2+}]_i$ was determined in IB without BSA+S supplemented with 10 mM NaCl in an LS55 spectrofluorometer as described above. The osmolarity of the HBSS measurement buffer solutions with various NaCl concentrations or NMDG-Cl was controlled and maintained between 290 and 300 mosmol/L. Imipramine was dissolved in water and added to give a final concentration of 250 μM during the dye activation step and the measurements. Curves of representative recordings were smoothened with a "moving average" algorithm ($F_s = 99$; FL WinLab version 4.00.03).

Determination of relative cellular ATP levels. A luminescence ATP detection assay kit (Abcam, Cambridge, UK) was used to determine relative cellular ATP levels in uninduced and induced A3st cells under various growth conditions. Cells were seeded in duplicate in 24-well plates at a starting density of 8000 cells/well in glucose/glutamine-free DMEM medium (Biochrom, Berlin, Germany). The medium was supplemented with 5 mM D-galactose, 6 mM L-glutamine, 1 mM sodium pyruvate, 10% dialyzed FBS, 15 μg/mL Bla, and 100 μg/mL Hyg. Cells were cultured for 24 hours, and then expression of A3 was induced by addition of tetracycline. Control cells were left untreated. After 24 hours the medium was exchanged either against Mg^{2+}-free HBSS medium (1x HBSS salts, 5 mM D-galactose, 6 mM L-glutamine, 1 mM sodium pyruvate, 10% dialyzed FBS, 15 μg/mL Bla, and 100 μg/mL Hyg) or HBSS medium (same composition as above) but supplemented with 0.8 mM $MgSO_4$. Control cells remained in the aforementioned DMEM medium. After another 6 hours of incubation the ATP assay was performed as follows. Two-hundred μl of the supplied detergent solution was directly added to the medium and the plate was incubated for 5 min in an orbital shaker. Then 200 μl of substrate solution was added to each well and the plate was incubated for another 5 min under constant shaking. The suspension of each well was then transferred to four wells of a 96 well plate (200 μl each) and after 10 min of dark adaptation luminescence was measured with an EnSpire multimode plate reader (PerkinElmer). Results were blank corrected against wells without cells but containing medium, detergent and substrate solution. The experiment was performed two times.

Statistical analyses. (1) A two-tailed Student's t-test was used to compare the differences between two means (i.e., influx in induced and uninduced cells, Fig. 3b). (2) A post hoc Holm-Sidak one-factor ANOVA (all pairwise multiple comparison) was used when three or more groups were compared (i.e., efflux experiments in induced and uninduced stable and transient cell lines in Fig. 2 or mitochondrial efflux, Fig. 7a). (3) A post hoc Dunn's one-factor ANOVA (multiple comparisons versus control group) was used when three or more groups were compared with a control (i.e., mitochondria efflux under various NaCl concentrations or temperature conditions, Fig. 8). (4) A post hoc Holm-Sidak two-factor ANOVA (all pairwise multiple comparison) was used to compare 2 factorial data sets (i.e., tet x different media for the determination of cellular ATP levels, Supplemental Fig. S5).

A Shapiro-Wilk normality test was used for (1), (2) and (3). Data are presented as means ± SE. Differences of $P < 0.05$ were considered significant. Statistical analyses were executed by using SigmaPlot 11.0 (Systat Software, Inc.).

References

1. Romani, A. M. Cellular magnesium homeostasis. *Archives of biochemistry and biophysics* **512,** 1–23, doi: 10.1016/j.abb.2011.05.010 (2011).
2. Nadler, M. J. *et al.* LTRPC7 is a Mg.ATP-regulated divalent cation channel required for cell viability. *Nature* **411,** 590–595, doi: 10.1038/35079092 (2001).
3. Schlingmann, K. P. *et al.* Hypomagnesemia with secondary hypocalcemia is caused by mutations in TRPM6, a new member of the TRPM gene family. *Nature genetics* **31,** 166–170, doi: 10.1038/ng889 (2002).
4. Zhou, H. & Clapham, D. E. Mammalian MagT1 and TUSC3 are required for cellular magnesium uptake and vertebrate embryonic development. *Proceedings of the National Academy of Sciences of the United States of America* **106,** 15750–15755, doi: 10.1073/pnas.0908332106 (2009).

5. Kolisek, M., Nestler, A., Vormann, J. & Schweigel-Rontgen, M. Human gene SLC41A1 encodes for the Na^+/Mg^{2+} exchanger. *American journal of physiology. Cell physiology* **302,** C318–326, doi: 10.1152/ajpcell.00289.2011 (2012).
6. Kolisek, M. *et al.* SLC41A1 is a novel mammalian Mg^{2+} carrier. *The Journal of biological chemistry* **283,** 16235–16247, doi: 10.1074/jbc.M707276200 (2008).
7. Kolisek, M. *et al.* Mrs2p is an essential component of the major electrophoretic Mg^{2+} influx system in mitochondria. *The EMBO journal* **22,** 1235–1244, doi: 10.1093/emboj/cdg122 (2003).
8. Schindl, R., Weghuber, J., Romanin, C. & Schweyen, R. J. Mrs2p forms a high conductance Mg^{2+} selective channel in mitochondria. *Biophysical journal* **93,** 3872–3883, doi: 10.1529/biophysj.107.112318 (2007).
9. Goytain, A. & Quamme, G. A. Identification and characterization of a novel family of membrane magnesium transporters, MMgT1 and MMgT2. *American journal of physiology. Cell physiology* **294,** C495–502, doi: 10.1152/ajpcell.00238.2007 (2008).
10. Kubota, T. *et al.* Mitochondria are intracellular magnesium stores: investigation by simultaneous fluorescent imagings in PC12 cells. *Biochimica et biophysica acta* **1744,** 19–28, doi: 10.1016/j.bbamcr.2004.10.013 (2005).
11. Pisat, N. P., Pandey, A. & Macdiarmid, C. W. MNR2 regulates intracellular magnesium storage in Saccharomyces cerevisiae. *Genetics* **183,** 873–884, doi: 10.1534/genetics.109.106419 (2009).
12. Schonfeld, P., Schuttig, R. & Wojtczak, L. Rapid release of Mg^{2+} from liver mitochondria by nonesterified long-chain fatty acids in alkaline media. *Archives of biochemistry and biophysics* **403,** 16–24, doi: 10.1016/S0003-9861(02)00206-0 (2002).
13. Cui, Y. *et al.* A novel mitochondrial carrier protein Mme1 acts as a yeast mitochondrial magnesium exporter. *Biochimica et biophysica acta* **1853,** 724–732, doi: 10.1016/j.bbamcr.2014.12.029 (2015).
14. Cui, Y., Zhao, S., Wang, X. & Zhou, B. A novel Drosophila mitochondrial carrier protein acts as a Mg^{2+} exporter in fine-tuning mitochondrial Mg^{2+} homeostasis. *Biochimica et biophysica acta* **1863,** 30–39, doi: 10.1016/j.bbamcr.2015.10.004 (2016).
15. Sahni, J. & Scharenberg, A. M. The SLC41 family of MgtE-like magnesium transporters. *Molecular aspects of medicine* **34,** 620–628, doi: 10.1016/j.mam.2012.05.012 (2013).
16. Schweigel-Rontgen, M. & Kolisek, M. SLC41 transporters–molecular identification and functional role. *Curr Top Membr* **73,** 383–410, doi: 10.1016/B978-0-12-800223-0.00011-6 (2014).
17. Visel, A., Thaller, C. & Eichele, G. GenePaint.org: an atlas of gene expression patterns in the mouse embryo. *Nucleic acids research* **32,** D552–556, doi: 10.1093/nar/gkh029 (2004).
18. Goytain, A. & Quamme, G. A. Identification and characterization of a novel mammalian Mg^{2+} transporter with channel-like properties. *BMC genomics* **6,** 48, doi: 10.1186/1471-2164-6-48 (2005).
19. Goytain, A. & Quamme, G. A. Functional characterization of the mouse [corrected] solute carrier, SLC41A2. *Biochemical and biophysical research communications* **330,** 701–705, doi: 10.1016/j.bbrc.2005.03.037 (2005).
20. Quamme, G. A. Molecular identification of ancient and modern mammalian magnesium transporters. *American journal of physiology. Cell physiology* **298,** C407–429, doi: 10.1152/ajpcell.00124.2009 (2010).
21. Kolisek, M. *et al.* Substitution p.A350V in Na^+/Mg^{2+} exchanger SLC41A1, potentially associated with Parkinson's disease, is a gain-of-function mutation. *PloS one* **8,** e71096, doi: 10.1371/journal.pone.0071096 (2013).
22. Volpe, S. L. Magnesium in disease prevention and overall health. *Adv Nutr* **4,** 378S–383S, doi: 10.3945/an.112.003483 (2013).
23. Jung, D. W. & Brierley, G. P. Magnesium transport by mitochondria. *J Bioenerg Biomembr* **26,** 527–535 (1994).
24. Salvi, M., Bozac, A. & Toninello, A. Gliotoxin induces Mg^{2+} efflux from intact brain mitochondria. *Neurochem Int* **45,** 759–764, doi: 10.1016/j.neuint.2004.01.001 (2004).
25. Meisner, H. & Klingenberg, M. Efflux of adenine nucleotides from rat liver mitochondria. *The Journal of biological chemistry* **243,** 3631–3639 (1968).
26. Kun, E. Kinetics of ATP-dependent Mg^{2+} flux in mitochondria. *Biochemistry* **15,** 2328–2336 (1976).
27. Tewari, S. G., Dash, R. K., Beard, D. A. & Bazil, J. N. A biophysical model of the mitochondrial ATP-Mg/P(i) carrier. *Biophysical journal* **103,** 1616–1625, doi: 10.1016/j.bpj.2012.08.050 (2012).
28. Akerman, K. E. Inhibition and stimulation of respiration-linked Mg^{2+} efflux in rat heart mitochondria. *J Bioenerg Biomembr* **13,** 133–139 (1981).
29. Rutter, G. A., Osbaldeston, N. J., McCormack, J. G. & Denton, R. M. Measurement of matrix free Mg^{2+} concentration in rat heart mitochondria by using entrapped fluorescent probes. *The Biochemical journal* **271,** 627–634 (1990).
30. Jung, D. W., Apel, L. M. & Brierley, G. P. Transmembrane gradients of free Na^+ in isolated heart mitochondria estimated using a fluorescent probe. *Am J Physiol* **262,** C1047–1055 (1992).
31. Boedtkjer, E., Praetorius, J. & Aalkjaer, C. NBCn1 (slc4a7) mediates the Na^+-dependent bicarbonate transport important for regulation of intracellular pH in mouse vascular smooth muscle cells. *Circulation research* **98,** 515–523, doi: 10.1161/01.RES.0000204750.04971.76 (2006).
32. Palty, R. *et al.* NCLX is an essential component of mitochondrial Na^+/Ca^{2+} exchange. *Proceedings of the National Academy of Sciences of the United States of America* **107,** 436–441, doi: 10.1073/pnas.0908099107 (2010).
33. Murphy, E. & Eisner, D. A. Regulation of intracellular and mitochondrial sodium in health and disease. *Circulation research* **104,** 292–303, doi: 10.1161/CIRCRESAHA.108.189050 (2009).
34. Donoso, P., Mill, J. G., O'Neill, S. C. & Eisner, D. A. Fluorescence measurements of cytoplasmic and mitochondrial sodium concentration in rat ventricular myocytes. *J Physiol* **448,** 493–509 (1992).
35. Baron, S. *et al.* Role of mitochondrial Na^+ concentration, measured by CoroNa red, in the protection of metabolically inhibited MDCK cells. *J Am Soc Nephrol* **16,** 3490–3497, doi: 10.1681/ASN.2005010075 (2005).
36. Kolisek, M. *et al.* PARK7/DJ-1 dysregulation by oxidative stress leads to magnesium deficiency: implications in degenerative and chronic diseases. *Clin Sci* (*Lond*) **129,** 1143–1150, doi: 10.1042/CS20150355 (2015).
37. Barbiroli, B. *et al.* Low brain intracellular free magnesium in mitochondrial cytopathies. *J Cereb Blood Flow Metab* **19,** 528–532, doi: 10.1097/00004647-199905000-00007 (1999).
38. Barbagallo, M. & Dominguez, L. J. Magnesium and aging. *Curr Pharm Des* **16,** 832–839 (2010).
39. Newsholme, P., Gaudel, C. & Krause, M. Mitochondria and diabetes. An intriguing pathogenetic role. *Adv Exp Med Biol* **942,** 235–247, doi: 10.1007/978-94-007-2869-1_10 (2012).
40. Exner, N., Lutz, A. K., Haass, C. & Winklhofer, K. F. Mitochondrial dysfunction in Parkinson's disease: molecular mechanisms and pathophysiological consequences. *The EMBO journal* **31,** 3038–3062, doi: 10.1038/emboj.2012.170 (2012).
41. Hjelm, B. E. *et al.* Evidence of Mitochondrial Dysfunction within the Complex Genetic Etiology of Schizophrenia. *Mol Neuropsychiatry* **1,** 201–219, doi: 10.1159/000441252 (2015).
42. Jia, D. P., Wang, S., Zhang, B. C. & Fang, F. Paraptosis triggers mitochondrial pathway-mediated apoptosis in Alzheimer's disease. *Exp Ther Med* **10,** 804–808, doi: 10.3892/etm.2015.2531 (2015).
43. Piskacek, M., Zotova, L., Zsurka, G. & Schweyen, R. J. Conditional knockdown of hMRS2 results in loss of mitochondrial Mg^{2+} uptake and cell death. *Journal of cellular and molecular medicine* **13,** 693–700, doi: 10.1111/j.1582-4934.2008.00328.x (2009).
44. Kuramoto, T. *et al.* A mutation in the gene encoding mitochondrial Mg^{2+} channel MRS2 results in demyelination in the rat. *PLoS genetics* **7,** e1001262, doi: 10.1371/journal.pgen.1001262 (2011).
45. Mastrototaro, L. *et al.* Insulin Modulates the Na^+/Mg^{2+} Exchanger SLC41A1 and Influences Mg^{2+} Efflux from Intracellular Stores in Transgenic HEK293 Cells. *J Nutr* **145,** 2440–2447, doi: 10.3945/jn.115.213918 (2015).

Acknowledgements

Our gratitude is due to Martin Marak, Katharina Wolf, and Uwe Tietjen (all Freie Universität Berlin) for competent technical support of the project. Our thanks are also extended to Dr. Theresa Jones for linguistic corrections. This work was supported by research grants from the German Research Foundation KO-3586/3-2 to MK and by an initiative grant from Free University of Berlin to GS.

Author Contributions

G.S. designed the study. L.M., G.S. and A.S. performed the experiments. G.S. and L.M. analysed the data. L.M., M.K. and J.R.A. contributed to the study design. G.S., L.M. and M.K. wrote the manuscript. All authors read, edited, and approved the manuscript.

Additional Information

Supplementary information accompanies this paper at http://www.nature.com/srep

Competing financial interests: The authors declare no competing financial interests.

How to cite this article: Mastrototaro, L. *et al.* Solute carrier 41A3 encodes for a mitochondrial Mg^{2+} efflux system. *Sci. Rep.* **6**, 27999; doi: 10.1038/srep27999 (2016).

Solute carrier 41A3 encodes for a mitochondrial Mg^{2+} efflux system

Lucia Mastrototaro, Alina Smorodchenko, Jörg R. Aschenbach, Martin Kolisek, Gerhard Sponder

Supplementary Information

Supplementary Figures

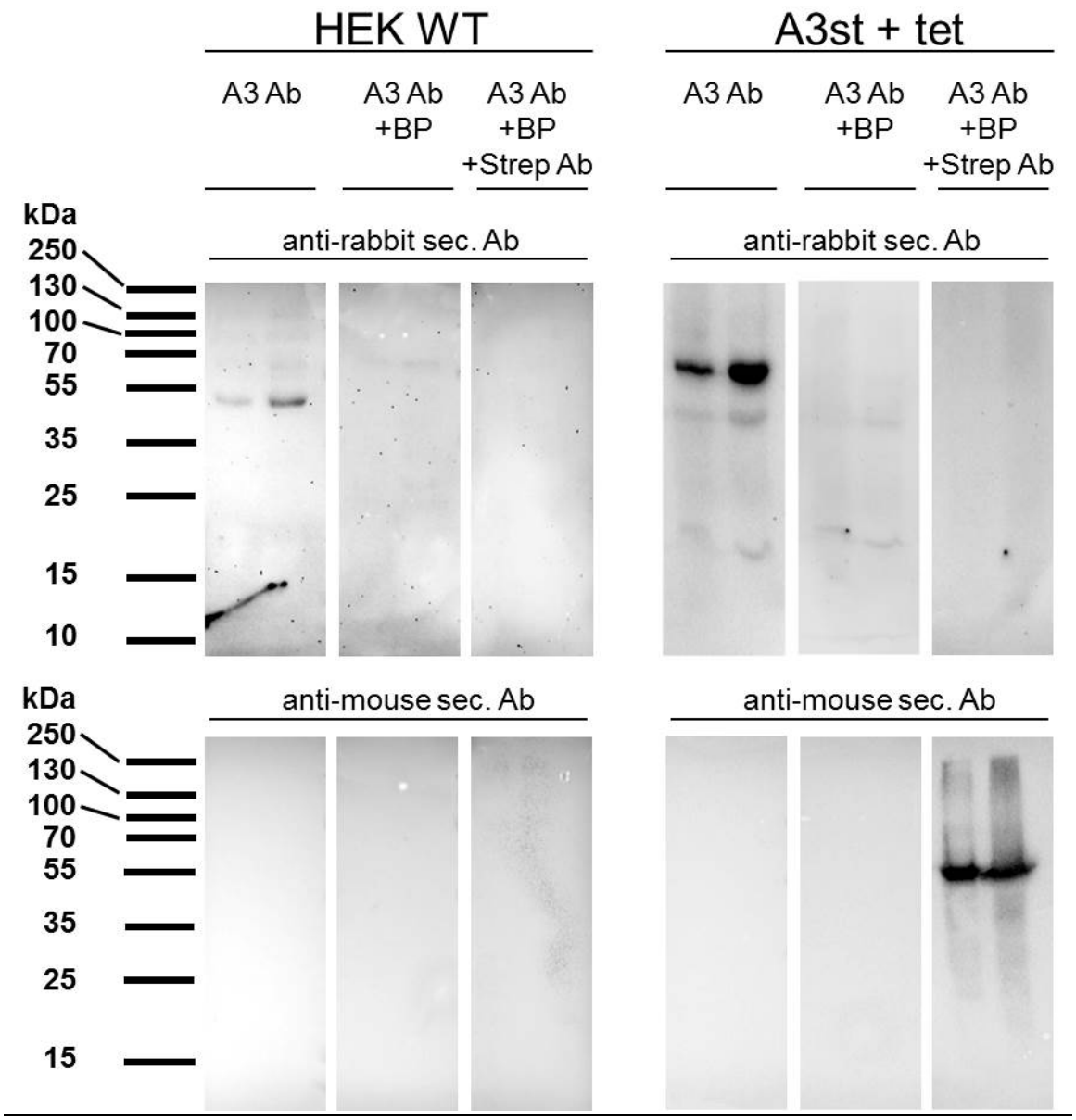

Supplementary Figure S1–Blocking peptide competition assay to verify the specificity of the antibody recognizing native SLC41A3.

Total protein extracts (left lane: 5 µg, right lane: 15 µg) of wild-type HEK293 cells (HEK WT) or tet-induced A3st cells (A3st + tet) were separated in triplicates on two 8.5% SDS-PAA gels and blotted on PVDF membranes. Membrane strips were either incubated with the anti-rabbit SLC41A3 antibody (A3 Ab), with a mixture of A3 Ab and a SLC41A3-specific blocking peptide (BP) or with a mixture of A3 Ab, the blocking peptide, and mouse anti-Strep Ab. After the primary incubation step, the first membrane was incubated with a secondary anti-rabbit antibody, the second membrane with an anti-mouse secondary antibody. Finally, proteins were visualized by chemiluminescence. In HEK WT cells (left panel) the A3 Ab efficiently recognized native SLC41A3 only in the absence of the blocking peptide. In A3st + tet cells (right panel) the A3 antibody recognized native SLC41A3 and the overexpressed Strep-tagged protein, no signal was detected in the presence of the blocking peptide. In contrary, the blocking peptide did not inhibit binding of the Strep-antibody to Strep-SLC41A3.

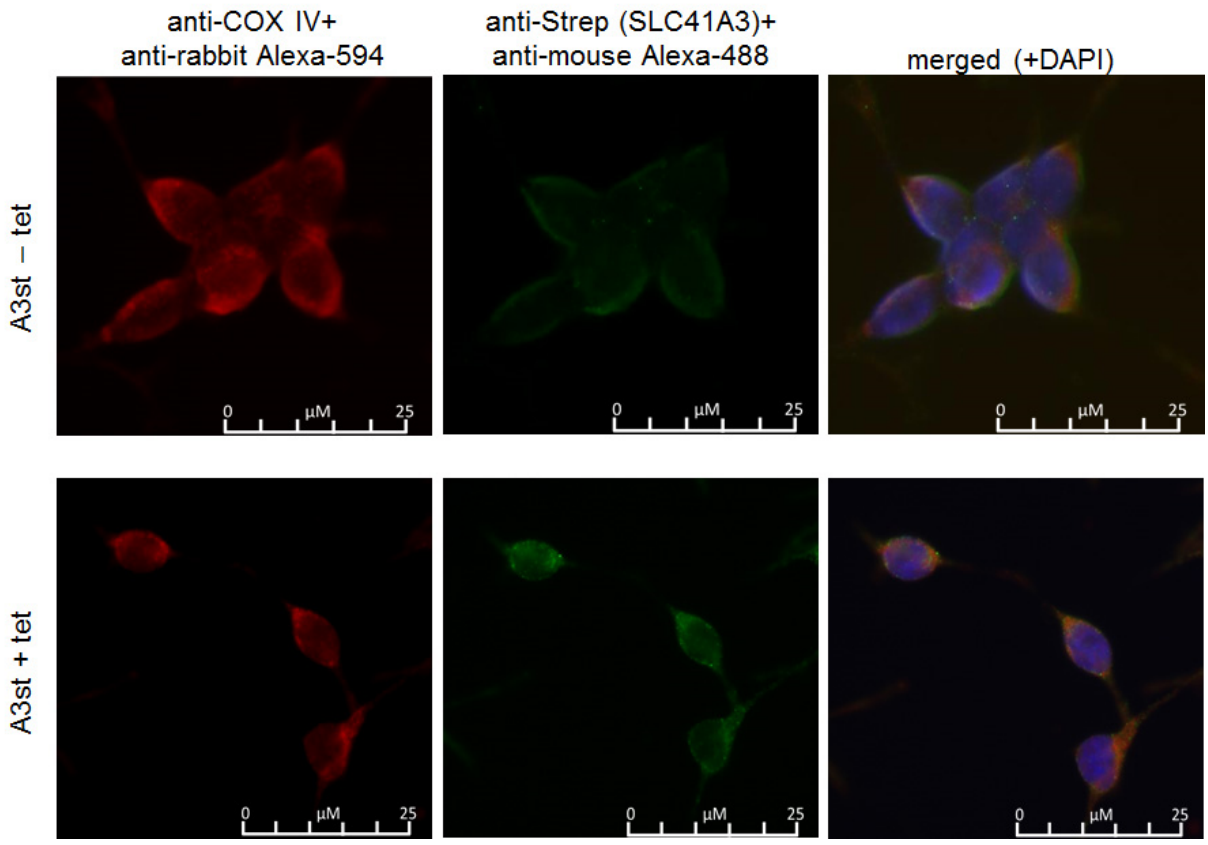

Supplementary Figure S2 – Fluorescence visualization of Strep-SLC41A3 and COX IV.

Triple-staining with anti-SLC41A3 antibody (red), anti-COX IV antibody (green), and DAPI (blue, only shown in merged) was performed in uninduced (A3st -tet) and induced (A3st +tet).

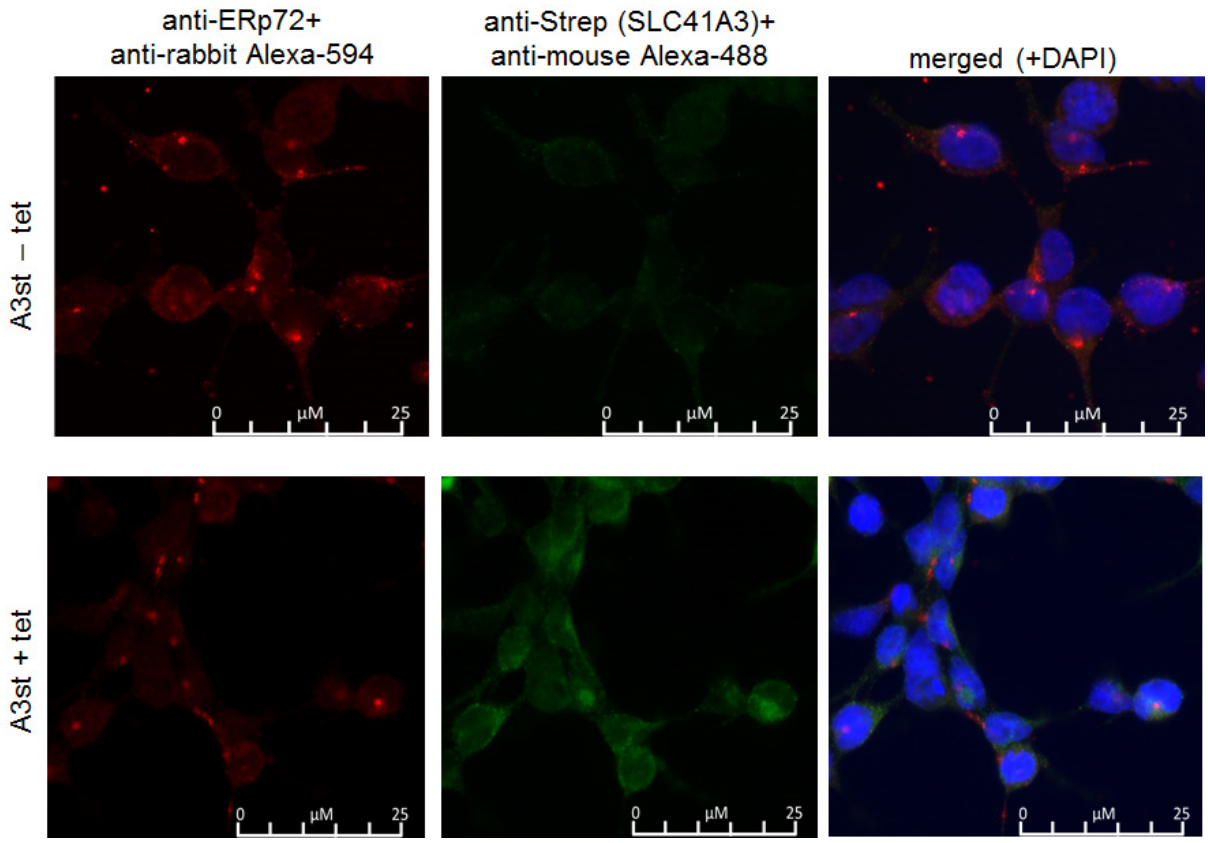

Supplementary Figure S3 – Fluorescence visualization of Strep-SLC41A3 and ERp72.

Triple-staining with anti-SLC41A3 antibody (red), anti-ERp72 antibody (green), and DAPI (blue, only shown in merged) was performed in uninduced (A3st -tet) and induced (A3st +tet).

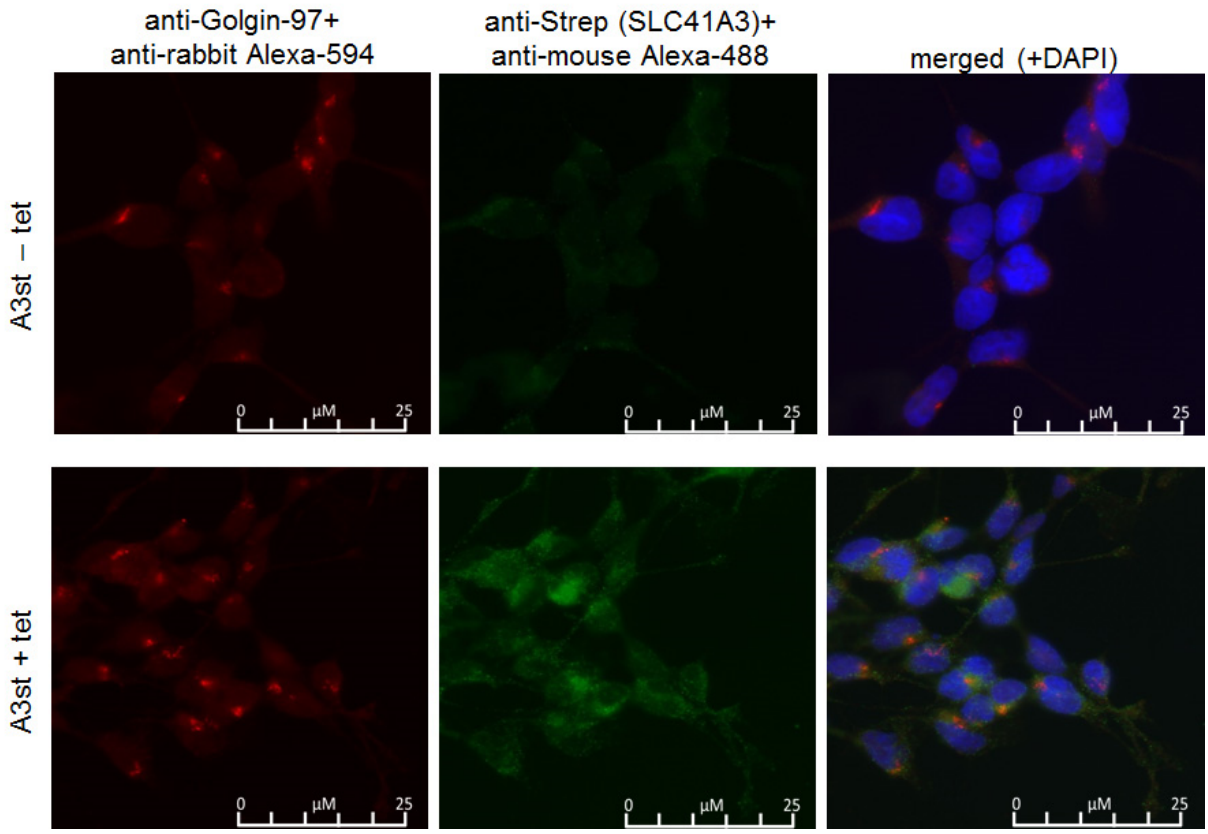

Supplementary Figure S4 – Fluorescence visualization of Strep-SLC41A3 and Golgin-97.

Double-staining with anti-SLC41A3 antibody (red), anti-Golgin-97 antibody (green), and DAPI (blue, only shown in merged) was performed in uninduced (A3st -tet) and induced (A3st +tet).

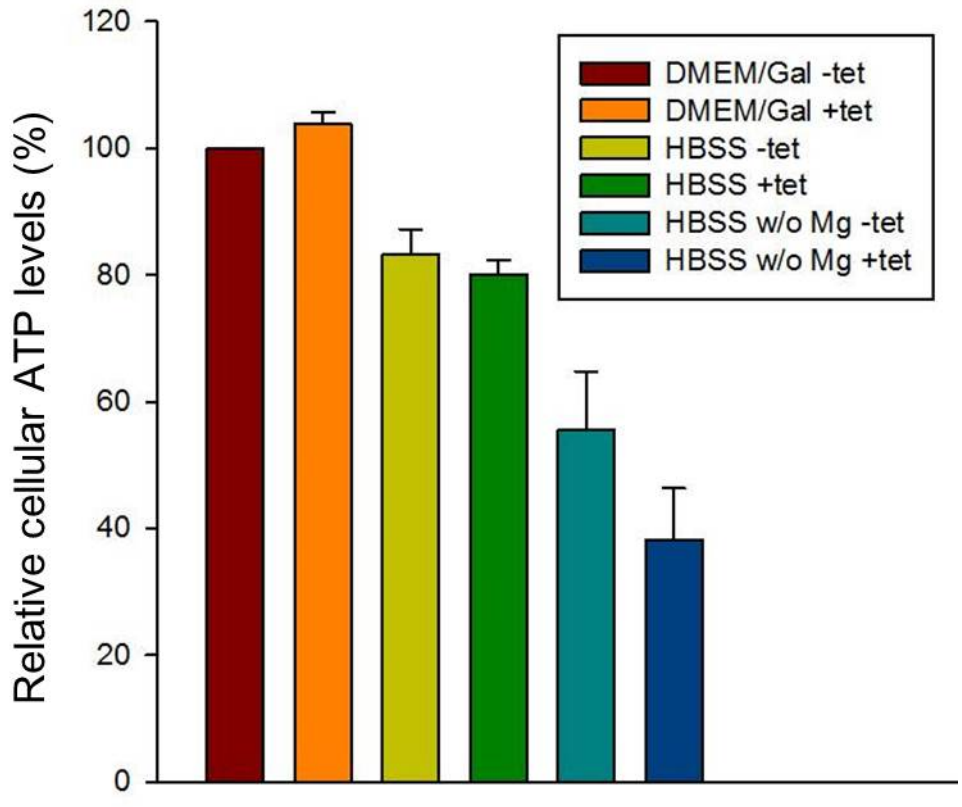

Supplementary Figure S5 – Relative cellular ATP levels in uninduced and induced A3st cells under various culture conditions.

ATP levels of uninduced (-tet) cells continuously grown in DMEM/Gal medium served as a control (100%), all other experimental conditions are given as percentage relative to the control level. Overexpression of A3 (+tet) in DMEM/Gal medium did not reduce ATP levels. In both uninduced and induced cells, HBSS medium containing $MgSO_4$ reduced cellular ATP by approximately 20%. A further reduction of cellular ATP was seen in Mg^{2+}-starvation medium which was more pronounced in A3 overexpressing cells.

5. DISCUSSION

An increasing number of disorders in humans and animals seems to be associated with an imbalanced magnesium homeostasis. In the last decades, many Mg^{2+} transporters have been well characterized and mutations in their genes induce impairment in Mg^{2+} homeostasis and therefore represent the cause of many disorders.

Recently SLC41A1 has been characterized as being a Na^{+}/Mg^{2+} exchanger (NME) able to form protein complexes *in vivo* (4, 5). Localized in the plasma membrane, it has been proposed as an essential component of intracellular magnesium homeostasis and the major Mg^{2+} efflux system of the cell.

In the present work SLC41A1 complex-forming ability was examined by using a split-ubiquitin yeast two hybrid (SU-YTH) assay; the proteins identified among the potential binding partners were mostly localized in the endoplasmic reticulum and Golgi apparatus but also in nucleus and plasma-membrane and were involved in translation, proper folding, and maturation (posttranslational modifications) of proteins. The most prominent interactor in the screen was EBP (emopamil binding protein), a protein involved in lipid and/or cholesterol biosynthesis, but further studies are necessary to establish any functional link between this protein and SLC41A1. Mass spectrometry-based analysis (MALDI-TOF-MS) revealed another interesting putative interactor, ACCA1, which was not identified as interactor in the functional SU-YTH assay. It is localized in ER and involved in lipid and/or cholesterol biosynthesis similar to EBP. Other members of the SLC superfamily and other solute transporters were identified as binding partners as well, but interactions between these proteins and SLC41A1 might be only transient and/or provoked by common pathways of their maturation in ER and/or GA and/or vesicular transport.

The activity of SLC41A1 has been connected with many pathophysiological conditions over the years, including cardiovascular (myocardial infarction, ischemic heart disease, essential hypertension, preeclampsia / eclampsia) (6, 120-124), metabolic (*diabetes mellitus* type 2) (81, 125), psychiatric (ADHD syndrome) (1) and neurodegenerative diseases (PD) (90).

The majority of these disorders are associated with aging, unhealthy life style, reduced food intake and exposure to environmental factors which contribute to their etiology. Often their pathogenesis is multifactorial and not fully understood. A typical case is PD, where only a small number of cases show a hereditary pattern of genetic defects or a *de novo* mutation in one PD-associated gene.

The present work aimed to characterize the coding variant of SLC41A1 carrying the amino-acid substitution p.A350V (c.1049C>T), which was found in one Caucasian PD patient (103). This mutation seems to be associated with PD because the gene SLC41A1 is part of the PD

susceptibility locus *PARK16*. The results presented here have revealed no changes regarding the cellular localization, phosphorylation status, or complex-forming ability of the p.A350V variant when compared with the wild-type protein; however, HEK293 cells overexpressing this variant are able to perform Mg^{2+} efflux more efficiently compared with the wild-type cells. Therefore it constitutes a 'gain of function' mutation which increases the Mg^{2+} efflux ability of SLC41A1; the latter likely has long-term consequences on cellular functions, particularly under conditions of low extracellular Mg^{2+} concentration. From these experimental data, it can be speculated that the chronic loss of Mg^{2+} from the cells and the latent intracellular magnesium deficiency can represent an important molecular mechanism which contributes to the PD pathophysiology. Although a precise molecular link between disturbed IMH and PD is currently not known, Na^{+}/ Mg^{2+} exchange mediated by SLC41A1 in neurons might represent a relevant therapeutic target for PD patients and a Mg^{2+} supplementation would be beneficial.

Magnesium deficiency (both systemic and intracellular) has long been suspected to be involved in several human diseases other than neurodegeneration, such as preeclampsia, nephron phthisis and metabolic syndrome (91, 103, 126).

Type 2 diabetes mellitus is often accompanied by alterations in the Mg status, and in particular DM2 patients show an increased prevalence of Mg^{2+} deficit. SLC41A1 represents the major mechanism responsible for the efflux of Mg^{2+} from cells and it is activated via cAMP-dependent PKA-mediated phosphorylation (127). Since intracellular cAMP levels are altered in response to hormonal stimuli, including insulin, the hypothesis was established that insulin may be the link between SLC41A1 and the pathophysiology of these ailments via the insulin receptor - phosphoinositide 3-kinase – Akt/protein kinase B (IR-PI3K-Akt/PKB) signaling pathway. Therefore, several series of experiments were conducted aiming at the characterization of SLC41A1 transport activity under insulin stimulation.

The *in vitro* study presented here examined the effect of insulin signaling via the IR-PI3K-PDE3b cascade on SLC41A1 NME activity in transgenic HEK293 cells and showed a significant inhibitory effect of insulin on SLC41A1 performance and an earlier onset of Mg^{2+} release from intracellular stores (such as mitochondria, endoplasmic reticulum, and Golgi apparatus).

So it can be speculated that insulin may be an essential regulator of intracellular magnesium homeostasis. Blocking the SLC41A1-mediated Mg^{2+} efflux might protect cells from an excessive loss of Mg^{2+} and thus protect from the consequences of hypomagnesaemia often observed in diabetes patients.

Taken together, these results support the importance of insulin management and Mg^{2+} supplementation in diabetes patients and provide a new molecular target to focus on for the prevention of the consequences of *diabetes*-associated hypomagnesaemia.

Many metabolic diseases and ageing-related neurodegenerative disorders, like PD, AD, Huntington's disease (HD) and amyotrophic lateral sclerosis (ALS), have been associated with mitochondrial dysfunction. There is strong evidence coming from genetic, biochemical and morphological analyses revealing that mitochondrial dysfunction occurs in the early stage of the pathogenesis (128, 129). Given that mitochondria serve as intracellular Mg^{2+} stores, a mitochondrial dysfunction might affect cellular Mg^{2+} homeostasis (130, 131) and this could be one reason for the intracellular Mg^{2+} deficiency observed in diabetes, PD, hypertension, etc.

The major Mg^{2+} influx system in mitochondria of yeast as well as higher eucaryotes is encoded by Mrs2. A recent study shows that *dmy/dmy* rats suffer from a mitochondrial disease and the molecular defect responsible for the demyelinating phenotype observed in adult rats is a “loss-of-function” mutation in the *Mrs2* gene (132). Therefore the authors concluded that Mg^{2+} homeostasis in central nervous system mitochondria is essential for the maintenance of myelin, even though the loss of the main mitochondrial Mg^{2+} influx system in rats is not lethal. Interestingly, Mrs2 silencing in HEK293 cells leads to a reduced capacity of mitochondrial Mg^{2+} uptake, loss of mitochondrial respiratory complex I, decreased mitochondrial membrane potential and eventually cell death (133). From these data it can be concluded that Mrs2 is the major transport protein for Mg^{2+} uptake into mitochondria and its expression is essential for the maintenance of respiratory complex I and cell viability.

Because so far nothing was known about putative mitochondrial Mg^{2+} efflux systems, one of the studies of the project aimed at the molecular and physiological characterization of SLC41A3. Since SLC41A3 is characterized by two MgtE domains, it was speculated to have a transport activity for Mg^{2+} similar to SLC41A1. Therefore the ability and mode of Mg^{2+} transport mediated by SLC41A3 were assayed by measuring the intracellular Mg^{2+} concentration and its changes with fast-filter spectrofluorometry (FFS), using the Mg^{2+}-sensitive fluorescent dye mag-fura 2.

First the ability of SLC41A3 to mediate Mg^{2+} influx was evaluated. Under influx conditions Mg^{2+} uptake was observed when the extracellular Mg^{2+} concentration was increased stepwise from 1 to 3 to 5 mM by adding $MgCl_2$ to the cell suspension but there was no difference between cells overexpressing the protein and the uninduced control cells; the observed Mg^{2+} uptake was therefore most likely not SLC41A3-mediated.

In the second step, the efflux ability of SLC41A3 was assessed and some differences were observed in regard of intracellular free Mg^{2+} in cells overexpressing SLC41A3 compared with the control, suggesting that SLC41A3 is somehow involved in Mg^{2+} transport. Surprisingly, overexpression of SLC41A3 led to an increase of the intracellular Mg^{2+} concentration. Given that the measurements were conducted in completely Mg^{2+}-free buffer, the increase of intracellular Mg^{2+} observed under these conditions cannot be due to an uptake of Mg^{2+} from the external buffer but it can only be explained by Mg^{2+} mobilization from internal stores.

Since the main internal stores of Mg^{2+} are mitochondria, double-stain immunofluorescence was performed in order to find out whether SLC41A3 was localized on the plasma-membrane, as suggested by computer predictions, or on intracellular membranes and a co-localization of SLC41A3 and COX (mitochondrial cytochrome c oxidase) was found. To further substantiate that SLC41A3 may be a mitochondrial transporter, double-stain microscopy was performed using a cell-permeant MitoTracker probe for labelling mitochondria together with the antibody recognizing native SLC41A3. The two signals colocalized well, confirming a mitochondrial localization of SLC41A3.

To further clarify the role of SLC41A3 in mitochondrial Mg^{2+} transport, efflux experiments were performed with intact mitochondria isolated from stably transfected cells overexpressing SLC41A3. The latter experiments showed that SLC41A3 is responsible for the extrusion of magnesium from mitochondria, and this transport is Na^+-dependent because it requires a physiological cytosolic Na^+ concentration (10 mM). Indeed it was reduced when the Na^+ concentration was lowered to 5 mM, blocked when there was no extramitochondrial Na^+ or when Na^+ was replaced by N-methyl-D-glucamine (NMDG) and it doubled with extramitochondrial Na^+ concentration of 40 mM. Finally SLC41A3 has been characterized as a mitochondrial Na^+/Mg^{2+} exchanger and not as a channel because its activity was reduced or even blocked when the measurements were performed at 16°C.

SLC41A3 can be assumed to be the link between altered internal Mg^{2+} mobilization and diabetes or neurodegeneration, because these diseases are characterized by aberrant mitochondrial homeostasis and the consequent loss of control over cellular energy turnover (134-137). Furthermore the results of this work support the hypothesis that insulin blocks Mg^{2+} efflux from the cells via SLC41A1 and promotes an early onset of Mg^{2+} release from internal stores likely activating SLC41A3 and therefore boosting a mitochondrial Mg^{2+} efflux. This opens up new treatment strategies to counterbalance the hypomagnesaemia often observed in age-related mitopathies.

Based on the knowledge that SLC41A1 and SLC41A3 represent molecular factors responsible for regulating cytosolic and mitochondrial Mg^{2+} homeostasis, a further magnesium-responsive gene involved in IMH was characterized, named CNNM2. It has previously been associated with regulation of serum magnesium concentrations (109) and its functional impairment in humans is associated with severe hypomagnesaemia (63), a condition which is typical for many brain diseases, neurodegenerative diseases and metabolic diseases as well.

A previous study of Kurth et al (114) showed CNNM2 transcripts to be overexpressed in a subpopulation of tested diabetic patients, but among them only one showed hypomagnesaemia with a plasma Mg^{2+} concentration below 0.72 mM. The other patients did not exhibit any correlation between *CNNM2* expression levels and plasma Mg^{2+} concentration. Therefore, it

seemed interesting to test the expression of CNNM2 and other MRGs *in vitro* in Jurkat and JVM-13 cells, respectively T lymphocytes and lymphoblasts, after a severe Mg^{2+} starvation, because these cells are normally exposed to changes in [Mg^{2+}] in blood. Respective data are controversial compared to the previous data obtained in leucocytes, as the present study clearly showed upregulation of CNNM2 upon Mg^{2+} starvation in both cell models. However, it might be that *in vitro* CNNM2 is upregulated in response to the intracellular Mg^{2+} deficiency or because of the existence of other diabetes-specific factors that may activate its overexpression. *In vivo* the correlation between CNNM2 levels and hypomagnesaemia may be missing because the body might activate other mechanisms to compensate for the magnesium deficiency.

It has recently been proposed that magnesium concentrations are tightly regulated by the transporters but there are also some homeostatic factors which indirectly influence Mg^{2+} transport. The present data showed that the overexpression of I1 and I2 of CNNM2 does not influence Mg^{2+} transport and total magnesium and therefore it can be speculated that CNNM2 may likely be the first magnesium homeostatic factor with no transport function.

Many transporters associate in homo- or hetero-oligomeric complexes in order to be functional (138). The molecular characterization of CNNM2 in the present studies revealed that both variants form protein complexes of higher order which might represent the functional form of the protein.

However, N-terminally tagged Strep-I1 and Strep-I2 have a different pattern of distribution, indeed I1 is mainly periplasmic/plasmalemmal while I2 is nuclear and perinuclear. It can be speculated that either the maturation and sorting of I1 and I2 in ER are different or that unprocessed I1 and I2 are targeted towards different compartments because of the missing exon 6 in I2 which might be crucial for the different localization and function of I1 and I2 in the cell. This data is in accordance with the split-ubiquitin results, which revealed a different spectrum of binding partners for the two variants. Indeed only 6 candidate interactors have been identified for I1, while the spectrum of potential interactors identified for I2 is much larger (around 50 proteins). The only common interactor is spectrin β chain (Brain) 1 (SPTBN1; UniProt ID Q01082). SPTBN1 is an integral component of β-amyloid plaques in AD (139) which, interacting with CNNM2, can stabilize the protein in cellular membranes in a way similar to α-synuclein.

Besides SPTBN1, other candidate interactors include PARK7/DJ1 for I1, PINK1, MPC1 and AMBRA1 for I2, which are all proteins associated with neurodegenerative disorders.

The identification of PARK7/DJ1 (PD-associated protein) and SPTBN1 (relevant in AD) as possible interaction partners of CNNM2 strengthens the hypothesis that molecular components involved in the regulation of IMH are directly or indirectly implicated in the pathophysiology of many neurodegenerative diseases and that a balanced IMH is essential for the neuronal activity (140). Taking into account that numerous cellular functions are magnesium-dependent, it is

evident that any change in the IMH may influence key physiological pathways (141) like energy metabolism, nucleic acids and proteins synthesis, ion homeostasis, and consequently may play a role in oxidative stress (142) and others processes associated with neurodegeneration. Because the neurons are metabolically active cells and particularly prone to oxidative stress and mitochondrial dysfunction, they are the first cells being affected by an unbalanced IMH (143, 144). Therefore a correct function of CNNM2 and consequently a balanced IMH are essential to prevent these processes.

The newly identified CNNM2 interactors PARK7/DJ1 and PINK1 are crucial in the maintenance of mitochondrial homeostasis and the protection against cell death (145, 146). PARK7/DJ1 has been shown to positively regulate the transcription activity of AR (147) which plays an important role in the regulation of SLC41A1 activity (148, 149). Therefore it can be assumed that PARK7/DJ1 regulates the expression of the Na^+/Mg^{2+} exchanger SLC41A1 and consequently it regulates the IMH via AR. If CNNM2 played a role in intracellular and/or extracellular Mg^{2+} sensing, then the hypothesis is justified that interaction of CNNM2 with PARK7/DJ-1 initiates the activation of AR, followed by *AREs*-mediated activation of SLC41A1 expression and increased Mg^{2+} efflux capacity of neurons.

PINK1 represents a critical pathway in controlling mitophagy, a process of autophagic turnover, recycling/elimination of damaged mitochondria in order to maintain mitochondrial integrity. Loss-of-function mutations in PINK1 cause mitochondrial dysfunction and are directly linked to PD (150-152). Assuming that CNNM2 is involved in Mg^{2+} sensing, it might detect a Mg^{2+} leak from damaged mitochondria and then interact with PINK1 and induce an upregulation of mitophagy.

Finally, the suggested interaction CNNM2–AMBRA1 is highly probable because intronic variants of both AMBRA1 (rs11819869) (153) and CNNM2 (rs7914558) were shown to be schizophrenia-related (111, 112). The involvement of both proteins in the pathology of schizophrenia further strengthens the hypothesis of an involvement of CNNM2 in the process of mitophagy. Mitophagy/autophagy is essential for neuronal function, as well as neuronal survival, and has recently been suggested to play a key role in the pathophysiology of schizophrenia (154, 155).

The interactions between PARK7/DJ-1 and CNNM2 (I1) and likely between CNNM2 (I2) and PINK1, and CNNM2 (I2) and AMBRA1, suggest that both variants of CNNM2 are not exclusively integral to the cytoplasmic membrane but they are also localized in membranes of organelles like mitochondria or lysosomes. These interactions support the hypothesis that CNNM2 is involved in processes such as protection against oxidative stress and maintenance of the "healthy" mitochondrial homeostasis and IMH. CNNM2 would therefore be part of a cross-talk mechanism between these processes and/or regulate the function of other proteins which directly transport magnesium. However, further studies are necessary to clarify its mode of action in the cell and its role in the pathophysiology of neurodegenerative diseases.

In conclusion, SLC41A1 is the key player responsible for Mg^{2+} extrusion across the plasma membrane and its activity undergoes a hormonal regulation via insulin and androgen receptor. SLC41A3 is the mitochondrial transporter responsible for Mg^{2+} efflux from internal stores to the cytosol. Besides, CNNM2 acting as intracellular and/or extracellular Mg^{2+} sensor might be responsible for the activation of SLC41A1 and SLC41A3 and for a subsequent Mg^{2+} redistribution between mitochondria and cytoplasm and cytoplasm and extracellular fluids according to the needs.

From the data collected in this thesis, it can be speculated that the three proteins function coordinately in order to maintain a balanced intracellular magnesium homeostasis which strictly depends on the magnesium influx/efflux across the plasma membrane and on the magnesium storage into the intracellular compartments.

SUMMARY

It is well known that magnesium deficiency or altered IMH can trigger many pathophysiological conditions, thus a correct functioning of Mg^{2+} transporters and channels is essential for normal cellular physiology. Mutations in many MRG induce hypomagnesemia which often represents one of the complications of many human ailments.

Based on previous data which have characterized SLC41A1 as a plasma membrane Na^{+}/Mg^{2+} exchanger (4, 5) and as being overexpressed in preeclamptic women (6), the present thesis aimed at a further characterization of SLC41A1 and Mg^{2+} efflux in some pathophysiological conditions. It further aimed at the molecular characterization of two others MRGs, CNNM2 and SLC41A3, in order to achieve a better understanding of Mg^{2+} homeostasis and to link the mechanisms of Mg^{2+} mobilization across the plasma membrane or between intracellular compartments with mitochondrial dysfunction and disease states (e.g.: Parkinson's disease (PD), diabetes, etc).

Proceeding from previous results of Kolisek et al (4, 5), describing SLC41A1 as the major Mg^{2+} efflux system of the cell, the first study examined the complex-forming ability of SLC41A1 *in vivo* and identified EBP and other members of the SLC superfamily as potential binding partners. Further experiments evaluated the transport activity of the PD-associated SLC41A1 variant pA350V and defined it as a "gain-of-function" mutation enhancing Mg^{2+} efflux compared with the wild-type protein. A next question was whether SLC41A1 transport activity could be influenced and regulated by insulin in order to explain the molecular basis of hypomagnesaemia often observed in diabetes patients. The present study shows that insulin reduces the SLC41A1-mediated Mg^{2+} efflux and, most importantly, it seems to have an effect on intracellular Mg^{2+} stores, since an earlier onset of Mg^{2+} release from intracellular stores was observed.

In the second part of this thesis, experiments were conducted on stably transfected HEK293 cells overexpressing SLC41A3 in order to uncover the function of SLC41A3 with regard to its ability to transport Mg^{2+}, its mode of Mg^{2+} transport and its role in cellular Mg^{2+} homeostasis. To assess the role of SLC41A3 for cellular Mg^{2+} homeostasis and gain insight into the regulation of transport activity and/or membrane insertion, knowledge about the precise cellular localization and the identification of the binding partners are essential. The present data reveal a specific mitochondrial localization for SLC41A3 and its function as mitochondrial Mg^{2+} efflux system. They further suggest that the effect of insulin on intracellular Mg^{2+} stores is most likely mediated via SLC41A3. Given that mitochondria serve as intracellular Mg^{2+} stores, a mitochondrial

dysfunction might affect cellular Mg^{2+} homeostasis and this could be one reason for intracellular Mg^{2+} deficiency observed in diseases such as diabetes, PD and hypertension.

The last part of the project focused on the physiological characterization of two isoforms of another Mg^{2+} responsive gene, CNNM2, because a mutation in this gene has been recently associated with severe familial hypomagnesaemia.

A previous study showed that CNNM2 is overexpressed in diabetic patients (114) but its expression does not correlate with Mg^{2+} plasma levels. However, the present study shows an overexpression of CNNM2 in Jurkat and JVM-13 cells after Mg^{2+} starvation. The protein has an extensive localization in the cells, including the mitochondrial membrane, and its putative interactors include proteins involved in the regulation of mitochondrial homeostasis (mitophagy, clearance of ROS). A further question was whether the two isoforms (I1 and I2) of CNNM2 are able to transport Mg^{2+}, but the data presented herein clearly indicate that CNNM2 transports Mg^{2+} neither in electrogenic nor in electroneutral mode in transgenic HEK293 cells overexpressing I1 or I2. This strongly suggests that CNNM2 might represent the first magnesium homeostatic factor without being a Mg^{2+} transporter *per se*. Instead CNNM2 can be postulated to sense the changes in extracellular and/or intracellular Mg^{2+} concentration and consequently activates other proteins responsible for Mg^{2+} mobilization in the cell.

From these data a role of CNNM2 in intracellular Mg^{2+} homeostasis can be assessed and it can be speculated that the two SLC41 proteins act cooperatively with CNNM2-mediated Mg^{2+} sensing in controlling the cellular magnesium homeostasis.

ZUSAMMENFASSUNG

SLC41A1, SLC41A3 und CNNM2: Magnesium-responsive Genes mit potentieller Beteiligung an humanen Krankheiten

Es ist allgemein anerkannt, dass ein Magnesiummangel oder eine veränderte intrazelluläre Mg^{2+}-Homöostase (IMH) viele pathophysiologische Zustände auslösen kann. Daher ist die einwandfreie Funktion von Mg^{2+}-Transportern und Mg^{2+}-Kanälen für physiologische Zellfunktionen essenziell. Mutationen in Mg^{2+}-regulierten Genen (MRG) können eine Hypomagnesiämie induzieren, die bei vielen Erkrankungen zu Komplikationen führen kann.

Basierend auf früheren Daten, die SLC41A1 als einen Na^{+}/Mg^{2+}-Austauscher in der Plasmamembran charakterisiert haben und als Gen, das bei Frauen mit Präeklampsie überexprimiert ist, war das Ziel dieser Arbeit eine weitere Charakterisierung von SLC41A1 und des durch dieses Protein vermittelten Mg^{2+}-Effluxes unter pathophysiologischen Zuständen. Ein weiteres Ziel dieser Arbeit war die funktionelle Charakterisierung der MRGs CNNM2 und SLC41A3 im Hinblick auf ihre Bedeutung für die intrazelluläre Mg^{2+}-Homöostase. Insbesondere sollten mögliche Beziehungen zwischen den Mechanismen des Mg^{2+}-Transportes über die Plasmamembran bzw. zwischen intrazellulären Kompartimenten mit mitochondrialer Dysfunktion und bestimmten Krankheitszuständen (z.B.: Morbus Parkinson, Diabetes, etc.) aufgedeckt werden.

Ausgehend von früheren Ergebnissen von Kolisek et al., die SLC41A1 als den Hauptmechanismus für den Mg^{2+}-Efflux aus der Zelle beschrieben hatten, untersuchte der erste Teil der Studie die Fähigkeit von SLC41A1 Proteinkomplexe zu bilden. Emopamil binding protein (EBP) und andere Vertreter der SLC Superfamilie wurden als potentielle Bindungspartner identifiziert. In weiteren Experimenten wurde die Transportaktivität der mit Morbus Parkinson assoziierten SLC41A1 Variante pA350V evaluiert und gezeigt, dass es sich um eine „gain-of-function“ Mutation handelt, die im Vergleich zum Wildtyp-Protein einen erhöhten Mg^{2+}-Efflux aus der Zelle bedingt.

Anschließend wurde die Fragestellung untersucht, ob die Transportaktivität von SLC41A1 durch Insulin beeinflusst werden kann, da bei Diabetes-Patienten oft eine Hypomagnesiämie beobachtet wird. Die vorliegenden Ergebnisse zeigen, dass Insulin den SLC41A1-vermittelten Mg^{2+}-Efflux reduziert und offensichtlich einen Effekt auf intrazelluläre Mg^{2+}-Speicher hat, da ein früheres Einsetzen der Mg^{2+}-Freisetzung aus intrazellulären Speichern beobachtet wurde.

Im zweiten Teil der Arbeit wurde eine stabil transfizierte, SLC41A3-überexprimierende HEK293 Zelllinie verwendet, um die Fähigkeit dieses Proteins, Mg^{2+} zu transportieren, näher zu untersuchen und seine Rolle in der zelluläre Mg^{2+}-Homöostase zu charakterisieren. Um die Regulation der Transportaktivität und die Rolle von SLC41A3 in der zelluläre Mg^{2+}-Homöostase zu verstehen, war es notwendig die zelluläre Lokalisation und etwaige Bindungspartner zu identifizieren. Die vorliegenden Daten zeigen eine spezifische Lokalisation in den Mitochondrien und eine Funktion als mitochondriales Mg^{2+}-Efflux System. Diese Ergebnisse legen nahe, dass der beobachtete Effekt von Insulin auf intrazelluläre Mg^{2+}-Speicher wahrscheinlich durch SLC41A3 vermittelt wird. Vorausgesetzt, dass Mitochondrien als intrazelluläre Mg^{2+}-Speicher fungieren, kann eine mitochondriale Dysfunktion auch die zelluläre Mg^{2+}-Homöostase beeinflussen und ein Grund für die bei Krankheiten wie Diabetes, Morbus Parkinson oder Bluthochdruck beobachtete intrazelluläre Mg^{2+}-Defizienz sein.

Der letzte Teil der Arbeit konzentrierte sich auf die physiologische Charakterisierung zweier Isoformen des Mg^{2+}-regulierten Gens CNNM2 (I1 und I2). Mutationen in diesem Gen sind mit schwerer, familiärer Hypomagnesiämie assoziiert. Eine vorangegangene Studie hatte gezeigt, dass CNNM2 in Diabetes-Patienten überexprimiert war, die Expression aber nicht mit den Mg^{2+}-Spiegel im Plasma korrelierte. In der vorliegenden Arbeit konnte aber eine Überexpression von CNNM2 in Jurkat und JVM-13 Zellen nach Mg^{2+}-Depletion gezeigt werden. Das Protein war in der Zelle weit verbreitet, auch in Mitochondrien, und seine potentiellen Interaktionspartner umfassen Proteine, die an der Regulation der Mitochondrien-Homöostase (Mitophagie, Beseitigung reaktiver Sauerstoffspezies) beteiligt sind. Es wurde auch untersucht, ob die beiden CNNM2-Isoformen in der Lage sind, Mg^{2+} zu transportieren. Die hier präsentierten Daten zeigen eindeutig, dass in HEK293 Zellen, die CNNM2 überexprimieren, das Protein weder in elektrogener noch in elektroneutraler Weise Mg^{2+} transportiert. Diese Ergebnisse legen nahe, dass CNNM2 der erste Mg^{2+}-homöostatische Faktor ist, der selbst keine Transportaktivität besitzt. Das Protein scheint die extrazelluläre und/oder intrazelluläre Mg^{2+}-Konzentration zu messen und darauffolgend andere Proteine, die für die Mg^{2+}-Mobilisierung in der Zelle verantwortlich sind, zu aktivieren.

Diese Daten charakterisieren CNNM2 als zentralen Faktor für die intrazelluläre Mg^{2+}-Homöostase und es kann angenommen werden, dass die beiden SLC41 Proteine kooperativ mit dem Mg^{2+}-Sensor CNNM2 die zelluläre Mg^{2+}-Homöostase regulieren.

REFERENCES

1. Nishizawa Y, Morii H, Durlach J. New Perspectives in Magnesium Research (Nutrition and Health). edn s, editor. London: Springer-Verlag Ltd.; 2007.
2. Bui DM, Gregan J, Jarosch E, Ragnini A, Schweyen RJ. The bacterial magnesium transporter CorA can functionally substitute for its putative homologue Mrs2p in the yeast inner mitochondrial membrane. J Biol Chem. 1999;274(29):20438-43.
3. Sponder G, Svidova S, Schweigel M, Vormann J, Kolisek M. Splice-variant 1 of the ancient domain protein 2 (ACDP2) complements the magnesium-deficient growth phenotype of Salmonella enterica sv. typhimurium strain MM281. Magnes Res. 2010;23(2):105-14.
4. Kolisek M, Launay P, Beck A, Sponder G, Serafini N, Brenkus M, et al. SLC41A1 is a novel mammalian Mg^{2+} carrier. J Biol Chem. 2008;283(23):16235-47.
5. Kolisek M, Nestler A, Vormann J, Schweigel-Rontgen M. Human gene SLC41A1 encodes for the Na^{+}/Mg^{2+} exchanger. Am J Physiol Cell Physiol. 2012;302(1):C318-26.
6. Kolisek M, Galaviz-Hernandez C, Vazquez-Alaniz F, Sponder G, Javaid S, Kurth K, et al. SLC41A1 is the only magnesium responsive gene significantly overexpressed in placentas of preeclamptic women. Hypertens Pregnancy. 2013;32(4):378-89.
7. Quamme GA. Molecular identification of ancient and modern mammalian magnesium transporters. Am J Physiol Cell Physiol. 2010;298(3):C407-29.
8. Goytain A, Quamme GA. Functional characterization of ACDP2 (ancient conserved domain protein), a divalent metal transporter. Physiol Genomics. 2005;22(3):382-9.
9. Fox C, Ramsoomair D, Carter C. Magnesium: its proven and potential clinical significance. South Med J. 2001;94:1195-201.
10. Saris NE, Mervaala E, Karppanen H, Khawaja JA, Lewenstam A. Magnesium. An update on physiological, clinical and analytical aspects. Clin Chim Acta. 2000;294:1-26.
11. Aikawa JK. Magnesium: Its Biological Significance. Boca Raton, FL: CRC Press; 1981.
12. Rude R. Magnesium disorders. J K, R T, editors. Philadelphia, PA: W.B. Saunders Company; 1996.
13. Maguire ME, Cowan JA. Magnesium chemistry and biochemistry. Biometals. 2002;15:203-10.
14. Touyz RM. Magnesium in clinical medicine. Front Biosci 2004;9:1278-93.
15. Elin RJ. Magnesium: the fifth but forgotten electrolyte. Am J Clin Pathol. 1994;102(5):616-22.
16. Tietz NW. Clinical Guide to Laboratory Tests. Philadelphia, PA: WB Saunders; 1990.
17. Kroll MH, Elin RJ. Relationships between magnesium and protein concentrations in serum. Clin Chem. 1985;31(2):244-6.

18. Lewenstam A, Maj-Zurawska M, Blomqvist N. Ionized magnesium - a new parameter in clinical analysis. . Clin Chem Enzym Commun. 1993;5:95-103.

19. Maj-Zurawska M. Clinical findings on human blood with the KONE ISE for Mg^{2+}. Scand J Clin Lab Invest Suppl. 1994;217:69-76.

20. Graham L, Caesar J, Burgen A. Gastrointestinal absorption and excretion of Mg^{28} in man. Metabolism 1960;9:646-59.

21. Romani A. Regulation of magnesium homeostasis and transport in mammalian cells. Arch Biochem Biophys. 2007;458(1):90-102.

22. Romani AM, Maguire ME. Hormonal regulation of Mg^{2+} transport and homeostasis in eukaryotic cells. Biometals. 2002;15(3):271-83.

23. Fatholahi M, LaNoue K, Romani A, Scarpa A. Relationship between total and free cellular Mg^{2+} during metabolic stimulation of rat cardiac myocytes and perfused hearts. Arch Biochem Biophys. 2000;374(2):395-401.

24. Raju B, Murphy E, Levy LA, Hall RD, London RE. A fluorescent indicator for measuring cytosolic free magnesium. Am J Physiol. 1989;256(3 Pt 1):C540-8.

25. Polancic JE. Magnesium: Metabolism, clinical importance, and analysis. Clin Lab Sci 1991;4:105-9.

26. De Rouffignac C, Quamme G. Renal magnesium handling and its hormonal control. Physiol Rev. 1994;74:305-22.

27. Weaver CM. Calcium and magnesium requirements of children and adolescents and peak bone mass. Nutrition. 2000;16(7-8):514-6.

28. Wacker WE, Parisi AF. Magnesium metabolism. N Engl J Med. 1968;278(14):772-6 concl.

29. Garfinkel L, Garfinkel D. Magnesium regulation of the glycolytic pathway and the enzymes involved. Magnesium. 1985;4(2):60-72.

30. Rubin H. Central role for magnesium in coordinate control of metabolism and growth in animal cells. Proc Natl Acad Sci USA. 1975;72:3551–5.

31. Switzer RL. Regulation and mechanism of phosphoribosylpyrophosphate synthetase. III. Kinetic studies of the reaction mechanism. J Biol Chem. 1971;246:2447–58.

32. Yang L, Arora K, Beard WA, Wilson SH, Schlick T. Critical role of magnesium ions in DNA polymerase beta's closing and active site assembly. J Am Chem Soc. 2004;126(27):8441-53.

33. Reynolds JL, Joannides AJ, Skepper JN, McNair R, Schurgers LJ, Proudfoot D, et al. Human vascular smooth muscle cells undergo vesicle-mediated calcification in response to changes in extracellular calcium and phosphate concentrations: a potential mechanism for accelerated vascular calcification in ESRD. J Am Soc Nephrol. 2004;15(11):2857-67.

34. Lemasters JJ, Nieminen AL, Qian T, Trost LC, Elmore SP, Nishimura Y, et al. The mitochondrial permeability transition in cell death: a common mechanism in necrosis, apoptosis and autophagy. Biochim Biophys Acta. 1998;1366(1-2):177-96.

35. Weglicki W, Quamme G, Tucker K, Haigney M, Resnick LM. Potassium, magnesium, and electrolyte imbalance and complications in disease management. Clin Exp Hypertens 2005;27(1):95-112.

36. Dacey MJ. Hypomagnesemic disorders. Crit Care Clin. 2001;17(1):155-73, viii.

37. Ceremuzynski L, Gebalska J, Wolk R, Makowska E. Hypomagnesemia in heart failure with ventricular arrhythmias. Beneficial effects of magnesium supplementation. J Intern Med. 2000;247(1):78-86.

38. Cappuccio FP. Sodium, potassium, calcium and magnesium and cardiovascular risk. J Cardiovasc Risk. 2000;7(1):1-3.

39. Mizushima S, Cappuccio FP, Nichols R, Elliott P. Dietary magnesium intake and blood pressure: a qualitative overview of the observational studies. J Hum Hypertens. 1998;12(7):447-53.

40. Touyz RM. Transient receptor potential melastatin 6 and 7 channels, magnesium transport, and vascular biology: implications in hypertension. Am J Physiol Heart Circ Physiol. 2008;294(3):H1103-18.

41. Altura BM, Altura BT. Tension headaches and muscle tension: is there a role for magnesium? Med Hypotheses. 2001;57:705-13.

42. Rude RK, Gruber HE, Norton HJ, Wei LY, Frausto A, Kilburn J. Reduction of dietary magnesium by only 50% in the rat disrupts bone and mineral metabolism. Osteoporos Int. 2006;17(7):1022-32.

43. Conradt A. [Pathophysiology and clinical aspects of pre-eclampsia]. Z Geburtshilfe Perinatol. 1985;189(4):149-61.

44. Jain S, Sharma P, Kulshreshtha S, Mohan G, Singh S. The role of calcium, magnesium, and zinc in pre-eclampsia. Biol Trace Elem Res. 2010;133(2):162-70.

45. Kao WH, Folsom AR, Nieto FJ, Mo JP, Watson RL, Brancati FL. Serum and dietary magnesium and the risk for type 2 diabetes mellitus: the Atherosclerosis Risk in Communities Study. Arch Intern Med. 1999;159(18):2151-9.

46. Masliah E, Rockenstein E, Veinbergs I, Mallory M, Hashimoto M, Takeda A, et al. Dopaminergic loss and inclusion body formation in alpha-synuclein mice: implications for neurodegenerative disorders. Science. 2000;287(5456):1265-9.

47. Ward KM, Niemela JE, Cecco SA, Rehak NN, Elin RJ, Balaban RS. Determination of the apparent dissociation constant of Mg-ATP (at T=37^{0}C, pH=7.2, I=0.15) using a combination of ^{31}P NMR spectroscopy and the fluorescence indicator Mag-fura-2.

48. Quamme GA. Renal magnesium handling: new insights in understanding old problems. Kidney Int. 1997;52(5):1180-95.

49. Gasbarrini A, Borle AB, Farghali H, Bender C, Francavilla A, Van Thiel D. Effect of anoxia on intracellular ATP, Na^{+}_{i} , Ca^{2+}_{i} , Mg^{2+}_{i} , and cytotoxicity in rat hepatocytes. J Biol Chem. 1992;267(10):6654-63.

50. Günther T. Mechanisms and regulation of Mg^{2+} efflux and Mg^{2+} influx. Miner Electrolyte Metab. 1993;19(4-5):259-65.

51. Romani A, Marfella C, Scarpa A. Regulation of magnesium uptake and release in the heart and in isolated ventricular myocytes. Circ Res. 1993;72(6):1139-48.

52. Shils ME. Magnesium. 8 ed. Shils ME, Olson JA, Shike M, editors. Philadelphia: Lea & Febiger; 1994.

53. Flatman PW. Mechanisms of magnesium transport. Annu Rev Physiol. 1991;53:259-71.

54. Beyenbach KW. Transport of magnesium across biological membranes. Magnes Trace Elem. 1990;9(5):233-54.

55. Romani AM, Scarpa A. Regulation of cellular magnesium. Front Biosci. 2000;5:D720-34.

56. Sahni J, Scharenberg AM. The SLC41 family of MgtE-like magnesium transporters. Mol Aspects Med. 2013;34(2-3):620-8.

57. Schmitz C, Perraud AL, Johnson CO, Inabe K, Smith MK, Penner R, et al. Regulation of vertebrate cellular Mg^{2+} homeostasis by TRPM7. Cell. 2003;114(2):191-200.

58. Schlingmann KP, Weber S, Peters M, Niemann Nejsum L, Vitzthum H, Klingel K, et al. Hypomagnesemia with secondary hypocalcemia is caused by mutations in TRPM6, a new member of the TRPM gene family. Nat Genet. 2002;31(2):166-70.

59. Walder RY, Landau D, Meyer P, Shalev H, Tsolia M, Borochowitz Z, et al. Mutation of TRPM6 causes familial hypomagnesemia with secondary hypocalcemia. Nat Genet. 2002;31(2):171-4.

60. Ryazanova LV, Rondon LJ, Zierler S, Hu Z, Galli J, Yamaguchi TP, et al. TRPM7 is essential for Mg^{2+} homeostasis in mammals. Nat Commun. 2010;1:109.

61. Deason-Towne F, Perraud AL, Schmitz C. The Mg^{2+} transporter MagT1 partially rescues cell growth and Mg^{2+} uptake in cells lacking the channel-kinase TRPM7. FEBS Lett. 2011;585(14):2275-8.

62. Zhou H, Clapham DE. Mammalian MagT1 and TUSC3 are required for cellular magnesium uptake and vertebrate embryonic development. Proc Natl Acad Sci U S A. 2009;106(37):15750-5.

63. Stuiver M, Lainez S, Will C, Terryn S, Gunzel D, Debaix H, et al. CNNM2, encoding a basolateral protein required for renal Mg^{2+} handling, is mutated in dominant hypomagnesemia. Am J Hum Genet. 2011;88(3):333-43.

64. Romani AM. Cellular magnesium homeostasis. Arch Biochem Biophys. 2011;512(1):1-23.

65. Zoratti M, Szabo I. The mitochondrial permeability transition. Biochim Biophys Acta. 1995;1241(2):139-76.

66. Kowaltowski AJ, Naia-da-Silva ES, Castilho RF, Vercesi AE. Ca^{2+}-stimulated mitochondrial reactive oxygen species generation and permeability transition are inhibited by dibucaine or Mg^{2+}. Arch Biochem Biophys. 1998;359(1):77-81.

67. Cui Y, Zhao S, Wang J, Wang X, Gao B, Fan Q, et al. A novel mitochondrial carrier protein Mme1 acts as a yeast mitochondrial magnesium exporter. Biochimica et Biophysica Acta. 2015 1853(3):724-32.

68. Brierley GP, Davis M, Jung DW. Respiration-dependent uptake and extrusion of Mg^{2+} by isolated heart mitochondria. Arch Biochem Biophys. 1987;253(2):322-32.

69. Khan MB, Sponder G, Sjoblom B, Svidova S, Schweyen RJ, Carugo O, et al. Structural and functional characterization of the N-terminal domain of the yeast Mg^{2+} channel Mrs2. Acta Crystallogr D Biol Crystallogr. 2013;69(Pt 9):1653-64.

70. Kolisek M, Zsurka G, Samaj J, Weghuber J, Schweyen RJ, Schweigel M. Mrs2p is an essential component of the major electrophoretic Mg^{2+} influx system in mitochondria. EMBO J. 2003;22(6):1235-44.

71. Jung DW, Apel L, Brierley GP. Matrix free Mg^{2+} changes with metabolic state in isolated heart mitochondria. Biochemistry. 1990;29(17):4121-8.

72. Kubota T, Shindo Y, Tokuno K, Komatsu H, Ogawa H, Kudo S, et al. Mitochondria are intracellular magnesium stores: investigation by simultaneous fluorescent imagings in PC12 cells. Biochim Biophys Acta. 2005;1744(1):19-28.

73. Hwang DL, Yen CF, Nadler JL. Insulin increases intracellular magnesium transport in human platelets. J Clin Endocrinol Metab. 1993;76(3):549-53.

74. Littledike ET, Arnaud CD. The influence of plasma magnesium concentrations on calcitonin secretion in the pig. Proc Soc Exp Biol Med. 1971;136(3):1000-6.

75. Gill JR, Jr., Bell NH, Bartter FC. Effect of parathyroid extract on magnesium excretion in man. J Appl Physiol. 1967;22(1):136-8.

76. Wolf FI, Di Francesco A, Covacci V, Cittadini A. cAMP activates magnesium efflux via the Na/Mg antiporter in ascites cells. Biochem Biophys Res Commun. 1994;202(3):1209-14.

77. Romani AM, Matthews VD, Scarpa A. Parallel stimulation of glucose and Mg^{2+} accumulation by insulin in rat hearts and cardiac ventricular myocytes. Circ Res. 2000;86(3):326-33.

78. Romani A, Scarpa A. Hormonal control of Mg^{2+} transport in the heart. Nature. 1990;346(6287):841-4.

79. Murphy E, Freudenrich CC, Lieberman M. Cellular magnesium and Na/Mg exchange in heart cells. Annu Rev Physiol. 1991;53:273-87.

80. Romani A, Dowell E, Scarpa A. Cyclic AMP-induced Mg^{2+} release from rat liver hepatocytes, permeabilized hepatocytes, and isolated mitochondria. J Biol Chem. 1991;266(36):24376-84.

81. Mastrototaro L, Tietjen U, Sponder G, Vormann J, Aschenbach JR, Kolisek M. Insulin Modulates the Na^{+}/Mg^{2+} Exchanger SLC41A1 and Influences Mg^{2+} Efflux from Intracellular Stores in Transgenic HEK293 Cells. J Nutr. 2015;145(11):2440-7.

82. Wabakken T, Rian E, Kveine M, Aasheim HC. The human solute carrier SLC41A1 belongs to a novel eukaryotic subfamily with homology to prokaryotic MgtE Mg^{2+} transporters. Biochem Biophys Res Commun. 2003;306(3):718-24.

83. Hattori M, Iwase N, Furuya N, Tanaka Y, Tsukazaki T, Ishitani R, et al. Mg^{2+}-dependent gating of bacterial MgtE channel underlies Mg^{2+} homeostasis. EMBO J. 2009 Nov 18;28(22):3602-12.

84. Hattori M, Tanaka Y, Fukai S, Ishitani R, Nureki O. Crystal structure of the MgtE Mg^{2+} transporter. Nature. 2007 Aug 30;448(7157):1072-5.

85. Ishitani R, Sugita Y, Dohmae N, Furuya N, Hattori M, Nureki O. Mg^{2+}-sensing mechanism of Mg^{2+} transporter MgtE probed by molecular dynamics study. Proc Natl Acad Sci U S A. 2008 Oct 7;105(40):15393-8.

86. Goytain A, Quamme GA. Functional characterization of human SLC41A1, a Mg^{2+} transporter with similarity to prokaryotic MgtE Mg^{2+} transporters. Physiol Genomics. 2005;21(3):337-42.

87. Goytain A, Quamme GA. Functional characterization of the mouse [corrected] solute carrier, SLC41A2. Biochem Biophys Res Commun. 2005;330(3):701-5.

88. Mandt T, Song Y, Scharenberg AM, Sahni J. SLC41A1 Mg^{2+} transport is regulated via Mg^{2+}-dependent endosomal recycling through its N-terminal cytoplasmic domain. Biochem J. 2011;439(1):129-39.

89. Nestler A, Sponder G, Rutschmann K, Mastrototaro L, Weise C, Vormann J, et al. Nature of SLC41A1 complexes: report on the split-ubiquitin yeast two hybrid assay. Magnes Res. 2013;26(2):56-66.

90. Kolisek M, Sponder G, Mastrototaro L, Smorodchenko A, Launay P, Vormann J, et al. Substitution p.A350V in Na^{+}/Mg^{2+} exchanger SLC41A1, potentially associated with Parkinson's disease, is a gain-of-function mutation. PLoS One. 2013;8(8):e71096.

91. Sponder G, Rutschmann K, Kolisek M. "Inside-in" or "inside-out"? The membrane topology of SLC41A1. Magnes Res. 2013;26(4):176-81.

92. Barbagallo M, Belvedere M, Di Bella G, Dominguez LJ. Altered ionized magnesium levels in mild-to-moderate Alzheimer's disease. Magnes Res. 2011;24(3):S115-21.
93. Miyake Y, Tanaka K, Fukushima W, Sasaki S, Kiyohara C, Tsuboi Y, et al. Dietary intake of metals and risk of Parkinson's disease: a case-control study in Japan. J Neurol Sci. 2011;306(1-2):98-102.
94. Lovitt B, Vanderporten EC, Sheng Z, Zhu H, Drummond J, Liu Y. Differential effects of divalent manganese and magnesium on the kinase activity of leucine-rich repeat kinase 2 (LRRK2). Biochemistry. 2010;49(14):3092-100.
95. Nie ZL, Wang ZM, Zhou B, Tang ZP, Wang SK. Magnesium intake and incidence of stroke: meta-analysis of cohort studies. Nutr Metab Cardiovasc Dis. 2013;23(3):169-76.
96. Johnson S. The multifaceted and widespread pathology of magnesium deficiency. Med Hypotheses. 2001;56(2):163-70.
97. Mousain-Bosc M, Roche M, Rapin J, Bali JP. Magnesium VitB6 intake reduces central nervous system hyperexcitability in children. J Am Coll Nutr. 2004;23(5):545S-8S.
98. Aden E, Carlsson M, Poortvliet E, Stenlund H, Linder J, Edstrom M, et al. Dietary intake and olfactory function in patients with newly diagnosed Parkinson's disease: a case-control study. Nutr Neurosci. 2011;14(1):25-31.
99. Barbiroli B, Martinelli P, Patuelli A, Lodi R, Iotti S, Cortelli P, et al. Phosphorus magnetic resonance spectroscopy in multiple system atrophy and Parkinson's disease. Mov Disord. 1999;14(3):430-5.
100. Satake W, Nakabayashi Y, Mizuta I, Hirota Y, Ito C, Kubo M, et al. Genome-wide association study identifies common variants at four loci as genetic risk factors for Parkinson's disease. Nat Genet. 2009;41(12):1303-7.
101. Simon-Sanchez J, Schulte C, Bras JM, Sharma M, Gibbs JR, Berg D, et al. Genome-wide association study reveals genetic risk underlying Parkinson's disease. Nat Genet. 2009;41(12):1308-12.
102. Yan Y, Tian J, Mo X, Zhao G, Yin X, Pu J, et al. Genetic variants in the RAB7L1 and SLC41A1 genes of the PARK16 locus in Chinese Parkinson's disease patients. Int J Neurosci. 2011;121(11):632-6.
103. Tucci A, Nalls MA, Houlden H, Revesz T, Singleton AB, Wood NW, et al. Genetic variability at the PARK16 locus. Eur J Hum Genet. 2010;18(12):1356-9.
104. Resnick LM, Altura BT, Gupta RK, Laragh JH, Alderman MH, Altura BM. Intracellular and extracellular magnesium depletion in type 2 (non-insulin-dependent) diabetes mellitus. Diabetologia. 1993;36(8):767-70.

105. de Baaij JH, Groot Koerkamp MJ, Lavrijsen M, van Zeeland F, Meijer H, Holstege FC, et al. Elucidation of the distal convoluted tubule transcriptome identifies new candidate genes involved in renal Mg^{2+} handling. Am J Physiol Renal Physiol. 2013;305(11):F1563-73.
106. Fleig A, Schweigel-Rontgen M, Kolisek M. Solute Carrier Family SLC41, what do we really know about it? Wiley Interdiscip Rev Membr Transp Signal. 2013;2(6).
107. Wang CY, Shi JD, Yang P, Kumar PG, Li QZ, Run QG, et al. Molecular cloning and characterization of a novel gene family of four ancient conserved domain proteins (ACDP). Gene. 2003;306:37-44.
108. Ignoul S, Eggermont J. CBS domains: structure, function, and pathology in human proteins. Am J Physiol Cell Physiol. 2005;289(6):C1369-78.
109. Meyer TE, Verwoert GC, Hwang SJ, Glazer NL, Smith AV, van Rooij FJ, et al. Genome-wide association studies of serum magnesium, potassium, and sodium concentrations identify six Loci influencing serum magnesium levels. PLoS Genet. 2010;6(8).
110. Dichgans M, Malik R, Konig IR, Rosand J, Clarke R, Gretarsdottir S, et al. Shared genetic susceptibility to ischemic stroke and coronary artery disease: a genome-wide analysis of common variants. Stroke. 2014;45(1):24-36.
111. Rose EJ, Hargreaves A, Morris D, Fahey C, Tropea D, Cummings E, et al. Effects of a novel schizophrenia risk variant rs7914558 at CNNM2 on brain structure and attributional style. Br J Psychiatry. 2014;204(2):115-21.
112. Ohi K, Hashimoto R, Yamamori H, Yasuda Y, Fujimoto M, Umeda-Yano S, et al. The impact of the genome-wide supported variant in the cyclin M2 gene on gray matter morphology in schizophrenia. Behav Brain Funct. 2013;9:40.
113. de Baaij JH, Stuiver M, Meij IC, Lainez S, Kopplin K, Venselaar H, et al. Membrane topology and intracellular processing of cyclin M2 (CNNM2). J Biol Chem. 2012;287(17):13644-55.
114. Kurth K. Validierung magnesiumsensitiver Gene als Biomarker für den intrazellulären Magnesiumstatus von Diabetes-mellitus-Typ-II-Patienten. Berlin: Freie Universität; 2013.
115. Rude RK. Magnesium. 11th ed. Ross AC, Caballero B, Cousins RJ, Tucker KL, Ziegler TR, editors. Baltimore: Lippincott Williams & Wilkins; 2012.
116. Intakes SCotSEoDR. Dietary Reference Intakes for Calcium, Phosphorus, Magnesium, Vitamin D, and Fluoride. Washington, DC: The National Academies Press; 1997.
117. Lopez-Ridaura R, Willett WC, Rimm EB, Liu S, Stampfer MJ, Manson JE, et al. Magnesium intake and risk of type 2 diabetes in men and women. Diabetes Care. 2004;27:134-40.

118. Ascherio A, Rimm EB, Giovannucci EL, Colditz GA, Rosner B, Willett WC, et al. A prospective study of nutritional factors and hypertension among US men. Circulation. 1992;86:1475-84.
119. Liao F, Folsom AR, Brancati FL. Is low magnesium concentration a risk factor for coronary heart disease? The Atherosclerosis Risk in Communities (ARIC) Study. Am Heart J. 1998;136(3):480-90.
120. Arsenian MA. Magnesium and cardiovascular disease. Prog Cardiovasc Dis 1993;35(4):271-310.
121. Altura BM, Altura BT. Role of magnesium in the pathogenesis of hypertension updated: relationship to its action on cardiac, vascular smooth muscle, and endothelial cells. edn n, editor. New York: Laragh, J. Brenner, B. M.; 1995. 1213–42 p.
122. Kisters K, Tokmak F, Kosch M, Hausberg M. Role of the Na^+/Mg^{2+} exchanger in hypertension. Am J Hypertens. 2003;16(1):95-6.
123. Picado MJ, de la Sierra A, Aguilera MT, Coca A, Urbano-Márquez A. Increased activity of the Na^+/Mg^{2+} exchanger in red blood cells from essential hypertensive patients. Hypertension. 1994;23(2):987-91.
124. Barbagallo M, Dominguez LJ, Brucato V, Galioto A, Pineo A, Ferlisi A, et al. New Perspectives in Magnesium Research. Nishizawa Y, Morii H, Durlach J, editors. London2007.
125. Volpe SL. Magnesium, the metabolic syndrome, insulin resistance, and type 2 diabetes mellitus. Crit Rev Food Sci Nutr. 2008 Mar;48(3):293-300.
126. Rayssiguier Y, Libako P, Nowacki W, Rock E. Magnesium deficiency and metabolic syndrome: stress and inflammation may reflect calcium activation. Magnes Res. 2010 Jun;23(2):73-80.
127. Günther T, Vormann J. Activation of Na^+/Mg^{2+} antiport in thymocytes by cAMP. FEBS Lett. 1992;297(1-2):132-4.
128. Lin MT, Beal MF. Review ArticleMitochondrial dysfunction and oxidative stress in neurodegenerative diseases. Nature. 19 October 2006;443:787-95.
129. de Moura MB, dos Santos LS, Van Houten B. Mitochondrial dysfunction in neurodegenerative diseases and cancer. Environ Mol Mutagen. 2010 Jun;51(5):391-405.
130. Shindo Y, Fujimoto A, Hotta K, Suzuki K, Oka K. Glutamate-induced calcium increase mediates magnesium release from mitochondria in rat hippocampal neurons. J Neurosci Res. 2010;88(14):3125-32.
131. Yamanaka R, Shindo Y, Hotta K, Suzuki K, Oka K. NO/cGMP/PKG signaling pathway induces magnesium release mediated by mitoKATP channel opening in rat hippocampal neurons. FEBS Lett. 2013;587(16):2643-8.

132. Kuramoto T, Kuwamura M, Tokuda S, Izawa T, Nakane Y, Kitada K, et al. A mutation in the gene encoding mitochondrial Mg^{2+} channel MRS2 results in demyelination in the rat. PLoS Genet. 2011;7(1):e1001262.
133. Piskacek M, Zotova L, Zsurka G, Schweyen RJ. Conditional knockdown of hMRS2 results in loss of mitochondrial Mg^{2+} uptake and cell death. J Cell Mol Med. 2009;13(4):693-700.
134. Barbiroli B, Iotti S, Cortelli P, Martinelli P, Lodi R, Carelli V, et al. Low brain intracellular free magnesium in mitochondrial cytopathies. J Cereb Blood Flow Metab. 1999;19(5):528-32.
135. Barbagallo M, Dominguez LJ. Magnesium and aging. Curr Pharm Des. 2010;16(7):832-9.
136. Newsholme P, Gaudel C, Krause M. Mitochondria and diabetes. An intriguing pathogenetic role. Adv Exp Med Biol. 2012;942:235-47.
137. Exner N, Lutz AK, Haass C, Winklhofer KF. Mitochondrial dysfunction in Parkinson's disease: molecular mechanisms and pathophysiological consequences. EMBO J. 2012;31(14):3038-62.
138. Traxler B, Beckwith J. Assembly of a hetero-oligomeric membrane protein complex. Proc Natl Acad Sci U S A. 1992 Nov 15;89(22):10852-6.
139. Sihag RK, Cataldo AM. Brain beta-spectrin is a component of senile plaques in Alzheimer's disease. Brain Res 1996;743:249-57.
140. Shindo Y, Yamanaka R, Suzuki K, Hotta K, Oka K. Intracellular magnesium level determines cell viability in the MPP(+) model of Parkinson's disease. Biochim Biophys Acta. 2015;1853(12):3182-91.
141. Swaminathan R. Magnesium metabolism and its disorders. Clin Biochem Rev. 2003;24(2):47-66.
142. Bussiere FI, Gueux E, Rock E, Girardeau JP, Tridon A, Mazur A, et al. Increased phagocytosis and production of reactive oxygen species by neutrophils during magnesium deficiency in rats and inhibition by high magnesium concentration. Br J Nutr. 2002;87(2):107-13.
143. Kasote DM, Hegde MV, Katyare SS. Mitochondrial dysfunction in psychiatric and neurological diseases: cause(s), consequence(s), and implications of antioxidant therapy. Biofactors. 2013;39(4):392-406.
144. Sas K, Robotka H, Toldi J, Vecsei L. Mitochondria, metabolic disturbances, oxidative stress and the kynurenine system, with focus on neurodegenerative disorders. J Neurol Sci. 2007;257(1-2):221-39.
145. Billia F, Hauck L, Grothe D, Konecny F, Rao V, Kim RH, et al. Parkinson-susceptibility gene DJ-1/PARK7 protects the murine heart from oxidative damage in vivo. Proc Natl Acad Sci U S A. 2003;110:6085-90.

146. Okatsu K, Oka T, Iguchi M, Imamura K, Kosako H, Tani N, et al. PINK1 autophosphorylation upon membrane potential dissipation is essential for Parkin recruitment to damaged mitochondria. Nat Commun. 2012;3:1016.
147. Takahashi K, Taira T, Niki T, Seino C, Iguchi-Ariga SM, Ariga H. DJ-1 positively regulates the androgen receptor by impairing the binding of PIASx alpha to the receptor. J Biol Chem. 2001;276:37556-63.
148. Kolisek M, Montezano AC, Sponder G, Anagnostopoulou A, Vormann J, Touyz RM, et al. PARK7/DJ-1 dysregulation by oxidative stress leads to magnesium deficiency: implications in degenerative and chronic diseases. Clin Sci (Lond). 2015;129(12):1143-50.
149. Romanuik TL, Wang G, Holt RA, Jones SJ, Marra MA, Sadar MD. Identification of novel androgen-responsive genes by sequencing of LongSAGE libraries. BMC Genomics. 2009;10(476).
150. Winklhofer KF, Haass C. Mitochondrial dysfunction in Parkinson's disease. Biochim Biophys Acta. 2010 Jan;1802(1):29-44.
151. Hoepken HH, Gispert S, Morales B, Wingerter O, Del Turco D, Mulsch A, et al. Mitochondrial dysfunction, peroxidation damage and changes in glutathione metabolism in PARK6. Neurobiol Dis. 2006;25:401-11.
152. Dawson TM, Ko HS, Dawson VL. Genetic animal models of Parkinson’s disease. Neuron 2010;66:646-61.
153. Heinrich A, Nees F, Lourdusamy A, Tzschoppe J, Meier S, Vollstädt-Klein S, et al. From gene to brain to behavior: schizophrenia-associated variation in AMBRA1 alters impulsivity-related traits. Eur J Neurosci. 2013;38:2941-5.
154. Merenlender-Wagner A, Malishkevich A, Shemer Z, Udawela M, Gibbons A, Scarr E, et al. Autophagy has a key role in the pathophysiology of schizophrenia. Molecular Psychiatry. 2015;20:126-32.
155. Merenlender-Wagner A, Shemer Z, Touloumi O, Lagoudaki R, Giladi E, Andrieux A, et al. New horizons in schizophrenia treatment: autophagy protection is coupled with behavioral improvements in a mouse model of schizophrenia. Autophagy. 2014;10(12):2324-32.

PUBLICATIONS

Peer reviewed publications

2016

- **Mastrototaro L**, Smorodchenko A, Aschenbach JR, Kolisek M, Sponder G: **Solute carrier 41A3 encodes for a mitochondrial Mg^{2+} efflux system.**
  Scientific Reports. 2016 Jun 15, 6:27999. doi: 10.1038/srep27999.

- Sponder G, **Mastrototaro L**, Kurth K, Merolle L, Zhang Z, Abdulhanan N, Smorodchenko A, Wolf K, Fleig A, Penner R, Iotti S, Aschenbach JR, Vormann J, Kolisek M: **Human CNNM2 is not a Mg^{2+} transporter *per se*.**
  Pflugers Archive – European Journal of Physiology. 2016 Apr, doi 10.1007/s00424-016-1816-7

2015

- **Mastrototaro L**, Tietjen U, Sponder G, Vormann J, Aschenbach JR, Kolisek M: **Insulin modulates the Na^{+}/Mg^{2+} exchanger SLC41A1 and influences Mg^{2+} efflux from intracellular stores in transgenic Hek293 cells.**
  The Journal of Nutrition. 2015 Nov;145(11):2440-2447

2013

- Kolisek M, Sponder G, **Mastrototaro L**, Smorodchenko A, Launay P, Vormann J, Schweigel-Röntgen M: **Substitution p.A350V in Na^{+}/Mg^{2+} exchanger SLC41A1, potentially associated with Parkinson's Disease, is a gain of function mutation.**
  PLoS One. 2013 Aug 15;8(8)

- Nestler A, Sponder G, Rutschmann K, **Mastrototaro L**, Weise C, Vormann J, Schweigel-Röntgen M, Kolisek M: **Nature of SLC41A1 complexes: report on split-ubiquitin yeast two-hybrid assay.**
  Magnesium Research. 2013 Apr-Jun;26(2):56-66

Abstracts in proceedings and participation in conferences

2016

- **Mastrototaro L**, Sponder G, Aschenbach JR, Kolisek M: **Magnesiotropic gene CNNM2 is not coding for a Mg^{2+} transporter.**
  DVG-Fachgruppe Physiologie und Biochemie
  Berlin- March 30-April 1st, 2016
  In Abstract book DVG, P. 42

- **Mastrototaro L**, Smorodchenko A, Aschenbach JR, Kolisek M, Sponder G: **Solute carrier 41A3 encodes for a mitochondrial Mg^{2+} efflux system.**
  DVG-Fachgruppe Physiologie und Biochemie
  Berlin- March 30-April 1st, 2016
  In Abstract book DVG, P. 113

- **Mastrototaro L**, Sponder G, Aschenbach JR, Kolisek M: **Mg-homeostatic factor CNNM2, not a simple story.**
  Magnesium in Translational Medicine
  Liptovsky Mikulas, Slovak Republic – February 18-21st, 2016
  In: Abstract book: Magnesium in Translational Medicine, P. 19

- Aschenbach JR, **Mastrototaro L**, Sponder G, Tjetien U, Abdulhanan N, Fröhlich N, Kolisek M: **Role of insulin in regulation of Na^{+}/Mg^{2+} exchanger SLC41A1.**
  Magnesium in Translational Medicine
  Liptovsky Mikulas, Slovak Republic – February 18-21st, 2016
  In: Abstract book: Magnesium in Translational Medicine, P. 11

- Sponder G, **Mastrototaro L**, Smorodchenko A, Aschenbach JR, Kolisek M: **Solute carrier 41A3 encodes for a mitochondrial Mg^{2+} efflux system.**
  Magnesium in Translational Medicine
  Liptovsky Mikulas, Slovak Republic – February 18-21st, 2016
  In: Abstract book: Magnesium in Translational Medicine, P. 26

2015

- **Mastrototaro L**, Sponder G, Aschenbach JR, Kolisek M: **Mutation p.A350V in Na^+/Mg^{2+} exchanger SLC41A1 elicits gain of function with potential relevance to Parkinson's disease.**
  Dahlem Research School PhD-Symposium
  Berlin, Freie Universität - March 20th, 2015
  In: Abstract book: PhD Symposium, P. 3

- Hille KT, Sponder G, Braun H, Deiner C, **Mastrototaro L**, Rosendahl J, Stumpff F: **Ruminal epithelial cells express multiple TRP channels.**
  94 Tagung der Deutschen Physiologischen Gesellschaft
  Magdeburg, Germany - March 5-7th, 2015
  In: Acta Physiologica, Oxford; **213**(699), P. 142

2014

- Aschenbach JR, **Mastrototaro L**, Bermudez-Pena C, Tietjen U, Marak M, Trappe S, Vormann J, Kolisek M: **Wirkung von Insulin und kurzkettigen Fettsäuren auf den SLC41A1-abhängigen Mg^{2+}-Efflux in einem Zellkulturmodell.**
  34. Magnesium- Symposium der Gesellschaft für Magnesium-Forschung e. V.
  Herne, Germany – October 24-25th,2014

- Kolisek M, Sponder G, **Mastrototaro L**, Tietjen U, Marak M, Aschenbach JR, Vormann J: **Magnesium homeostasis and neurodegeneration.**
  34. Magnesium-Symposium der Gesellschaft für Magnesium-Forschung
  Herne, Germany – October 24-25th,2014

- **Mastrototaro L,** Sponder G, Aschenbach JR, Vormann J, Kolisek M: **Does CNNM2 represent further molecular evidence for an involvement of an imbalanced intracellular Mg^{2+} homeostasis (IMH) in neurodegeneration?**
  1st European Magnesium Workshop dedicated to Magnesium in Translational Medicine
  Smolenice Castle , Slovak Republic - May 11-15th, 2014
  In: Abstract book: Magnesium in Translational Medicine, P. 23.

- Aschenbach JR, **Mastrototaro L**, Bermudez-Pena C, Tietjen U, Marak M, Trappe S, Vormann J, Kolisek M: **Short chain fatty acids activate SLC41A1-dependent Mg^{2+} efflux and seem to antagonize the inhibitory effect of insulin.**

1st European Magnesium Workshop dedicated to Magnesium in Translational Medicine
Smolenice Castle , Slovak Republic - May 11-15th, 2014
In: Abstract book: Magnesium in Translational Medicine, P. 23

- Kolisek M, Sponder G, **Mastrototaro L**, Aschenbach JR, Vormann J: **Magnesium homeostasis and neurodegeneration.**
  1st European Magnesium Workshop dedicated to Magnesium in Translational Medicine
  Smolenice Castle , Slovak Republic - May 11-15th, 2014
  In: Abstract book: Magnesium in Translational Medicine, P. 5

- **Mastrototaro L,** Sponder G, Aschenbach JR, Kolisek M: **Characterization of the transporter SLC41A3 in HEK293 transgenic cell line.**
  93rd Annual Meeting of the German Physiological Society
  Mainz, Germany - March 13-15th, 2014
  In: Acta Physiologica, Oxford; **210**(Suppl. 695), P. 126

- Sponder G, **Mastrototaro L**, Smorodchenko A, Schweigel-Roentgen M, Aschenbach JR, Kolisek M: **Mutations in the Na^+/Mg^{2+} exchanger SLC41A1 might be involved in Parkinson's disease etiology.**
  21. Tagung der Fachgruppe Physiologie und Biochemie der Deutschen Veterinärmedizinischen Gesellschaft
  Zürich – February 13-15th, 2014
  In: 21. Tagung der Fachgruppe Physiologie und Biochemie der Deutschen Veterinärmedizinischen Gesellschaft – Deutsche Veterinärmedizinische Gesellschaft (Hrsg.) München: Ludwig-Maximilians-Univ. P. V39

2012

- **Mastrototaro L,** Sponder G, Aschenbach JR, Vormann J, Kolisek M: **Mag-fura 2 characterization of SLC41A3 in HEK293 transgenic cell line.**
  XIII International Magnesium Symposium
  Mexico, Merida- October 16-19th, 2012
  In: Magnesium research; **25**(4), P. 42

DANKSAGUNG

At the end of my thesis, I would like to thank all these people who made this dissertation possible and an unforgettable experience for me; I would never have been able to finish it without the guidance of my committee members, help from friends, and support from my family.

Foremost, I would like to express my sincere gratitude to my advisor **Prof. Aschenbach** for the opportunity he gave me to work in his institute and to accomplish my PhD studies. He has been a fantastic mentor for me and his guidance helped me in the entire research and writing of this thesis, which he patiently corrected. I am thankful for his constant constructive criticisms, for being available at any time for advices, for encouraging my research and engaging me in new ideas, for his constant support, and for allowing me to grow as a scientist. His advices on both research and my career have been essential, I learned a lot in the past four years and I am grateful he insisted that I speak German.

Besides my advisor, I would like to thank the second committee member **Dr. Chris Weise**, for his interest in my work and for his scientific advices, comments, annotations, and insightful discussions about the research. He also provided me with the opportunity to work in his lab and perform the mass spectrometry experiments presented in this thesis.

My special appreciation and thanks go to **Dr. Martin Kolisek** who encouraged me to make a doctoral program abroad from Italy and provided me with the opportunity to make my PhD thesis in his group. He is the funniest supervisor and one of the smartest people I know. He has been my primary resource for getting my science questions. I am grateful to him for holding me to a high research standard, demanding strict validations for each research result, and thus teaching me how to do research. Aside from the scientific help, his sense of humour made my staying in Berlin much easier, despite our initial language problems.

I want to thank present and past members of the **Institute of Physiology**, all the technical assistants, doctoral students, and everyone else in the institute for providing a great working environment, for their help, and chats. A special thank you to **Katerina Wolf**, a wonderful person with great lab skills, for giving me precious advices in the PCR world, for always being helpful in solving technical problems, and for being stubborn in speaking german to me! A second special thank you to **Martin Marak**, a good technician, enjoyable working partner, a great cook, and a good friend!

I would like to thank all my friends and colleagues for their skill in spreading happiness on those scientifically dark days.

Gerhard Sponder: I am very grateful for his patience, motivation, enthusiasm, and immense knowledge in molecular biology and cloning. Taken together, this makes him a great “teacher”. It would have been a lonely lab without him, we worked closely in all the experiments presented in this thesis and we have even been able to clone a ‘Gerardo gene’ together! He taught me how to be precise, accurate, and meticulous in cutting membranes for western blot, as well as in performing every experiment! I know that I could always ask him for advice and opinions on lab related issues and he often helped me cranking out reports and abstracts in a very short time. Most importantly, he has been a friend, the person I could always go to, for every problem and concerns, whether it was for professional or private reasons. I will forever be grateful to him for the support and help he gave me when I first moved to Berlin and I had to go through many bureaucracy issues and finally I will not forget his help in moving all my stuff during the many moves…6 or 7 times?

Azzurra: I am thankful that she persisted in being friendly with me and that after some time, I finally gave up and realized how great of a person I was missing. I cannot list all the good moments we shared together, I can just express my immense gratitude for her, for all the laughing times, the tears and mutual encouragements during our PhD, for cheering me up and standing by me through the good and bad times, during the thesis writing hell, and my scientific and personal failures. I thought it was not possible to find a soulmate in a friend but now I am convinced that it is possible. I know that when we will be old, she will still be there as a supportive and caring friend.

Nasrin: I was not sure we could get along when she first entered my office, but it didn’t take me very long to change my mind. Thanks for the many evenings filled with wine and interesting but also dumb discussions, for the introduction to Arabic food, for helping me quickly proofread this thesis, for listening to my crazy stories, and for always being there during my latest breakdowns. I think of her as my big sister, always checking on me, and talking to me as an adult when I forget to be an adult myself!

Kim and Gabri: the nicest couple I have ever met! I am grateful to Gabri for his inevitable morning jokes that bring light to my days at work and to Kim for the many talks and advices. Thanks to both of them for the many times they took care of me when the only thing I needed was my family and they have been family here in Berlin. Thanks for the great nights filled with food, drinks, and countless laughs that we have had together.

Carmen: my first friend in Berlin, who soon became my mexican sister. I will never forget the innumerable crazy times, funny activities, and not well planned travels we did together, including our last minute “cheap” flight to Oslo...I am still wondering why was it so cheap?!? We grew up together when we came to Berlin and we had to face so many unfamiliar and sometimes awkward situations for us little latin girls. She is a wonderful and generous friend who has been through a lot, I admire her positive outlook and her ability to always smile despite the situation. Thanks for being there when I went through one of the hardest period of my life then and now, even though thousands kilometres divide us!

Lucia, Federica, Alessandra: my Italian funny and friendly office mates. Thanks for coming to the institute, either for long or short time. It is not easy to meet nice persons and know from the beginning they would leave at some point, but I am happy that I have had the chance to meet them. I had a great time with each of them at work and after work. Together, we found the way to smile in the lab when everything seemed catastrophic: with Lucia when the cells got contaminated for such a long period of time with some unknown “creatures”; with Federica when the autoclave exploded and we were able to create “a piece of art”; with Alessandra when she could work with other people without a language in common!

Thank you to **Vicky** who helped me many times with administrative issues during the past 4 years and who has become a good friend!
Thnk you to **Alma** for being my party planner and for the numerous chats about northern coldness and latin warmth!
Thank you to **Jorine** for the “many talks and few beers” shared, and for always being friendly and cheerful about everything.
I thank my long-time friends in Italy (too many to list here but you know who you are!) for the support and friendship they gave me, even though we spent the past 4 years apart.

Last but not the least I would like to thank **my family**. Words cannot express how grateful I am to my parents for all of the sacrifices they had to make for me. They supported me spiritually and financially throughout all my studies in University and reminded me to never give up because I could accomplish whatever I was “racing” for; I would never have made it this far without them.
Thank you to my sister and my brother, sometimes too busy with their own lives, but always proud of me and encouraging me to become ‘someone’, or, as they have called me since we were kids, ‘the genius of our family’!
Being apart has not been easy and it will never be, but I know I always have my family to count on when times are rough.

Selbständigkeitserklärung

Hiermit bestätige ich, dass ich die vorliegende Arbeit selbständig angefertigt habe. Ich versichere, dass ich ausschließlich die angegebenen Quellen und Hilfen Anspruch genommen habe.

Lucia Mastrototaro